Indian J. Chem. Vol. 27A No. 9 pp 747-828
September 1988
CODEN:IJOCAP ISSN:0019-5103
27A(9) 747-828 (1988)

1029
Date 23/1/89

Indian Journal of
CHEMISTRY

SECTION A
(Inorganic, Physical, Theoretical & Analytical)

Published by
PUBLICATIONS & INFORMATION DIRECTORATE, CSIR, NEW DELHI
in association with
THE INDIAN NATIONAL SCIENCE ACADEMY, NEW DELHI

A RANGE OF HIGH PRECISION, HIGH QUALITY RECORDING INSTRUMENTS FOR THE DISCRIMINATING RESEARCH SCIENTIST

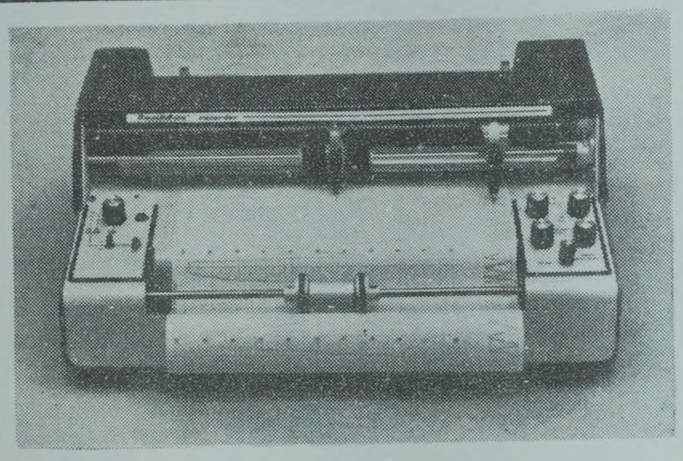

Series 5000 Strip Chart Recorder

The series 5000 Strip Chart Recorder and the series 2000 XY Recorder are well proven instruments incorporating State of the Art Circuitry. A wide range of models offer tremendous flexibility to the user. With over 5000 installations, these instruments are the preferred choice of discriminating users all over India.

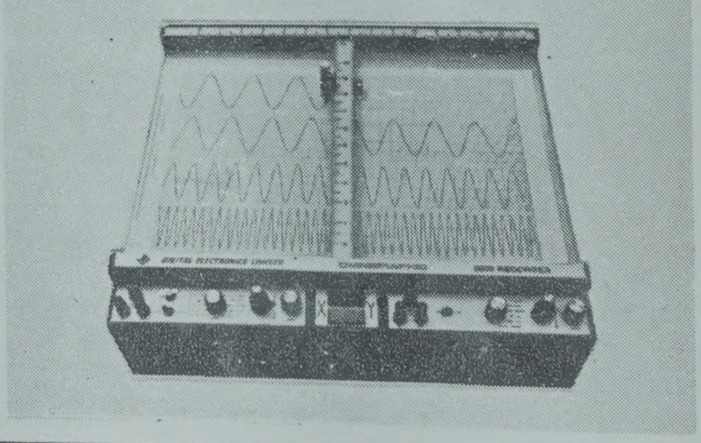

Series 2000 XY Recorder

Another quality product from

DIGITAL ELECTRONICS LIMITED

Reliability in Recording Instruments.

Digilog House 74/II, Marol Industrial Area MIDC, Andheri (East), Bombay- 400 093 Tel: 634 09 01, 632 86 76 Grams: 'DIGILOG'

A Company in collaboration with houston instrument

Special Effects/DE/25/86

INDIAN JOURNAL OF CHEMISTRY

Section A: Inorganic, Physical, Theoretical & Analytical Chemistry

Editorial Board

Prof. C.N.R. Rao
Director
Indian Institute of Science
Bangalore 560 012

Prof. R.P. Rastogi
Vice-Chancellor
Banaras Hindu University
Varanasi 221 005

Prof. A.R. Vasudeva Murthy
Department of Inorganic &
Physical Chemistry
Indian Institute of Science
Bangalore 560 012

Prof. J.C. Kuriacose
Department of Chemistry
Indian Institute of Technology
Madras 600 036

Prof. D.V.S. Jain
Department of Chemistry
Panjab University
Chandigarh 160 014

Prof. P. Natarajan
Department of Inorganic Chemistry
University of Madras
Madras 600 025

Prof. N.K. Ray
Department of Chemistry
University of Delhi
Delhi 110 007

Prof. A. Chakravorty
Department of Inorganic Chemistry
Indian Association for the
Cultivation of Science
Calcutta 700 032

Prof. S. Mitra
Tata Institute of Fundamental Research
Bombay 400 005

Dr K.N. Rao
Chemistry Division
Bhabha Atomic Research Centre
Trombay, Bombay 400 085

Prof. S.M. Khopkar
Department of Chemistry
Indian Institute of Technology
Powai, Bombay 400 076

Prof. P.T. Manoharan
Department of Chemistry
Indian Institute of Technology
Madras 600 036

Dr A.C. Dash
Department of Chemistry
Utkal University
Bhubaneswar 751 004

Shri S.P. Ambasta, Editor-in-Chief
(*Ex-officio*)

Editors

S.S. Saksena — B.C. Sharma — S. Sivakamasundari

Assistant Editor

S.K. Bhasin

Published by the Publications & Information Directorate (CSIR), Hillside Road, New Delhi 110 012

Editor-in-Chief: S.P. Ambasta

Copyright, 1988, by the Council of Scientific & Industrial Research, New Delhi 110 012

The Indian Journal of Chemistry is issued monthly in two sections: A and B. Communications regarding contributions for publication in the journal should be addressed to the Editor, Indian Journal of Chemistry, Publications & Information Directorate, Hillside Road, New Delhi 110 012.

Correspondence regarding subscriptions and advertisements should be addressed to the Sales & Distribution Officer, Publications & Information Directorate, hillside Road, New Delhi 110 012.

The Publications & Information Directorate (CSIR) assumes no responsibility for the statements and opinions advanced by contributors. The Editorial Board in its work of examining papers received for publication is assisted, in an honorary capacity by a large number of distinguished scientists, working in various parts of India.

Annual Subscription: Rs. 300.00 £ 70.00 $ 100.00; 50% discount admissible to research workers and students and 25% discount to non-research individuals on annual subscription.

Single Copy: Rs. 30.00 £ 7.00 $ 10.00

Payments in respect of subscriptions and advertisements may be sent by cheque, bank draft, money order or postal order marked payable to Publications & Information Directorate, Hillside Road, New Delhi 110 012.

Claims for missing numbers will be allowed only if received within 3 months of the date of issue of the journal plus the time normally required for postal delivery of the journal and the claim.

AUTHOR INDEX

Ananthaswamy J 768

Bandyopadhyay Ranajit K 819
Bansal Avanija 753
Bansal W R 747
Bhattacharjee Gurudas 790

Chandra Pal A V 822
Chaudhari S K 797
Choube A C 756

Dash Anadi C 772
De G S 778
Deoki Nandan 794
Dongare M K 756
Dwivedi P C 753

Gangopadhyay Ashis Kumar 778
Gaur Santwana 806
Ghosh Parthasarathi 819
Giridhara Reddy K 812
Gupta A R 794

Havanur G H 803
Hussain Reddy K 812

Indrasenan P 809
Ishwara Bhat J 786

Jagannadha Charyulu K 822

Kalavathi S V 822
Katti S S 797
Keshavan B 815
Kir Sedet 825
Kundu Kiron K 764
Kutty T R N 828

Mahale V B 803
Malhotra Kamini 747
Mehta G R 799
Mehta R K 806
Mishra Pratima 783
Mulla I S 756

Nigam Prem C 783

Omprakash K L 822
Onar A Nur 825

Padma D K 759
Patil K J 799
Pradhan Jyotsnamayee 772

Ranga S P 806
Reddy M L N 822
Revankar V K 803
Rudra Sibaprasad 764

Saikia Ranjumoni 790
Sarkar Asit R 819
Seetharamappa J 815
Sharma Shobha 806
Sidhu K S 747
Singh Ashok Kumar 790
Sinha A P B 756
Sobhana Devi G 809
Srivastava Archana 753
Srivastava P C 827
Syed Mohamed K 759

Talukdar Himansu 764
Temizer Aytekin 825
Thimme Gowda B 786

Venkata Reddy D 812
Venkateswarlu Ch 768

Wazalwar A B 799

Indian Journal of Chemistry

Sect A: Inorganic, Physical, Theoretical & Analytical

VOLUME 27A NUMBER 9 SEPTEMBER 1988

CONTENTS

Benzophenone-sensitized Photoreduction of N-Phenyl-*p*-benzoquinoneimine & Phenothiazine-3-one in Isopropyl Alcohol, Benzhydrol & Ethylene Glycol 747
K S Sidhu*, W R Bansal & Kamini Malhotra

Interaction of Anilines with 2,3-Dichloro-5,6-dicyano-*p*-benzoquinone: Spectroscopic & Kinetic Studies 753
P C Dwivedi*, (Mrs) Avanija Bansal & (Miss) Archana Srivastava

Reaction of Magnesium Silicide & Silicon Tetrachloride/Trichlorosilane in Presence of Hydrogen 756
I S Mulla, A C Choube, M K Dongare* & A P B Sinha

A Novel Synthetic Route for the Preparation of Ammonium & Alkali Metal Tetrafluoroborates & Alkyl Substituted Ammonium Tetrafluoroborates using Pyridinium Tetrafluoroborate as the Precursor 759
K Syed Mohamed & D K Padma*

Deprotonation Energetics of Disodium Adenosine Triphosphate in Water from EMF Measurements 764
Himansu Talukdar, Sibaprasad Rudra & Kiron K Kundu*

Thermodynamics of Electrolyte Solutions: Activity Coefficients of NaCl in NaCl + $MnCl_2$ + H_2O System at 25°C 768
Ch Venkateswarlu & J Ananthaswamy*

Effect of Solvent on Reactions of Coordination Complexes: Part 6—Kinetics of Solvolysis of *cis*-(Bromo)(2-aminothiazole)-bis(ethylenediamine)cobalt(III) in Acetone + Water Media 772
Anadi C Dash* & Jyotsnamayee Pradhan

Kinetic & Mechanistic Studies on Substitution Reaction of Aquo-ligands from *cis*-Diaquo-bis(biguanide)cobalt(III)/chromium(III) Ions in Aqueous Medium 778
Ashis Kumar Gangopadhyay & G S De*

Kinetics of Oxidation of Triethylenetetraamine by Hexacyanoferrate(III) 783
(Miss) Pratima Mishra & Prem C Nigam*

Kinetics & Mechanism of Oxidation of Semicarbazide by Chloramine-B, Bromamine-B & Dichloramine-B 786
B Thimme Gowda* & J Ishwara Bhat

Reactions of N-(2,4-Dinitrophenoxy)-9,10-dihydroanthracene-9,10-*endo*-α,β-succinimide with Hydroxide Ion, Piperidine, Cyclohexylamine & Morpholine: Evidence for Base Catalysis 790
Ranjumoni Saikia, Ashok Kumar Singh & Gurudas Bhattacharjee*

Continued overleaf

Notes

Anion Hydration & Hydrogen Isotope Effects in Dehydration of Chloride Form of Anion Exchange Resins 794
Deoki Nandan & A R Gupta*

Excess Molar Volumes of Binaries of Ethylbenzene with Chlorobenzene, Nitrobenzene, Aniline & Benzyl Alcohol 797
S K Chaudhari & S S Katti*

Apparent Molal Volumes & Compressibilities of Electrolytes in Aqueous & Aqueous Urea Solutions 799
K J Patil*, A B Wazalwar & G R Mehta

Mixed Ligand Complexes of Oxotitanium (IV) & Tin(IV) with Dihydrazones 803
G H Havanur, V K Revankar & V B Mahale*

Synthesis & Characterisation of Co(II), Ni(II), Cu(II), Zn(II), Cd(II), UO_2^{2+} & VO^{2+} Chelates of *o*-(N-α-Pyrrolidimino)propanoic Acid & *o*-(N-α-Pyrrolidimino)benzoic Acid 806
Santwana Gaur, S P Ranga, Shobha Sharma & R K Mehta*

Uranyl Nitrate Complexes of Some Schiff Bases Derived from Substituted Benzaldehydes & Amino Compounds 809
G Sobhana Devi & P Indrasenan*

Iron(III) Complexes of 2,4-Dihydroxybenzophenone Semicarbazone (DBPS) & Thiosemicarbazone (DBPT) & Determination of Iron(III) using DBPS & DBPT 812
K Hussain Reddy, K Giridhara Reddy & D Venkata Reddy*

Synthesis, Characterisation & Fungicidal Activity of the Complexes of N-Alkylphenothiazines with Titanium(IV) 815
B Keshavan* & J Seetharamappa

Interaction of Divalent Metal Ions with Uracil: Part IV—Mixed Ligand Complexes of Mn(II), Fe(II), Co(II), Ni(II) & Cu(II) with Uracil & Different Amines 819
Asit R Sarkar*, Parthasarathi Ghosh & Ranjit K Bandyopadhyay

Formation Constants of the Complexes of Some Bivalent Metal Ions with a New Tridentate Schiff Base, 7-Hydroxy-8-[(2-mercaptophenyl)iminomethyl]-4-methyl-2*H*-1-benzopyran-2-one 822
(Mrs) S V Kalavathi & K L Omprakash*, K Jagannadha Charyulu, A V Chandra Pal & M L N Reddy*

Differential Pulse Polarographic Determination of Proquazone 825
Aytekin Temizer*, Sedef Kir & A Nur Onar

Book Reviews

The Theory of Thermodynamics (Author: J R Waldram) 827
R C Srivastava

High Pressure Chemistry and Biochemistry (Editors: R Van Eldik & J Jones) 827
T R N Kutty

Authors for correspondence are indicated by (*)

Indian Journal of Chemistry
Vol. 27A, September 1988, pp. 747-752

Benzophenone-sensitized Photoreduction of N-Phenyl-*p*-benzoquinoneimine & Phenothiazine-3-one in Isopropyl Alcohol, Benzhydrol & Ethylene Glycol

K S SIDHU*, W R BANSAL & KAMINI MALHOTRA

Department of Chemistry, Punjabi University, Patiala 147 002

Received 16 *November* 1987; *revised and accepted* 1 *February* 1988

The results of the title ihvestigtion show that whereas N-phenyl-*p*-benzoquinoneimine (PBQ) and phenothiazine-3-one (PT) physically quench triplet benzophenone (^{3}BP) in competition with hydrogen abstraction by ^{3}BP from alcohols, these substrates also undergo quantitative reduction to corresponding phenols via the ketyl radicals involving chemical sensitization. The reduced product also quenches the sensitizer through electron transfer at rates comparble to quenching rates by the substrates. The quantum yield data have been rationalised and a reaction scheme consistent with the observations and in close agreement with the kinetic expressions has been presented and various rate constants evaluated. Bulk of evidence is in support of the reduction taking place through hydrogen atom transfer to the carbonyl oxygen rather than to the azomethine nitrogen in these quinoneimines.

The photochemistry of $>C=O$ (refs 1-3) and of $>C=N$ (refs 4-6) chromophores which are isoelectronic, has been studied in great depth. Among the various reactions, viz. addition[7,8], isomerization[9,10], rearrangement[11,13], cyclization[14,16] etc., the photoreduction[16,17] is mechanistically the most important one. The carbonyls undergo photoreduction[3] essentially from (n, pi*) state whereas the imines react from any one of the excited states. Furthermore, the electronically excited imines undergo rapid radiationless decay because of ready *E-Z* isomerism about the carbon-nitrogen double bond[17] and the quantum yield in these systems is much less.

The title compounds incorporate both $C=O$ and $C=N$ moieties in their molecular framework and hence it was considered worthwhile to investigate their sensitization via triplet benzophenone in order to have an insight into the mechanism of their photoreduction from the standpoint of the relative reactivity of the two groups and of any intramolecular physical and chemical processes between them.

Materials and Methods

Benzophenone (BP) (GR, Bush) was used as such. N-Phenyl-*p*-benzoquinoneimine (PBQ) was prepared by the method of Fetizon *et al.*[18] and was recrystallized from pet ether (60-80°C). Phenothiazine-3-one (PT) was prepared by the method of Bodea *et al.*[19] and was purified chromatographically over silica gel [benzene-methanol, 9:1 (v/v)]. Purity of both these compounds was further checked by TLC, melting points and spectral characteristics. All other reagents were purified by the known methods.

A medium pressure mercury lamp (125 watt, Gallenkemp, UK model LH-530) with a built-in filter having emission at 366 nm was used for irradiation. The radiation beam was collimated through blackened tube (diam 1.5 cm and length 4 cm). Absorption coefficients for PBQ, PT and BP in methanol at 366 nm were found to be 7.7×10^2, 1.3×10^4 and 70 M^{-1} cm^{-1} respectively. Concentration of BP with respect to quinoneimines was varied so as to ascertain a limit beyond which essentially all light was absorbed by BP and in subsequent experiments this concentration of BP was used.

A square quartz cell (1 cm × 1 cm × 4 cm) fitted with an air tight teflon stopper was used as the photolysis cell.

The system was deoxygenated by flushing purified nitrogen. Nitrogen (99%) was purified by passing it over freshly reduced finely divided copper deposited over kieselguhr (60-80 mesh) and kept at 200°C and subsequently through liquid nitrogen traps. Traces of water in nitrogen were removed by passing it through a column of activated silica gel. The purified nitrogen was presaturated with solvents. Freeze-pump thaw cycle technique was also employed for deaeration in some experiments. Freezing was done by liquid nitrogen and pumping with an all glass pumping system capable of attaining 10^{-6} torr pressure.

For product identification deoxygenated solutions of PBQ and PT ($\sim 10^{-2}$ mol dm^{-3}) in benzene containing BP (0.2 mol dm^{-3}) and IPA

(2 mol dm^{-3}) were irradiated at 366 nm till the colour of the solutions disappeared. Photolysed solutions were subjected to TLC on silica gel G plates under N_2 atmosphere using benzene as an irrigant. 3-Hydroxydiphenylamine (HDPA) and 3-hydroxyphenothiazine (HPT) were identified as the products of photoreduction of PBQ and PT respectively by direct comparison (co-TLC, UV) with authentic samples. Benzopinacol was detected in both the systems; however we failed to detect the presence of benzhydrol. The deoxygenated solutions of PBQ and PT ($\sim 10^{-4}$ mol dm^{-3}) containing BP (0.1 mol dm^{-3}) and IPA (1 mol dm^{-3}) on photolysis and subsequent oxidation by exposure of the product solutions to air gave quantitative recovery of the parent imines. This demonstrated that HDPA and HPT are the only products of PBQ and PT systems respectively.

Absorbance measurements on two pre-calibrated spectrophotometers (Hilger and Watts-H 700; Erma, model LS-7) gave identical results. Measurements were also made on an interference filter colorimeter (Erma, model AE-11). The interference filters were of the narrowest range and precautions were taken to have many closely spaced points in the calibration graph.

Potassium ferrioxalate actinometer was employed for measuring the intensity of absorbed light. Under conditions of complete absorption, $I_0 = 6.3 \times 10^{-7}$ einstein min^{-1} dm^{-3}. Under the conditions of incomplete absorption the intensity

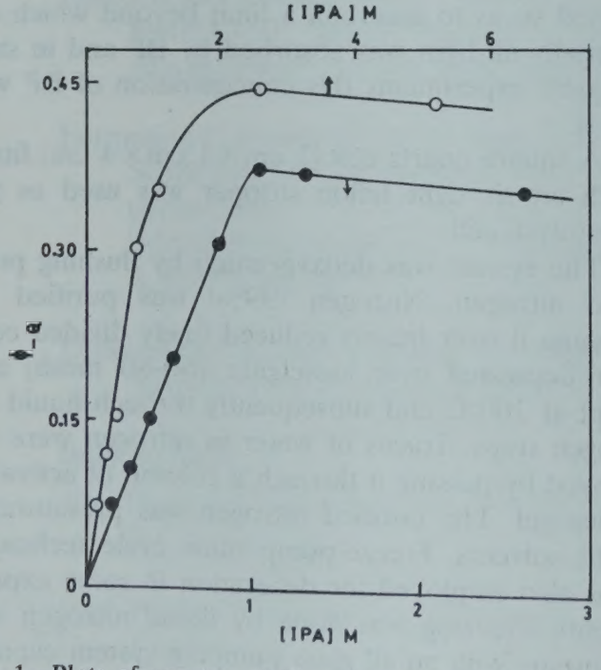

Fig. 1—Plots of quantum yield of disappearance of substrate (ϕ_{-Q}) versus concentration of hydrogen donors (a) For IPA; solvent = benzene; (−○−) is for $[PT]_0 = 2.3 \times 10^{-4}$ mol dm^{-1}, $[BP] = 0.2$ mol dm^{-1} and (−●−) is for $[PBQ]_0 = 1.9 \times 10^{-4}$ mol dm^{-3} $[BP] = 2.0 \times 10^{4}$ mol dm^{-3}

(I_a) was a complex function of the geometry of the photolysis cell. However, because of nearly parallel beam it was assumed here that I_a (total) = $I_0(1\text{-}10^{-\text{O.D. total}})$. I_a (total) was further aportioned to species in proportion to their optical densities (O.D's) at the wavelength of interest.

Results and Discussion

Photoreduction of PBQ and PT by direct absorption of light at 366 nm is accompanied by negligible quantum yields[20]. Triplet BP abstracts a hydrogen atom from alcohols to give ketyl radicals[1] and the abstraction rates, which are to some extent solvent-dependent, vary with the nature of alcohol. But the abstraction rates are far below the viscosity-controlled diffusion rates and accordingly for elucidation of the mechanism the quantum yields of the disappearance of the substrates were examined with IPA, benzhydrol and ethylene glycol as hydrogen donors and the results are given in Fig. 1. In each case the quantum yield increases linearly with increase in [alcohol] and reaches a plateau at higher [alcohol]; in the case of IPA the plateaus have negative slopes. In the case of PBQ the maximum quantum yields with IPA, benzhydrol and ethylene glycol are 0.37, 0.26 and 0.042 respectively (Since ethylene glycol is not miscible with benzene, the solvent in this case is acetonitrile). The rate of hydrogen abstraction in benzene is lower than in acetonitrile[21,22] and the lower quantum yields cannot be attributed to a change in the medium. In the case of PT the quantum yields with IPA and benzhydrol are 0.44 and 0.36 respectively. The rate of hydrogen abstraction from benzhydrol is higher than that from IPA by a factor of 3 to 10 (see ref. 1). The lowering of quantum yield with benzhydrol can be attributed to the difference in the ketyl radicals produced in the two systems (see Eqs 1 and 2).

$$^3BP \xrightarrow{Ph_2CHOH} 2Ph_2\dot{C}OH \quad \ldots (1)$$

$$^3BP \xrightarrow{(CH_3)_2CHOH} Ph_2\dot{C}OH + (CH_3)_2\dot{C}OH \quad \ldots (2)$$

It is reported that the diphenylcarbinol pair is initially produced within the solvent cage and it fails to couple measurably in the cage. After escape the radicals undergo a series of hydrogen atom exchange reactions before finally disappearing in a combination process to give benzopinacol[23]. The corresponding hydrogen atom transfer from dimethylcarbinol to BP (Eq. 3)

$$(CH_3)_2\dot{C}OH + BP \longrightarrow (CH_3)_2CO + Ph_2\dot{C}OH \ldots (3)$$

Table 1--Effect of Viscosity on Quantum Yield at Various [PBQ][a]

Ethylene glycol mol dm^{-3}	η (cp)	ϕ_{-PBQ}		
		[PBQ] = 8.7×10^{-5} mol dm^{-3} $I_a = 5.5 \times 10^{-7}$ (b)	[PBQ] = 1.8×10^{-4} mol dm^{-3} $I_a = 5.6 \times 10^{-7}$ (b)	[PBQ] = 2.4×10^{-4} mol dm^{-3} $I_a = 4.45 \times 10^{-7}$ (b)
0	0.34	—	0.180	0.084
0.89	0.40	—	0.177	—
1.79	0.46	0.315	0.171	0.075
2.69	0.54	—	0.170	—
3.58	0.66	0.240	0.249	0.075
4.48	0.80	—	0.360	—
5.40	0.98	0.441	0.480	0.33

(a) Solvent = CH_3CN; [IPA] = 1.3 mol dm^{-3}; [BP] = 0.02 mol dm^{-3}

(b) BP and PBQ both absorb at 366 nm. The reported absorbed intensities are for BP and have been corrected in terms of the net light absorbed and filter effect due to PBQ.

is known from very early studies. A recent CIDNP investigation has given the rate for this reaction = 2.75×10^8 M^{-1} s^{-1} (ref. 24). The diffusion limited rate in benzene = 1×10^{10} M^{-1} s^{-1} and a consideration of the concentrations of PBQ and PT in the systems show that the reaction (3) is favoured by at least a factor of 8 in PBQ and by a factor of 16 in PT over the reaction (4) which can be at the most be diffusion-controlled.

$$PBQ(\text{or } PT) + (CH_3)_2\dot{C}OH \rightarrow PB\dot{Q}H(\text{or } P\dot{T}H) + (CH_3)_2CO \quad \ldots (4)$$

This leads to the conclusion that although the differences in quantum yields with two alcohols in the case of PBQ and PT are of the right order as per this reasoning, the differences do not appear to result from the above. It is likely that hydrogen bonding from alcohols plays a role. The rate constant for reaction (3) infact, has a lower value in the medium used here.

The negative slopes at the plateaus show some inefficiency in the reactions at higher IPA concentrations. It may be noted that earlier workers have also observed higher rates of photoreduction in dilute alcohols[25]. The linear increase in the initial stages, as is evident from Fig. 1 is representative of the competition between reactions (5) and (6)

$$^3BP \xrightarrow{>C(H)OH} B\dot{P}H + > \dot{C}OH \quad \ldots (5)$$

$$^3BP \rightarrow BP \text{ (deactivation)} \quad \ldots (6)$$

The lower quantum yield in ethylene glycol cannot be ascribed to the effect of viscosity on hydrogen abstraction rate, which is lower than the diffusion rate in ethylene glycol (3×10^8 M^{-1} s^{-1}). The effect has to be due to the difference in the rates of hydrogen abstraction from ethylene glycol, as revealed by the results in Table 1.

The overall trend is that increase in viscosity increases the quantum yield, the increase being more marked at higher PBQ concentrations. The effect is thus due to the processes in which PBQ participates. The effect is unusual and mechanistically very significant. A detailed examination has thus been made at [PBQ] = 1.8×10^{-4} mol dm^{-3}. The quantum yield increases markedly beyond $\eta = 0.5$ cp, the initial linearity being due to some balancing effects. The results in the sequel go to show that PBQ and PT deactivate ^{3}BP, most likely in an exothermic energy transfer process. Such a process has to have a rate higher than 10^9 M^{-1} s^{-1} and an increase in viscosity certainly brings about a decrease in this rate. The decreased deactivation results in a net increase in the reduction.

In view of the observed features of these reactions and known properties of BP sensitizer, the processes which need to be considered are shown in Scheme 1. The rate constant, k_3 for the pseudo-unimolecular deactivation by the solvent varies with the solvent and = 7×10^6 s^{-1} (ref. 26) in benzene and = 1.5×10^5 s^{-1} (ref. 27) in IPA. 'Q' (PBQ or PT) has triplet states below ^{3}BP (ref. 20) and exothermic energy transfer is known to be diffusion-controlled[28], i.e. $k_5 \simeq$ diffusion rate. The excited singlet and triplet states of 'Q' cause no chemical reaction as shown by direct photolysis and naphthalene sensitization results[20]. The excited 'Q' therefore ends up in ground state 'Q' through deactivation. A steady state treatment for the rate of disappearance of 'Q' gives the rate expression (7)

$$\Phi_{-Q} = \frac{\alpha k_6[BPH_2]}{k_3 + k_4[BP] + k_5[Q] + k_6[BPH_2]} \quad \ldots (7)$$

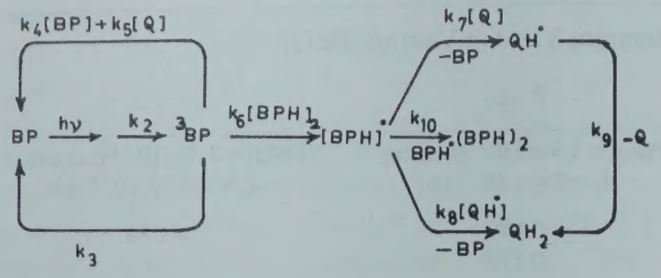

Scheme 1

In the derivation of Eq. (7) terms in which radical concentrations appear to have been neglected as compared to other concentration terms after giving due weightage to the respective rate constants. For example, the rate constant for the formation of benzopinacol (k_{10}) $= 3 \times 10$ M^{-1} s^{-1} (ref. 29) and when it is multiplied with [$\dot{B}PH$] the product has been taken to be negligible with respect to the sum of other terms. The coefficient, α, is a fraction of the reaction ending up in QH_2. The other fraction goes to benzopinacol. This coefficient is a function of [Q]. At [Q] = 0; $\alpha = 0$. With increase in [Q], α increases but only to a limiting value because of reaction (8)

$$\dot{Q}H + BP \rightarrow Q + B\dot{P}H \qquad \ldots (8)$$

It may be noted that the corresponding reaction with dimethylcarbinol radical has $k = 2.75 \times 10^8$ M^{-1} s^{-1} (ref. 24).

When [BPH_2] or [$(CH_3)_2C(H)OH$] is small the rate expression (7) reduces to Eq. (9)

$$\Phi_{-Q} = \frac{\alpha k_6[BPH_2]}{k_3 + k_4[BP] + k_5[Q]} \qquad \ldots (9)$$

At high [BPH_2]

$$\Phi_{-Q} = \alpha \qquad \ldots (10)$$

The linearity in the first part of the curves with intercepts = 0 in Fig. 1 is correctly predicted by Eq. (9). The near independence of the rate in [alcohol] is as per Eq. (10).

The rate expression (7) predicts Stern-Volmer type relationship (11) at constant [BP] and [BPH_2] for the deactivation of ^{3}BP by Q.

$$\frac{1}{\Phi_{-Q}} = \frac{1}{\alpha} + \frac{k_3}{\alpha k_6[BPH_2]} + \frac{k_4[BP]}{k_6[BPH_2]} + \frac{k_5[Q]}{k_6[BPH_2]} \qquad \ldots (11)$$

The plots of $1/\Phi_{-Q}$ versus [Q] show a very good fit of the data (see Fig. 2). The slopes give; $k_5/\alpha k_6[IPA] = 1.5 \times 10^3$ M^{-1} for PBQ and $k'_5/\alpha' k_6[IPA] = 1.0 \times 10^4$ M^{-1} for PT. Substituting the

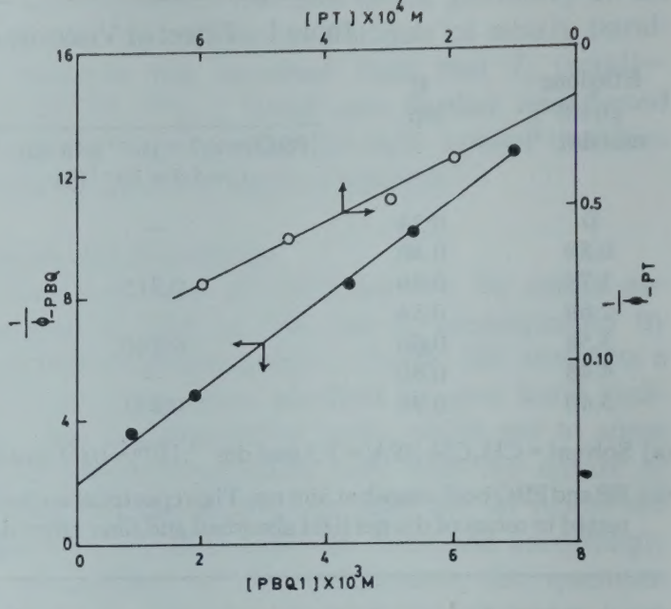

Fig. 2—Plot of $1/\phi_{-Q}$ versus [Q] (solvent = benzene, [BP] = 0.2 mol dm^{-3} (−●−), [IPA] = 1.3 and 2.6 mol dm^{-3} (−○−).

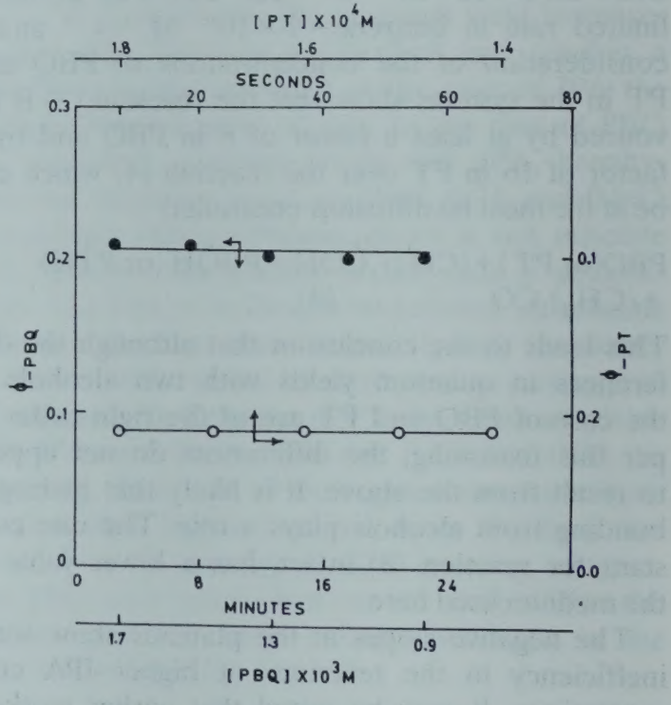

Fig. 3—Plot of ϕ_{-Q} versus time of irradiation (solvent = benzene, [BP] = 0.2 mol dm^{-3} (−●−); [IPA] = 1.3 and 2.6 mol dm^{-3} (−○−).

values of α's and [IPA]'s (cf. Fig. 3), gives $k_5/k_6 = 7.2 \times 10^2$ and $k'_5/k'_6 = 1.1 \times 10^4$; $k_6 = 1.0 \times 10^6$ M^{-1} s^{-1} and this gives $k_5 = 7.2 \times 10^8$ and $k'_5 = 1.1 \times 10^{10}$ M^{-1} s^{-1}. These values are of the right order of magnitude for such deactivation processes.

In the evaluation of quantum yields from the disappearance of the substrates, only those values which were below 10% conversion of the substrate were taken into consideration. However, the results at larger conversions are unusual. Inspite of the fact that the substrate disappears from the

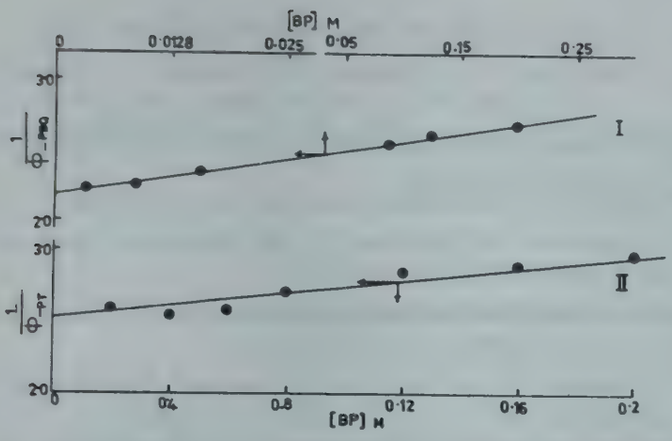

Fig. 4—Plots of $1/\phi_{-Q}$ versus [BP] (solvent = benzene; and [IPA] = 1.3 mol dm^{-3}; curve I for $[PBQ]_0 = 1.9 \times 10^{-4}$ mol dm^{-3} and curve II for $[PT]_0 = 2.2 \times 10^{-4}$ mol dm^{-3}).

reaction the quantum yields do not change much (Fig. 3). It was felt that the product itself may be quenching the reaction. This was actually found to be so. It is observed that HDPA at a concentration of 5.2×10^{-4} mol dm^{-3} quenches the reaction by a factor of 2.5. There is no filter effect and it has to be due to quenching of ^{3}BP. This quenching is likely to be through an electron transfer process as observed in the case of amines[30]. The quantum yields in the photoreduction, thus, remain unchanged because the quenching by substrate was replaced by quenching by the product in equimolar quantities. It may be noted that all such quenching reactions have comparable rates.

Equation (11) also predicts a linear relationship between $1/\phi_{-Q}$ versus [BP] at constant [Q] and [BPH_2]. Plots of this relationship are given in Fig. 4. The results are in very good agreement with the proposed mechanism. The slopes give $k_4/k_6 = 1.2$ and 1.3 for PBQ and PT respectively. Substituting the value of $k_6 = 1.0 \times 10^6$ $M^{-1}s^{-1}$ the average value of $k_4 = 1.3 \times 10^6$ $M^{-1}s^{-1}$. In benzene an excimer formation between the excited state and ground state molecules of BP (see Eq. 12) has been proposed and rate constant $= 1.6 \times 10^5$ $M^{-1}s^{-1}$ evaluated for the deactivation process[31].

$$^3BP + BP \rightarrow \text{excimer} \rightarrow 2BP \qquad \ldots(12)$$

The other available values for this deactivation are 3×10^3 $M^{-1}s^{-1}$ in benzene[32] and $8 \times 10^5 M^{-1}s^{-1}$ in acetonitrile[33]. The present value is somewhat higher but if the difference between the values in benzene and acetonitrile is considered, it is apparent that this value is solvent-dependent. In the present system alcohols have been used and the benzophenone in the ground state is hydrogen bonded. This bonding is lost in the *n*, pi* transition and therefore the deactivation here is through the process (13)

$$^3BP + BP \ldots HOR \rightarrow BP \ldots HOR + BP \qquad \ldots(13)$$

This can have a higher rate than the process in which uncomplexed BP is involved.

Reaction in which QḢ is formed deserves further consideration (Scheme 1). There are two atoms, oxygen and nitrogen, in each quinoneimine molecule and any one can be the site for abstraction. The resulting radicals from the two abstractions are of course very different (see Scheme 2). Though in molecules containing only carbonyl and azomethine[17] groups alone reactions (14) and (15) respectively take place in the case of quinoneimines competition can be envisaged between reactions (14) and (15). This competition should be very much in favour of reaction (15) because:

(a) Oxygen is more electronegative. It is to be noted that hydrogen abstraction apparently takes place through electron transfer followed by proton transfer.

(b) O − H bond (463 kJ mol^{-1}) is stronger than N − H bond (388 kJ mol^{-1}).

(c) Radical resulting from reaction (14) is stabler than that from reaction (15) because of the difference in the resonance stabilization energy of the two radicals as apparent from the possible structures for the two radicals. It is thus postulated that the final product arises from the ketyl radicals formed in reaction (15).

It is apparent that quinoneimines are reduced in the present systems through chemical sensitization and are unique because of their concomitantly quenching the sensitizer through physical interaction. The photoreduced product also quenches the sensitizer which makes them much more interesting and mechanistically revealing.

References

1 Turro N J, *Modern molecular photochemistry*, (The Benjamin/Commings Publishers, California), 1978.
2 Kan R O, *Organic photochemistry*, (W.A. Benjamin, New York) (1965) Chapter 6.
3 Neckers D C, *Mechanistic organic photochemistry*, (Rheinhold publishing Corp, New York) (1967).
4 Fischer M, *Chem Ber*, **100** (1967) 3599.
5 Toshima N, Asao S, Takada K & Hirai H, *Terahedron Lett*, (1970) 5123.
6 Padwa A & Koehn W P, *J org Chem*, **40** (1975) 1896.
7 Searles S & Clasen R A, *Tetrahron Lett*, (1967) 3913.
8 Dorsheln W, Tiefenthaler H, Groth H, Cerutti P & Schmid H, *Helv Chim Acta*, **50** (1967) 1759.
9 Wettermark G & Doglioth, *J chem Phys*, **40** (1964) 1486.
10 Nelson D A, *Chem Comm*, (1968) 377.
11 Beak P & Miesel J L, *J Am chem Soc*, **89** (1967) 2375.
12 Tiefenthaler H, Dorscheln W, Goth H & Schmid H, *Tetrahedron Lett*, (1964) 2999.

13 Lahmani F & Ivanhoff N, *Tetrahedron Lett* (1967) 3913.
14 Cave M P & Schlessinger R H, *Tetrahedron Lett*, (1964) 2109.
15 Badjer G M, Joshna C P & Lewis G E, *Tetrahedron*, (1964) 3811.
16 Grellman K H & Tauer E, *Tetrahedron Lett*, (1967) 1909.
17 Padwa A, Dharan M, Smolanoff J & Wetmore S I, *Pure appl Chem*, **33** (1973) 269.
18 Fetizon M, Balogh V & Golfier M, *J org Chem*, **36** (1971) 1339.
19 Bodea C & Raileanu M, *Chem Abs*, **58** (1963) 3420b.
20 Unpublished results from this laboratory.
21 Berger M, Camp R N, Demetrescu I, Giering L & Steel C, *Isr J Chem*, **16** (1977) 311.
22 Seaiano J C, *J Photochem*, **2** (1984) 81.
23 Schuster D I & Karp P B, *J Photochem*, **12** (1980) 333.
24 Den Hollander J A, Hartel A J & Schippers P H, *Tetrahedron*, **33** (1977) 211.
25 Henne A & Fischer H, *Helv Chim Acta*, **58** (1975) 1598.
26 Bartholomew R F, Davidson R S, Lambeth P F, Mekeller J F & Turner P N, *J chem Soc Perkin II*, (1972) 577.
27 Thielen J V, The in T V & Schryver F C, *Tetrahedron Lett*, (1971) 3031.
28 Porter G & Wilkinson F, *Proc Royal Soc*, (1966) 264A.
29 Yoshida H & Warashina T, *Bull chem Soc Japan*, **44** (1971) 2950.
30 Davidson R S, Lambeth P F & Santhanam M, *J chem Soc Perkin Trans II* (1972) 2351.
31 Schuster D I & Weil J M, *J Am chem Soc*, **95** (1973) 4091.
32 Giering L, Berger M & Steel C, *J Am chem Soc*, **91** (1969) 5390.
33 Schuster D E, Weil T M & Halpern A M, *J Am chem Soc*, **94** (1972) 8248.

Indian Journal of Chemistry
Vol. 27A, September 1988, pp 753-755

Interaction of Anilines with 2,3-Dichloro-5,6-dicyano-*p*-benzoquinone: Spectroscopic & Kinetic Studies

P C DWIVEDI*, (Mrs) AVANIJA BANSAL† & (Miss) ARCHANA SRIVASTAVA
Department of Chemistry, Harcourt Butler Technological Institute, Kanpur 208 002

Received 21 *September* 1987; *revised* 15 *December* 1987; *accepted* 29 *December* 1987

Interaction of aniline, and *o*-, *m*- and *p*-toluidines with 2,3-dichloro-5,6-dicyano-*p*-benzoquinone (DDQ) has been studied spectrophotometrically. The blue coloured solutions obtained by mixing anilines and DDQ solution instantaneously change into green (λ_{max}, 540 nm) and finally become yellow (λ_{max}, 350 nm) in all the solvents studied. Pseudo-first order rate constants have been evaluated at both 540 nm and 350 nm. Possible participation of electron donor-acceptor complexes between anilines and DDQ in the reaction is indicated.

Aromatic amines are known to act as electron donors and form electron donor-acceptor (EDA) complexes with a number of electron acceptors[1,2]. Some aromatic amines are reported to undergo chemical reaction with strong electron acceptors through EDA complexes[3-5]. Nagakura and coworkers[6] studied the interaction of aniline with chloranil (CA) and the formation of product was rationalised via EDA and σ-complexes as intermediates. 2,3-Dichloro-5,6-dicyano-*p*-benzoquinone (DDQ) is a much stronger electron acceptor than structurally similar CA[7]. The electron acceptor strength of DDQ is comparable to that of tetracyanoethylene (TCNE)[8]. Therefore, it is expected to undergo chemical reactions with a variety of electron donors. Murlikrishna and coworkers[9] studied EDA interaction between piperidines and DDQ and reported the formation of mono- and disubstituted products via a substitution reaction. We have recently investigated the interaction of aza-aromatics with DDQ[10] wherein the occurrence of a reaction through EDA complex was proposed. However, systematic studies on the interaction of anilines with DDQ have not been reported so far. It was, therefore, worthwhile to undertake spectroscopic and kinetic investigations on the interaction of aniline and *o*-, *m*- and *p*-toluidines with DDQ.

Materials and Methods

All the anilines were commercial products and were purified before use. Chloroform (BDH, AR) and dichloromethane (E. Merck, LR) were dried and distilled before use. DDQ was purified by recrystallising several times from chloroform.

Electronic absorption spectra were measured on a Beckman-DU spectrophotometer fitted with variable temperature cell compartment using matched silica cells of 1 cm pathlength. Freshly prepared stock solutions were used for measurements. Pseudo-first order rate constants (k) (in the presence of a large excess of donor) at 540 nm and 350 nm were evaluated employing Eqs (1) and (2), respectively.

$$k = \frac{2.303}{t} \log \frac{D_0}{D_t} \qquad \ldots (1)$$

$$k = \frac{2.303}{t} \log \frac{D_\infty - D_0}{D_\infty - D_t} \qquad \ldots (2)$$

Here D_0, D_t and D_∞ are the absorbances measured immediately after mixing aniline with DDQ, after time t and at the end of the reaction, respectively. Some typical plots employed for these calculations are shown in Fig. 1. The energies of activation were evaluated by measuring the temperature dependence of k in the range 288-310 K.

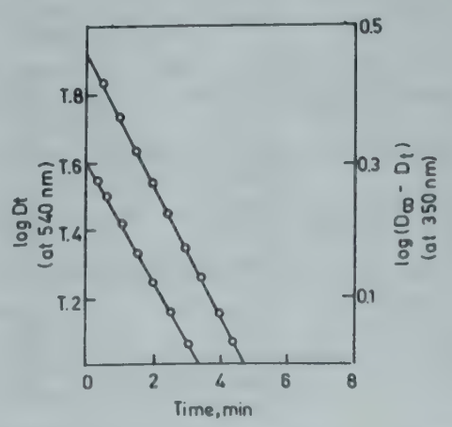

Fig. 1—Pseudo-first order rate plots for the aniline + DDQ system in $CHCl_3$ solution at 298 K [(1) at 540 nm and (2) at 350 nm]

†Analytical Service Lab Group, R and D Centre for Iron and Steel, Steel Authority of India Ltd, Ranchi

Results and Discussion

Absorption spectra

Anilines on mixing with DDQ produce blue coloured solutions which instantaneously change into green (λ_{max}, 540 nm) and finally become yellow (λ_{max}, 350 nm) in all the solvents studied. As the blue solution turned green before spectral measurements, its absorption could not be measured. The blue colour may be attributed to the formation of EDA complexes between anilines and DDQ which are unstable under the experimental conditions. It may be mentioned here that aniline forms a stable EDA complex with CA[6] below 200 K but on raising temperature aniline reacts with CA to give 2,5-dichloro-3,6-dianilino-*p*-benzoquinone as the reaction product. It is, thus, possible that the EDA complexes formed between anilines and DDQ (which is more reactive than CA) are unstable in the temperature range 288-310 K. The intensity of the 540 nm band decreases with time whereas that of the 350 nm band continues to increase until the end of the reaction as evidenced by Fig. 2. This shows that the 350 nm band is due to the final reaction product. On analogy with the reaction of CA with aniline[6], we may expect the final product to be 2-chloro-5-cyano-3,6-dianilino-*p*-benzoquinone. This is supported by the elemental analyses of the product. The 540 nm band may be assigned to a monosubstituted product (either 2,3-dichloro-5-cyano-6-anilino-*p*-benzoquinone or 2-chloro-5,6-dicyano-3-anilino-*p*-benzoquinone). The monosubstituted product, however, could not be isolated.

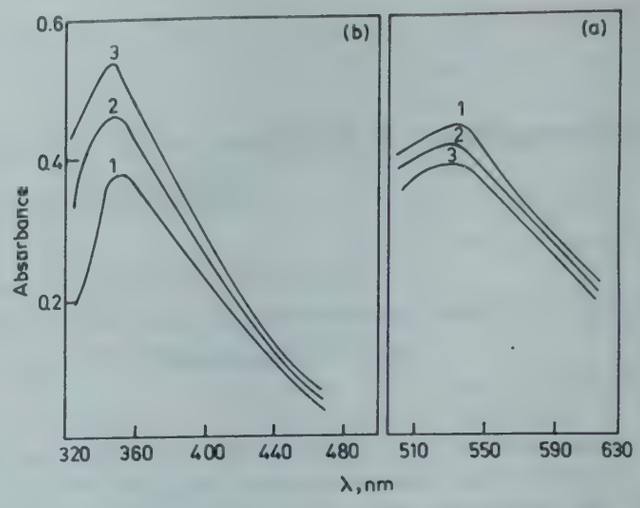

Fig. 2—Time dependent absorption spectra of aniline + DDQ system in $CHCl_3$ ([Aniline] = 0.15 mol dm^{-3} and [DDQ] = 1.0×10^{-3} mol dm^{-3} for curve − a and [Aniline] = 0.018 mol dm^{-3} and [DDQ] = 1.2×10^{-4} mol dm^{-3} for curve-b; (1) fresh solution; 2 and 3, after 5 and 10 min respectively)

Kinetic data

To explore the possibility of the EDA complexes as the reaction intermediates in the reactions of DDQ with anilines, we have carried out the kinetic measurements on these systems. Pseudo-first order rate constants (k) were obtained spectrophotometrically at 540 and 350 nm. The k values increase with increase in donor strength of anilines and follow the order: *p*-toluidine > *o*-toluidine > *m*-toluidine > aniline. The donor strength of these compounds, as judged from their ionization potentials (Table 1) also follows the same order. The E_a values (Table 1) decrease as k increases. These k and E_a values seem to suggest

Table 1—Kinetic Data on the Interaction of Anilines with DDQ at 298 K

Electron donor	Ip (ev)	Solvent	Dielectric constant	At 540 nm			At 350 nm		
				k^a (min^{-1})	E_a (kJ mol^{-1})	$\Delta S\dagger$ (JK^{-1} mol^{-1})	k^a (min^{-1})	E_a (kJ mol^{-1})	$\Delta S\dagger$ (JK^{-1} mol^{-1})
Aniline	7.70	$CHCl_3$	4.5	0.414	13	−242	0.184	34	−180
		$CHCl_3 + CH_2Cl_2$ (1:1)	6.6	0.438	10	−251	0.218	23	−215
		CH_2Cl_2	9.1	0.484	8	−258	0.253	17	−234
m-Toluidine	7.66	$CHCl_3$	4.5	0.495	10	−251	0.219	25	−188
		$CHCl_3 + CH_2Cl_2$ (1:1)	6.6	0.529	8	−258	0.242	18	−229
		CH_2Cl_2	9.1	0.576	6	−264	0.276	13	−247
o-Toluidine	7.62	$CHCl_3$	4.5	0.541	8	−252	0.253	19	−226
		$CHCl_3 + CH_2Cl_2$ (1:1)	6.6	0.587	6	−262	0.276	14	−242
		CH_2Cl_2	9.1	0.633	5	−267	0.311	10	−254
p-Toluidine	7.48	$CHCl_3$	4.5	0.587	7	−256	0.299	14	−241
		$CHCl_3 + CH_2Cl_2$ (1:1)	6.6	0.600	5	−265	0.345	10	−255
		CH_2Cl_2	9.1	0.668	4	−270	0.369	7	−263

(a) Uncertainty in k values is less than ± 1%

that the reactions proceed through the initial formation of EDA complexes in all the systems investigated.

Further, the k values increase and E_a values decrease with increase in solvent polarity. The rate constants at 540 nm are larger (and E_a smaller) than those at the 350 nm, indicating the existence of an intermediate in the transformation of the monosubstituted product to the disubstituted product of the reaction. In the absence of an intermediate, the two rate constants are found to be equal in the reactions of the EDA complexes[11,12]. Nagakura and coworkers[6] considered reactions (3) and (4) in the interaction of aniline with CA:

$$D + A \rightleftarrows \text{EDA complex} \rightarrow \text{Product} \quad \ldots (3)$$

$$D + A \rightleftarrows \text{EDA complex} \rightarrow \text{Intermediate} \rightarrow \text{Product} \quad \ldots (4)$$

The plots of concentration of the product ([P]) (calculated by solving the rate equations) versus time (t) in the initial stage of reaction (4) were quadratic in nature and closely resembled the experimental [P] versus t plots. This was taken as an evidence for the existence of an intermediate in the reaction of aniline with CA. In the present investigation, the plots of experimental [P] (measured in terms of the absorbance of the product) versus t exhibit initial quadratic behaviour (see Fig. 3). This observation provides further support to the existence of the intermediate in the transformation of the monosubstituted product to the disubstituted product.

The reaction of DDQ with anilines may, therefore, be rationalised as shown in Scheme 1:

$$\text{Aniline} + \text{DDQ} \overset{\text{very fast}}{\rightleftarrows} \underset{\text{(blue solution)}}{\text{EDA complex}} \overset{\text{fast}}{\rightarrow} \text{mono-substituted-product} \underset{\text{(step I)}}{\overset{\text{slow}}{\longrightarrow}} \text{Intermediate}$$

(green solution, λ_{max}, 540 nm)

(step II) ↓ Fast

disubstituted product

(yellow solution λ_{max}, 350 nm)

Scheme 1

The $\Delta S^{\ddagger}$ values for the transformation of the monosubstituted product to the intermediate (step-I) are larger and negative than those for the transformation of the intermediate to the final disubstituted product (step-II), the magnitude being higher in more polar solvents. This indicates that the transition state in step-I is more polar than the initial state (which is likely to be the monosubstituted product) and also that the transition state in step-II differs in polarity from the initial state (the intermediate).

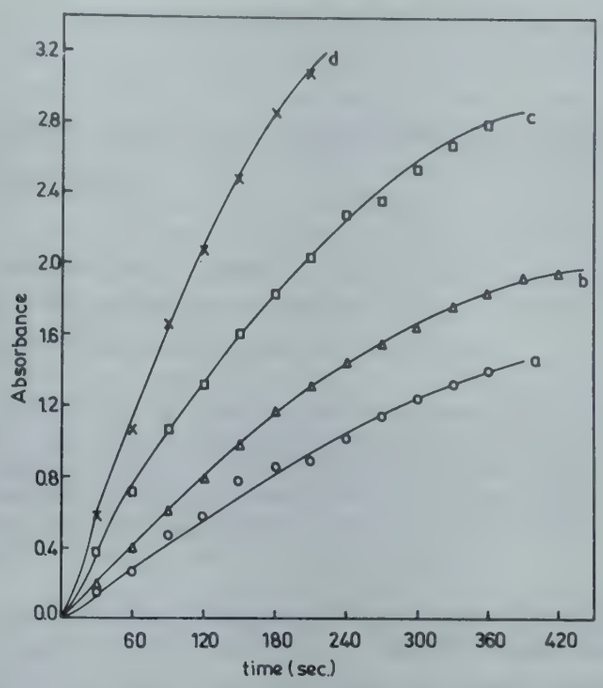

Fig. 3—Time versus absorbance plots for product formation at 288K in $CHCl_3$ ([Amine] = 2.0×10^{-2} mol dm^{-3} and [DDQ] = 1.0×10^{-4} mol dm^{-3}; curves a, b, c and d for aniline, *m*-toluidine, *o*-toluidine and *p*-toluidine, respectively)

References

1 Zweig A, Lancasten J E, Neglia M T & Jura W H, *J Am chem Soc*, **86** (1964) 4130.

2 Iwata S, Tanaka J & Nagakura S, *J Am chem Soc*, **88** (1966) 894.

3 Liptay W & Tamberg N, *Z Elektrochem*, **66** (1962) 59.

4 Eastman J W, Engelsma G & Calvin M, *J Am chem Soc*, **84** (1962) 1339.

5 Rappoport Z, *J chem Soc*, (1963) 4498.

6 Nogami T, Yoshihara K, Hosoya H & Nagakura S, *J phys Chem*, **73** (1969) 2670.

7 Srivastava R D & Prasad G, *Bull chem Soc Japan*, **43** (1970) 1611.

8 Hammond P R, *J chem Soc*, (1963) 3113.

9 Murlikrishna U & Krishnamurthy M, *Indian J Chem*, **25A** (1986) 949.

10 Dwivedi P C, Bansal A, Banga A K & Srivastava A, *Indian J Chem*, **26A** (1987) 389.

11 Lautenberger W J & Miller J G, *J phys Chem*, **74** (1970) 2722.

12 Dwivedi P C & Banga A K, *J phys Chem*, **85** (1981) 1768.

13 Yamaoka T & Nagakura S, *Bull chem Soc Japan*, **43** (1970) 355.

14 Nogami T, Yamaoka T, Yoshihara K & Nagakura S, *Bull chem Soc Japan*, **44** (1971) 380.

Indian Journal of Chemistry
Vol. 27A, September 1988, pp. 756-758

Reaction of Magnesium Silicide & Silicon Tetrachloride/Trichlorosilane in Presence of Hydrogen†

I S MULLA, A C CHOUBE, M K DONGARE* & A P B SINHA
Physical Chemistry Division, National Chemical Laboratory, Pune 411 008

Received 3 *December* 1987; *revised and accepted* 12 *February* 1988

The formation of silane (SiH_4) has been observed during the reaction of silicon tetrachoride and hydrogen ($SiCl_4 + H_2$) with magnesium silicide (Mg_2Si) at 400-500°C. The silane formed decomposes to give silicon in the vicinity of Mg_2Si charge. A mixture of trichlorosilane + H_2 reacts with Mg_2Si at 250°C to afford silane which has been separated and decomposed to high purity silicon. The reaction of $SiHCl_3 + H_2$ with Mg_2Si gives optimum conversion when $SiHCl_3$:H_2 ratio is 1:4 at the reaction temperature of 250°C.

A major proportion of high purity silicon used in semiconductor industry is produced by the Siemen's process[1] which involves chemical vapour deposition of trichlorosilane (TCS) onto hot silicon filament. However, the process has some basic disadvantages such as low conversion efficiency of TCS to Si, high energy requirements in the process and problems associated with separation and recycling of byproduct silicon tetrachloride (STC).

Recently SiH_4 (silane) as well as dichlorosilane (DCS), SiH_2Cl_2, have been tried[2] for the production of silicon on pilot plant scale. The advantage of using silane is that its boiling point is lower than that of TCS and it is easier to purify it to a higher level than any other chlorosilane. Union Carbide Corporation[3] has developed a process for the preparation of SiH_4 by hydrogenation of $SiCl_4$ under high pressure and by successive disproportionation of intermediate chlorosilanes to SiH_4.

Silane can also be generated by the reaction of Mg_2Si and NH_4Br at low temperature[4]. We have tried to prepare SiH_4 by hydrogenation of $SiCl_4$ (STC) as well as $SiHCl_3$ (TCS), using various hydrogenating catalysts. It has been observed by us that in the presence of Mg_2Si and H_2, TCS and STC can be converted into silane. The reaction of Mg_2Si, STC and TCS was studied in detail and the results are given in this paper.

Materials and Methods

The experimental set-up for the preparation of silane is shown in Fig. 1. A mixture of Mg powder (AR) and silicon (metallurgical grade) in the weight ratio of 64:36 (50 g) was heated in a previously weighed quartz tubular reactor (B) for 6 hr under H_2 atmosphere at 480-500°C. This treatment was found to be adequate to form Mg_2Si, as confirmed by X-ray diffraction. The temperature of the reactor tube was then reduced to the desired reaction temperature (250-500°C) and a mixture of H_2 and STC (300 g) was passed through it. The ratio of H_2/STC was maintained by (i) adjusting the bath temperature

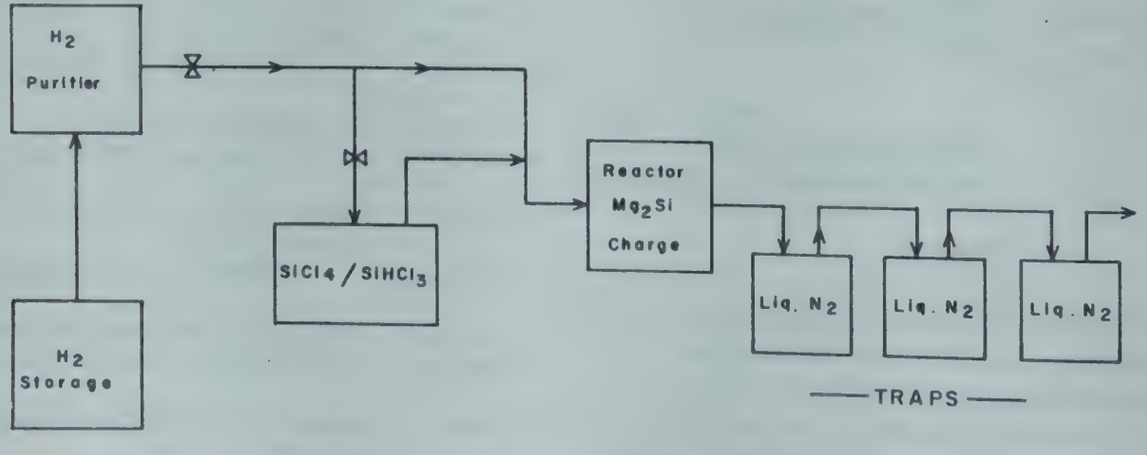

Fig. 1—Schematic diagram of experimental set-up

†NCI Communication No. 4348.

of STC and (ii) the quantity of H_2 bubbled through STC.

The condensable portion of the exit gas was condensed using three liquid nitrogen traps successively. The condensed portion was first scrubbed through distilled deionized water to hydrolyse any chlorosilane which had escaped condensation and finally through silver nitrate solution to estimate silane, as silane reacts quantitatively with $AgNO_3$, reducing it to metallic silver and giving free silicon[5]. The condensed gases were analysed by gas chromatography.

On completion of the experiment the reactor tube was cooled to room temperature and was weighed immediately to minimise any absorption of moisture. The powder was boiled with distilled deionized water to dissolve $MgCl_2$. The Mg and Cl in solution were estimated quantitatively. The unreacted Mg_2Si was decomposed by AR HCl (1:1) and Mg was again estimated quantitatively from the $MgCl_2$ solution. The silica was removed by reacting the residue with HF and subsequent evaporation in a platinum crucible and finally free silicon was weighed. The purity of Si was determined spectrographically.

The temperature of reactor was varied from 300 to 500°C and the effect of temperature on the efficiency of reduction ($SiCl_4$ to Si) was studied. Ratio of $H_2/SiCl_4$ was also varied at each temperature.

In another set of experiments, Mg_2Si was prepared as above, STC was passed over it in the absence of H_2. Here, pure N_2 was used as the carrier gas. In this case also the analytical processes were repeated as narrated above.

Results and Discussion

On cooling the reactor at the end of the experiment it was observed that a mirror like silicon deposition had occurred on the walls of the reactor tube away from the original Mg_2Si which was indicative of the formation of a volatile compound of silicon presumably SiH_4. The reactor tube was weighed immediately and the increase in weight was noted. $MgCl_2$ and unreacted Mg_2Si were removed as described earlier and finally free silicon was weighed. The reaction was poor below 400°C. At 500°C the amount of Mg_2Si remaining unreacted was less than 2%. STC and H_2 were kept in excess. The entire unreacted STC was collected in the traps.

The formation of silane, TCS, SiH_2Cl_2(DCS), SiH_3Cl(MCS) is confirmed in all experiments by gas chromatographic analysis using Perkin-Elmer (Sigma 3B) gas chromatograph and Sigma 15 data station. An SE-52 column (length = 12 inches; int. diam. = 1/8 inch) was used for the analysis.

The various probable primary and secondary reactions alongwith thermodynamic parameters are listed in Table 1.

Amongst the various reactions given in Table 1, reaction (i) is thermodynamically highly favourable, still it does not appear to be occurring when the reaction is carried out in the absence of H_2 using N_2 as carrier gas. Neither mirror-like deposition on the walls of reactor tube nor formation of $MgCl_2$ was detected hence reaction is considered to take place as per Eq. (ii) or Eq. (iii) (see Table 1). The formations of TCS, DCS, MCS are due to the secondary reactions[7] (iv) and (v) (Table 1) which are also thermodynamically favourable.

Mg_2Si contains small amounts of Mg and MgO as revealed by the X-ray diffraction pattern of Mg_2Si, Mg, $MgO.Mg_2Si$ is used for hydrogen storage[8-10] and its adsorption-desorption property has been studied. The Mg:MgO and Mg_2Si adsorb hydrogen used for hydrogenation, the molecular hydrogen dissociates and reacts with STC (see reactions viviii) leading to reaction (iii) (Table 1).

Table 1—Probable Primary Reactions and Thermodynamic Parameters*

Probable reaction	ΔF (kcal mol^{-1}) (800 K)	ΔF (kcal mol^{-1}) (600 K)	ΔH (kcal mol^{-1}) (300 K)
Primary reactions			
(i) $Mg_2Si + SiCl_4 = 2\ MgCl_2 + 2\ Si$	−92	−97	−114.28
(ii) $Mg_2Si + SiCl_4 + 2\ H_2 = 2\ MgCl_2 + Si + SiH_4$	−71	−74	−106.95
(iii) $Mg_2Si + SiCl_4 + 4H_2 = 2\ MgCl_2 + 2\ SiH_4$	−47	−56	−99.65
Secondary reactions			
(iv) $SiH_4 + SiCl_4 = SiHCl_3 + SiH_3Cl$	−16.08	−14.85	−17.90
(v) $SiCl_4 + SiH_4 = 2\ SiH_2Cl_2$	−7.74	−6.06	−10.30

*Free energy changes (ΔF) and heat of formation (ΔH) are calculated from thermodynamic values given in Janaf Thermochemical Table[6].

$$2\ Mg_2Si + H_2 \rightarrow 2\ Mg_2Si(-H)^* \quad \ldots(vi)$$

$$8\ Mg_2Si - H + SiCl_4 \rightarrow 8\ Mg_2Si + SiH_4 + 4\ HCl \quad \ldots(vii)$$

$$Mg_2Si + 4\ HCl \rightarrow 2\ MgCl_2 + SiH_4 \quad \ldots(viii)$$

The HCl formed in the reaction (viii) reacts with Mg_2Si leading to the formation of silane which is one of the conventional methods for preparation of silane from Mg_2Si (see ref. 9).

From these observations it can be inferred that silane is formed during the hydrogenation of STC in the presence of Mg_2Si, which further decomposes to Si at the reaction temperature 500°C.

Experiments on the same lines were carried out to study the hydrogenation of trichlorosilane (TCS) using Mg_2Si and hydrogen. For this purpose a mixture of TCS and H in the molar ratio of 1:4 was preheated at 500°C and then passed over the Mg_2Si charge which was heated upto 220°C. A cracking sound was heard at 220°C which increased in its magnitude with increase in temperature upto 250°C. The reaction was carried out for 4 hr and the effluent gases were condensed in the liquid nitrogen traps and gases were analysed by the online gas chromatograph. The analysis showed presence of silane, lower chlorosilanes and unreacted TCS, STC and hydrochloric acid.

After completion of the reaction, the Mg_2Si charge was cooled to room temperature under H_2 atmosphere. A thin layer of shining silicon was deposited on the inner wall of the reactor in the vicinity of Mg_2Si, with marginal increase in the weight of the charge.

In another experiment the effluent gases of $SiHCl_3$ and H_2 reaction in the presence of Mg_2Si were passed through a separate silica tube reactor heated at 500°C. After completion of the reaction the reactor tube was cooled to room temperature under H_2 atmosphere. It was found that a thick coating of silicon was deposited in the separate tube. This is a clear indication of formation of silane in the hydrogenation of TCS in the presence of Mg_2Si at 250°C, which further decomposes to Si at 500°C in the second reactor.

There was a marginal increase in the weight of Mg_2Si charge after the reaction. The molecular hydrogen passing over hot Mg_2Si gets converted (dissociated) into atomic hydrogen which in turn reduces TCS to silane. The plausible chemical reactions can be written as follows:

$$Mg_2Si + 2\ SiHCl_3 + 6\ H_2 \rightarrow 2\ MgCl_2 + 3\ SiH_4 + 2\ HCl \quad \ldots(ix)$$

$$3\ Mg_2Si + 4\ SiHCl_3 + 12\ H_2 \rightarrow 6\ MgCl_2 + 7\ SiH_4 \quad \ldots(x)$$

The formation of silane from TCS and STC by hydrogenation in the presence of Mg_2Si is an interesting reaction and needs further investigation for its commercial exploitation.

References

1 Runnyan W R, *Silicon semiconductor technology* (McGraw-Hill, New York), 1965.

2 *Union Carbide Corporation Final Report DOE/JPL.* Contract No. 954334 pp. 210 (DOE Technical Information Centre, Springfield VA), 1979.

3 Iya,Sridhar K, *J Cryst Growth*, **75** (1986) 88.

4 Johnson W C & Hogness J R, *J Am chem Soc*, **56** (1934) 1252.

5 Ellis H R & Weston F E, *Trans Faraday Soc*, **6** (1910) 152.

6 Janaf Thermochemical Table, Aug. 1965.

7 Clasen H, *Angew Chem*, **70** (1958) 179-80.

8 Ono S, Ishido Y, Imanari K & Tabata T, *J less common Materials*, **88** (1982) 57.

9 Guinet P, Halotier D & Perround P, *Comm Eur Communities [Rep] EUR*, 1977, EUR, 6170.

10 Guinet P, Halotier D & Perround P, *Comm Eur Communities [Rep] EUR*, 1978, *EUR* 6085.

*Represents H atom adsorbed (formed by dissociation of H_2) on Mg_2Si surface.

Indian Journal of Chemistry
Vol. 27A, September 1988, pp. 759-763

A Novel Synthetic Route for the Preparation of Ammonium & Alkali Metal Tetrafluoroborates & Alkyl Substituted Ammonium Tetrafluoroborates using Pyridinium Tetrafluoroborate as the Precursor

K SYED MOHAMED† & D K PADMA*
Department of Inorganic and Physical Chemistry, Indian Institute of Science, Bangalore 560 012

Received 19 *August* 1987; *revised and accepted* 18 *December* 1987

Ammonium and alkali metal tetrafluoroborates have been prepared by the cation exchange reaction of pyridinium tetrafluoroborate with the corresponding hydroxides/halides. The reaction of pyridinium tetrafluoroborate with primary, secondary and tertiary alkyl amines at room temperature gives rise to mono-, di- and tri-alkylammonium tetrafluoroborates, respectively. The yields are good and the samples are of high purity. The products have been characterised by elemental analysis, IR and PMR spectroscopy. The spectral data for most of the compounds are reported for the first time.

Tetrafluoroborates salts are widely used both in research and industry. Some of the applications are in electrolytic polishing of ammonium[1], metal finishing operations[2], bright dipping solutions for Sn-Pb alloys in printed circuits and other electrical components[3], catalyst in organic synthesis[4,5], high temperature fluxes, battery components and boriding of steel surfaces[8]. The availability of pure salts is of decided advantage for the applications mentioned above. However, the methods so far reported for their preparation are not satisfactory as regards purity of products, simplicity of methods employed and yields. We report here a simple, one-step procedure for the synthesis of title compounds at room temperature, employing pyridinium tetrafluoroborate for exchange reactions.

Materials and Methods

All the reagents employed in the present study were of LR/AR grade.

The precursor, pyridinium tetrafluoroborate ($C_5H_5NHBF_4$) was synthesised by the reaction of pyridinium poly(hydrogen fluoride) with boric oxide or boric acid[9]. Recrystallized samples, m.p. 210°C, when treated with ammonium and alkali metal hydroxide/chlorides underwent cation exchange and formed the corresponding ammonium and alkali metal tetrafluoroborates. This preparative mode has been extended to the preparation of alkyl substituted ammonium tetrafluoroborates in good yields and high purity.

The infrared spectra of the compounds were recorded both in nujol mull and KBr using a Perkin Elmer 599 spectrophotometer, ^1H (TMS standard) and ^{19}F ($CFCl_3$ standard) NMR spectra were recorded on Varian T60 and Varian FT 80A (74-84 MHz) NMR spectrometers using D_2O or DMSO-d_6 as solvents. ^{13}CNMR spectra were recorded on a Brucker WH-270 MHz F-T NMR, X-ray powder diffraction patterns were recorded with a Phillips 1050/70 X-ray diffractometer using Cu Kα radiation.

Preparation of ammonium tetrafluoroborate

To a solution of pyridinium tetrafluoroborate, (5 g) was added a very slight excess of ammonium hydroxide (1:1) solution dropwise. Pyridine was found to be liberated and was extracted with chloroform thrice. The aqueous solution was filtered and evaporated slowly on a water-bath at 60°-70°C when a solid was obtained, it was dried *in vacuo* over phosphorus pentoxide, yield 92%.

Preparation of alkali metal (Na, K, Rb and Cs) tetrafluoroborates

To a solution of pyridinium tetrafluoroborate (5 g) was added calculated amount of sodium hydroxide solution (30 ml, 1.0 *N*), potassium chloride (2.5 g in 10 ml of water), rubidium bromide (2.0 g in 5 ml of water) or cesium bromide (1.5 g in 5 ml of water). Pyridine was found to be liberated in the process. In the case of sodium tetrafluoroborate the pyridine was extracted with chloroform and the solution concentrated. The yield was 94%. In the other cases, the precipitate formed was filtered, washed with alcohol-water mixture

†Present address: Department of Chemistry, Govt. Arts College, Krishnagiri, Tamilnadu.

and dried in a hot air oven (~ 105°C). The yield was 96%, 96% and 90% for the potassium, rubidium and cesium salts respectively.

The compounds have been characterised by chemical analysis (Table 1) and X-ray powder diffraction pattern (Table 2). The BF_4^- and the boron contents of all the compounds were estimated gravimetrically using nitron acetate as precipitant[10] and titrimetrically by the method of Tatarskii *et al*[11].

Table 1 – Analytical and Infrared Spectra data of Ammonium and Alkali Metal Tetrafluoroborates

MBF_4	Found (calc.), %		IR frequencies (cm^{-1})	Probable assignments
	BF_4^-	Boron		
			3330 s	ν(N – H)
			1430 s	δ(N – H)
			1295 m	
NH_4BF_4*	82.01	—	1100-1000 b,vs	$\nu_3(F_2)$: ν(B – F)
	(82.82)		765 w, 720 w	
			530 s, 520 s	$\nu_4(F_2)$: δ(B – F)
				$\nu_3(F_2)$: ν(B – F)
$NaBF_4$	77.86	9.72	1100-1040 b,vs	
	(79.05)	(9.84)	770 w, 1305 w	$\nu_4(F_2)$: δ(B – F)
			527 m, 516 m	$\nu_3(F_2)$: ν(B – F)
KBF_4	68.31	8.55	1080-1300 b,vs	
	(68.99)	(8.58)	770 m, 740 w	$\nu_4(F_2)$: δ(B – F)
			530 s, 518 s	$\nu_3(F_2)$: ν(B – F)
$RbBF_4$	50.16	6.19	1075-1025 b,vs	
	(50.40)	(6.27)	765 w	$\nu_4(F_2$: δ(B – F)
			525 s, 518 s	$\nu_3(F_2$: ν(B – F)
$CsBF_4$	39.55	4.90	1090-1000 b,vs	
	(39.51)	(4.92)	530 m, 517 s	$\nu_4(F_2)$: δ(B – F)

* Nitrogen estimation : calc. = 13.36% : found = 13.25%.

Table 2 – X-ray Powder Diffraction Pattern Data of Ammonium and Alkali Metal Tetrafluoroborates (in Å)

NH_4BF_4		$NaBF_4$		KBF_4		$RbBF_4$		$CsBF_4$	
d_{obs}	d_{lit}	d_{obs}	d_{lit}	d_{obs}	d_{lit}	d_{obs}	d_{lit}	d_{obs}	d_{lit}
5.75	5.70	3.41	3.41	3.88	3.88	3.99	3.98	4.82	4.83
4.53	4.50	3.39	3.39	3.49	3.50	3.85	3.84	4.65	4.66
3.88	3.84	2.85	2.84	3.40	3.40	3.63	3.62	4.21	4.20
3.67	3.65	2.32	2.31	3.27	3.26	3.53	3.52	4.08	4.08
3.58	3.55	2.15	2.14	3.07	3.07	3.37	—	3.82	3.82
3.11	3.18	2.04	2.03	2.81	2.80	3.18	3.17	3.74	3.73
2.93	2.89	2.01	2.00	2.75	2.74	2.89	2.88	3.55	3.55
2.87	2.84	1.84	1.83	2.33	2.32	2.81	2.83	3.36	3.35
2.56	2.53	1.82	1.81	2.21	2.20	2.53	2.52	3.05	3.04
2.34	2.33	1.56	1.56	2.08	2.08	2.40	2.38	2.95	2.96
2.30	2.28	1.51	1.50	2.03	2.02	2.35	2.33	2.52	2.52
2.18	2.16			1.83	1.82	2.33	2.32	2.47	2.46
1.66	1.65					2.27	2.27	2.39	2.39
						2.16	2.15	2.31	2.30
								2.27	2.27
								2.24	2.23

Preparation of monoalkly ammonium tetrafluoroborates

Pyridinium tetrafluoroborate (5 g) dissolved in 15 ml of water was kept in ice-cooled water. To this solution was added 2.6 ml of propylamine dropwise with stirring. Pyridine was found to be liberated which was extracted with chloroform. The aqueous solution was concentrated to dryness on a water-bath maintained at 50-60°C and the solid so obtained dried over P_4O_{10}. The yield of *n*-propylammonium tetrafluoroborate was 91%.

Six other monoalkylammonium tetrafluoroborates were prepared in a similar manner employing methyl amine (25/30%), ethyl amine (40%), isopropyl amine, *n*-butyl amine, *t*-butyl amine, benzyl amine and cyclohexyl amine.

All the monoalkylammonium tetrafluoroborates were found to be hygroscopic and were preserved over P_4O_{10}. The analytical results are given in Table 3.

Preparation of di- and tri-alkylammonium tetrafluoroborates

Dimethyl-, diethyl- and trimethyl-ammonium tetrafluoroborates were prepared by adopting the same procedure as described for monoalkylammonium tetrafluoroborates. For the other di- and tri-alkylammonium salts a modified procedure was adopted.

Pyridinium tetrafluoroborate (5 g) was taken in a beaker and cooled in an ice-bath; to it was added di-*n*-propyl amine (4.5 ml) dropwise. The reaction was instantaneous and exothermic. For

Table 3 – Preparation and Analyses of Mono-alkylammonium Tetrafluoroborate (RNH_3BF_4)

Compound prepared	Yield (%) (M.P., °C)	Found (calc.), %	
		Nitrogen	BF_4^-
$CH_3NH_3BF_4$	98	11.72	72.24
	(180)	(11.78)	(73.06)
$C_2H_5NH_3BF_4$	95	10.50	64.98
	(146)	(10.54)	(65.36)
n-$C_3H_7NH_3BF_4$	91	9.37	58.53
	(150)	(9.53)	(59.13)
i-$C_3H_7NH_3BF_4$	90	9.59	58.39
	(100)	(9.53)	(59.13)
n-$C_4H_9NH_3BF_4$	93	8.64	53.09
	(194)	(8.71)	(53.98)
t-$C_4H_9NH_3BF_4$	93	8.72	53.68
	(174)	(8.70)	(53.98)
$C_6H_{11}NH_3BF_4$	94	7.44	45.98
	(134)	(7.49)	(46.47)
$C_6H_5CH_2NH_3BF_4$	90	7.10	44.28
	(126)	(7.18)	(44.56)

about 30 min, the solution was stirred and maintained at 0-5°C. The liberated pyridine was extracted with ether, the precipitate filtered off on suction, washed well with ether till free from pyridine. The compound was dried over P_4O_{10}; yield 90%.

The other salts were prepared in a similar manner, making use of calculated amounts of amines and the prepared salts were stored over P_4O_{10}. Analytical results are given in Table 4, Table 5 gives the ^1H NMR data for the alkylammonium tetrafluoroborates.

Results and Discussion

Ammonium and alkali metal tetrafluoroborates

The analytical data and spectral data (Tables 1 and 2) indicate that the products are of high purity.

The infrared spectra of NH_4BF_4 and other alkali metal fluoroborates (Table 1) show a very strong broad absorption in the region 1100-1000 cm^{-1} which is characteristic of the tetrafluoroborate ion and a sharp doublet in the region 515-530 cm^{-1}. The former strong band has been assigned to ν_3 (B−F stretching) and the latter doublet to ν_4 (B−F bending) of the tetrahedral BF_4 ion. The splitting of ν_4 and the appearance of the other bands are attributed to the lowering of site symmetry of the anion[12]. In addition to the above absorptions, NH_4BF_4 shows two more peaks; one at 3330 cm^{-1} and the other at 1430 cm^{-1} which are due to the ammonium ions. The X-ray powder diffraction pattern results (Table 2) are in good agreement with the values reported in literature[13] indicating the purity of the compounds.

Alkyl substituted ammonium tetrafluoroborates

Tables 3 and 4 indicate that yields are good and the products are of high purity. The PMR spectral data are presented in Table 5. The IR data (spectra available with the authors) for all the salts show a medium split band in the region 500-530 cm^{-1} and a characteristic broad band in the region 1150-1000 cm^{-1}. These can be assigned (as with the alkali metal salts) to ν_3 (B−F stretching) and ν_4 (B−F bending) frequencies of the BF_4^- ion.

In the infrared spectra of alkylammonium tetrafluoroborates, a strong broad absorption in the region 3200-3800 cm^{-1} is observed. This has been assigned to the merging of the N−H and C−H stretching vibrations, both of which occur in this region. In dialkylammonium salts, the N−H stretching vibrations appear in the region 3160-3270 cm^{-1}. In trialkylammonium salts, the ν(N−H) and ν(C−H) appear below 3000 cm^{-1}. Several other bands in the region 2800-2300 cm^{-1} might be due to the amine salt combination bends[14]. The other absorptions are due to the organic moieties present in the molecule.

Table 4 – Analytical Data of Di- and Tri-alkylammonium Tetrafluoroborates

Compounds prepared	Yield (%) (M.P., °C)	Found (calc.), %	
		Nitrogen	BF_4^-
$(CH_3)_2NH_2BF_4$	94	10.62	65.03
	(220)	(10.54)	(65.36)
$(C_2H_5)_2NH_2BF_4$	93	8.58	54.09
	(169	(8.70	(53.98)
$(n\text{-}C_3H_7)_2NH_2BF_4$	90	7.32	45.84
	(235)	(7.40)	(45.98)
$(n\text{-}C_4H_9)_2NH_2BF_4$	88	6.28	39.93
	(235)	(6.45)	(40.04)
$(i\text{-}C_4H_9)_2NH_2BF_4$	84	6.38	40.25
	(235)	(6.45)	(40.04)
$(C_6H_5CH_2)_2NH_2BF_4$	85	4.90	30.28
	(186)	(4.91)	(30.48)
$(O)C_4H_8NH_2BF_4$	91	8.00	49.24
	(141)	(8.01)	(49.65)
$(CH_3)_3NHBF_4$	90	9.50	59.03
	(204)	(9.54)	(59.13)
$(C_2H_5)_3NHBF_4$	92	7.37	46.02
	(106)	(7.41)	(45.97)

The ^1H NMR spectra (DMSO-d_6 solvent, TMS-internal standard) (Table 5) of all the alkylammonium tetrafluoroborates identify the organic moieties. The N−H resonances were identified by deuterium exchange. In some cases, the α-protons were found to couple with the N−H protons and these couplings were found to be relieved on deuterium exchange.

It is of interest to mention that other methods so far reported do not give such high yields or purity. The methods reported for the preparation of substituted (alkyl or aryl) ammonium tetrafluoroborates are: (i) decomposing the adducts of boron trifluoride and amines[15], (ii) reaction between ether solution or the amine with boron trifluoride etherate[16], and (iii) by the reaction of tetrafluoroboric acid (HBF_4) and amines[17-19]. The tetrafluoroboric acid is found to be always in equilibrium with its hydrolysis products, $BF_4^- + H_2O \rightarrow [BF_3OH]^- + HF$. Equilibrium constant is 2.8×10^{-3} at 25°C (ref. 20). The salts prepared by using this acid would, therefore, be associated with these impurities. The present method has the advantage of eliminating the drawbacks of the earlier methods such as the presence of difficultily removable impurities, the poor yields and

Table 5 – ^{1}H NMR Data of Mono-, Di- and Tri-alkylammonium Tetrafluoroborates [δ)ppm)]

$CH_3NH_3BF_4$	$C_2H_5NH_3BF_4$	n-$C_3H_7NH_3BF_4$	i-$C_3H_7NH_3BF_4$	n-$C_4H_9NH_3BF_4$
2.5 s ($-CH_3$)	1.23 t ($-CH_3$)	1.0 t (CH_3)	1.3 d ($-\!<^{CH_3}_{CH_3}$)	0.9 ($-CH_3$)
7.08 s ($-NH_3$)	2.92 q ($-CH_2-$)	1.66 mlt (β-CH_2)	3.3 mlt ($-CH<$)	1.43 mlt (β and γ-CH_2)
4.21 ($-NH_3$) on deuteration	7.23 b, s ($-NH_3$)	2.83 t (α-CH_2)	7.26 s ($-NH_3$)	2.8 t (α-CH_2)
	5.47 s ($-NH_3$) on deuteration	6.46 s ($-NH_3$)	5.56 s ($-NH_3$) on deuteration	7.3 b ($-NH_3$)
		4.66 s ($-NH_3$) on deuteration		4.0 b ($-NH_3$) on deuteration
t-$C_4H_9NH_3BF_4$	$C_6H_5CH_2NH_3BF_4$	$C_6H_{11}-NH_3BF_4$	$(CH_3)_2NH_2BF_4$	$(C_2H_5)_2NH_2BF_4$
1.33 s ($<^{CH_3}_{CH_3}_{CH_3}$)	4.01 s ($-CH_2-$)	1.66 b (10 ring protons except α-proton)	2.63 s ($-CH_3$)	1.23 t ($-CH_3$)
	7.4 s (C_6H_5-)		7.7 b ($-NH_2$)	2.96 q ($-CH_2$)
7.16 s (-NH_3)	7.56 s (-NH_3)	2.96 mlt (α-proton)	4.53 ($-NH_2$) on	7.53 b ($-NH_2$)
4.5 s ($-NH_2$) on deuteration		7.23 b (-NH_3)	deuteration	4.86 ($-NH_2$) on deuteration
		5.16 b ($-NH_3$) on deuteration		
$(n$-$C_3H_7)_2NH_2BF_4$	$(n$-$C_4H_9)_2NH_2BF_4$	$(i$-$C_4H_9)_2NH_2BF_4$	(O)C_4H_8 NH_2BF_4	
1.0 t ($-CH_3$)	0.95 ($-CH_3$)	1.0 d ($-\!<^{CH_3}_{CH_3}$)	3.16 mlt (N$<^{CH_2}_{CH_2}$)	
1.7 mlt (β-CH_2)	1.58 mlt (β and γ-CH_2)	2.0 mlt ($-CH<$)	3.8 mlt (O$<^{CH_2}_{CH_2}$)	
2.9 b (α-CH_2- coupled with NH_2 protons)	2.9 t (α-CH_2) 6.73 b ($-NH_2-$)	2.76 d ($-CH_2-CH<$)	7.63 s ($-NH_2-$)	
2.9 t (ondeuteration) 8.06 b ($-NH_2$)	4.16 b ($-NH_2-$) on deuteration	NH absorption was not seen	4.5 s ($-NH_2-$) on deuteration	
$(C_6H_5CH_2)_2NH_2BF_4$	$(CH_3)_3NHBF_4$	$(C_2H_5)_3NHBF_4$		
4.16 s ($-CH_2-$) 7.43 s (C_6H_5-)	2.86 s ($-CH_3$) NH was not observed	1.3 t ($-CH_3$) 3.16 mlt ($-CH_2-$) coupled with $>$NH)		
NH_2 absorption was not seen clearly		3.16 q ($-CH_2$) on deuteration NH was not observed		

s – singlet, q – quartet, d – doublet, mlt – multiplet, t – triplet, b – broad.

the necessity of employing elaborate experimental procedures. This novel procedure is simple, one-pot reaction, occurring at room temperature (25°C).

The pK_a values of the alkyl amines (8.7-11.2) employed are higher than that of pyridine (5.17) and therefore they displace pyridine from pyridinium tetrafluoroborate with great ease. The displacement reactions could be summarised in terms of the following scheme:

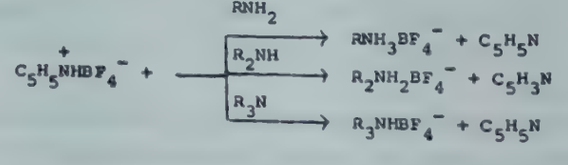

References

1 Jumer J F, *Met Finish*, **56** (1958) 44; **56** (1958) 60.
2 Hudson R M, Butler J J & C J Warning, *Met Finish*, **74** (1976) 37.

3 Beckwith M & Hau G F, *US Pat.* 3888778 (March 13, 1973).
4 O'Conner D E & Wyness G R, *US Pat.* 3808245 (Apr. 30 1974).
5 Pawlenko S, *US Pat.* 334107 (Oct. 24, 1967).
6 Boika V, *USSR Pat.* 495178 (Dec. 15, 1975).
7 Lauck H, *Ger Pat.* 2334660 (Jan 23, 1975).
8 Von Matüschka G, *Kunstofftechnik*, **11** (1972) 304.
9 Kalbandkeri R G, Syed Mohamed K, Padma D K & Vasudeva Murthy A R, *Polyhedron*, **4** (1985) 787.
10 Lucchesi C A & DeFord D D, *Analyt Chem*, **29** (1957) 1169.
11 Taterskii S V, Kornilova E N & Sheinina F A, *Trudy Komissii, Anal Khim Acad Nauk SSSR*, 3 (1951) 287; Chem Absts 47 (1953) 2642h.
12 Cote G L & Thompson H N, *Proc Roy Soc*, **210A** (1951) 217.
13 X-ray powder diffraction file (Joint Committee on Powder Diffraction Standards, Pennsylvania), 19103 (1967), 1-0335, 11-671, 1-0820 and 9-394.
14 Hoard J L & Blair V, *J Am chem Soc*, **51** (1935) 1985.
15 Harris J J & Rudner B, *Inorg Chem*, **8** (1969) 1258.
16 Muller Eugen & Huber-Emden Helmut, *Ann Chem*, **649** (1961) 70.
17 Muller Eugen, Buber-Emden Helmut & Rundel Wolfgang, *Ann Chem*, 6323 (1959) 34.
18 Harris J J, *Inorg Chem*, **5** (1966) 1627.
19 Cook D, *Can J Chem*, **39** (1961) 2009.
20 Ryss I G, *J gen Chem*, (*USSR*), **16** (1946) 531.

Indian Journal of Chemistry
Vol. 27A, September 1988, pp. 764-767

Deprotonation Energetics of Disodium Adenosine Triphosphate in Water from EMF Measurements

HIMANSU TALUKDAR, SIBAPRASAD RUDRA & KIRON K KUNDU*
Physical Chemistry Laboratory, Jadavpur University, Calcutta 700 032

Received 10 *March* 1988; *accepted* 11 *May* 1988

The two-stage deprotonation constants (K_3) and (K_4) of disodium adenosine triphosphate (Na_2H_2A) in water have been determined from EMF measurements of cells comprising H_2 and Ag-AgCl electrodes at five equidistant temperatures ranging from 15° to 35°C. The standard free energies ($\Delta G°$), entropies ($\Delta S°$) and enthalpies ($\Delta H°$) of deprotonation processes in water have also been evaluated. These observations are expected to be important in relation to the complex biochemical phenomena of ATP with biofluids.

Adenosine triphosphate (ATP) occupies a key position in various biochemical processes. Consequently, like other properties the extent of deprotonation and the associated energetics of ATP(H_4A) form vital thermochemical quantities that will help understand its role in vital biological processes.

Unfortunately, despite unusual interests the knowledge of deprotonation energetics of ATP and its analogues is quite limited. Of the few significant studies made so far, those due to Phillips *et al.*[1] and Taqui Khan and Martell[2] are worth-noting. Phillips *et al.* reported the ionization constants of secondary phosphate hydrogens of mono-, di- and tri-adenosine phosphates at three temperatures and the related thermodynamic parameters. Taqui Khan and Martell reported the ionization constants of both primary and secondary phosphate hydrogens of ATP (i.e. pK_3 and pK_4 of H_2A^{-2}) at four different temperatures and the related thermodynamic quantities in 0.1 *m* KNO_3 solution instead of pure water. However, in both these studies a simple potentiometric method using glass and calomel electrodes was used. Notably, neither of these procedures in principle furnished true thermodynamic data because of lack of strict correspondence between *p*H readings and -log (hydrogen ion activity) besides the involved uncertainties of temperature coefficients of liquid junction. Evidently the thermochemical data based on these studies are likely to be suspect. Consequently, it would be highly useful to determine deprotonation energetics of ATP, especially of (H_2A^{-2}) using cells without liquid junction and particularly involving H_2 and Ag-AgX (X = Cl, Br and I) electrodes. In the present paper we report our findings on the depronation constants K_3 and K_4 related to third and fourth step deprotonation of ATP (H_4A) in water and the related thermodynamic quantities, as determined using Harned-Ehler[3] type cells (A) and (B) respectively

Pt, H_2 (g, 1 atm)/$Na_2H_2A(m_1)$, $Na_3HA(m_2)$, $NaCl(m_3)$/AgCl-Ag ... (A)

Pt, H_2 (g, 1 atm)/$Na_3HA(m_1)$, $Na_4A(m_2)$, $NaCl(m_3)$/AgCl-Ag ... (B)

at five equidistant temperatures ranging from 15° to 35°C.

Materials and Methods

Adenosine triphosphate disodium salt (Sigma Chemical Co., grade A-2383; purity 98-99%) was used after drying in a vacuum desiccator (kept at 5-10°C) without further pretreatment. Its purity was checked by alkalimetry as well as by UV spectroscopy using the method of Bock *et al.*[4], and was found to lie within 98-99%.

Stock solutions of both ATP and NaCl (GR, E Merck) were prepared by dissolving weighed amounts of the substances in known amounts of water. Stock NaOH (GR, E Merck) solutions were also prepared separately and their molalities were obtianed by alkalimetric titration using phenolphthalein as indicator. The stock cell solutions were then prepared by mixing appropriate weighed amounts of each of the three solutions and those of different ionic strengths (I) by mass dilution with the solvents, which varied from 0.01 to 0.1 unit. Solutions of lower ionic strength were not used in order to avoid the possible interference of CO_2 (if any) to the concentrations of alkali. All solutions were prepared in well stoppered Jena bottles. The concentrations of the acids in the cell solutions were often checked both before and after the emf runs and no appreciable changes were detected.

Table 1—EMF Values at Different Temperatures for Different Cell Solutions in Pure Water for the Third Dissociation Constant of ATP

I	$m_{Cl^-} \times 10^3$ (mol kg^{-1})	$m_{H_2A^{-2}} \times 10^3$ (mol kg^{-1})	$m_{HA^{-3}} \times 10^3$ (mol kg^{-1})	emf (V)				
				15°	20°	25°	30°	35°
0.01	1.58	0.36	1.21	0.6712	0.6733	0.6754	0.6765	0.6770
0.02	3.70	0.52	2.45	0.6567	0.6581	0.6594	0.6605	0.6613
0.04	7.40	1.04	4.90	0.6377	0.6384	0.6395	0.6408	0.6427
0.06	11.20	1.70	7.27	0.6263	0.6269	0.6275	0.6284	0.6298
0.08	14.90	2.27	9.70	0.6224	0.6226	0.6230	0.6233	0.6236
0.10	18.70	2.85	12.13	0.6187	0.6187	0.6188	0.6188	0.6188

Table 2—Emf Values at Different Temperatures for Different Cell Solutions in Pure Water for the Fourth Dissociation Constant of ATP

I	$m_{Cl^-} \times 10^3$ (mol kg^{-1})	$m_{HA^{-3}} \times 10^3$ (mol kg^{-1})	$m_{A^{-4}} \times 10^3$ (mol kg^{-1})	emf (V)				
				15°	20°	25°	30°	35°
0.01	2.08	0.69	0.38	0.7757	0.7834	0.7902	0.7968	0.8033
0.02	4.17	1.38	0.77	0.7539	0.7606	0.7674	0.7736	0.7801
0.04	8.33	3.75	1.53	0.7321	0.7386	0.7445	0.7512	0.7565
0.06	12.52	4.13	2.30	0.7189	0.7249	0.7308	0.7369	0.7429
0.08	16.69	5.51	3.07	0.7104	0.7166	0.7223	0.7280	0.7335
0.10	20.00	6.60	3.68	0.7054	0.7112	0.7171	0.7225	0.7281

General experimental procedures including the preparation of the Ag-AgCl and H_2(Pt) electrodes, and the measurements of emf were similar to those described earlier[5,6]. The equilibrium was attained in about 2-3 hr. The constancy of emf readings to about ±0.1 mV for 1 hr was taken as the criterion of equilibrium. The emfs of the cells were measured using a Leeds and Northrup K_4-potentiometer filled with a moving coil galvanometer (Cambridge Instrument Co.) as the null point detector.

Results

The measured emfs of cells (A) and (B) corrected to $p_{H_2} = 1$ atm, gave the value of E. the emf data (E) of cells (A) and (B) at different temperatures and the corresponding molalities of NaCl, Na_2H_2A and Na_3HA for cell (A) and those of NaCl, Na_3HA and Na_4A for cell (B) for each of the solvent mixtures are given in Tables 1 and 2 respectively. pK_3 and pK_4 values of the acid salts in water were obtained using the functions pK'_3 and pK'_4 defined by Eqs (1) and (2), respectively

$$pK'_3 = \frac{[E-(E^0_m)_{Ag\text{-}AgCl}]}{2.303\,R\,T/F} + \log \frac{m_{H_2A^{-2}}\, m_{Cl^-}}{m_{HA^{-3}}} + \log \frac{\gamma_{Cl^-}\,\gamma_{H_2A^{-2}}}{\gamma_{HA^{-3}}} \quad \ldots (1)$$

$$pK'_4 = \frac{[E-(E^0_m)_{Ag\text{-}AgCl}]}{2.303\,R\,T/F} + \log \frac{m_{HA^{-3}}\, m_{Cl}}{m_{A^{-4}}} + \log \frac{\gamma_{Cl^-}\,\gamma_{HA^{-3}}}{\gamma_{A^{-4}}} \quad \ldots (2)$$

Table 3—Values of pK_3 and pK_4 of Disodium Adenosine Triphosphate in Water and of Coefficients A_1 and A_2 of Polynomial (4) at Different Temperatures

pK_3	A_1	A_2	pK_3	A_1	A_2
	3rd step dissociation				
	Temp 15°C			Temp 20°C	
4.62	−2.721	7.130	4.59	−2.909	7.385
	Temp 25°C			Temp 30°C	
4.55	−2.970	7.360	4.48	−2.678	6.567
	Temp 35°C				
4.39	−2.084	5.081			
	4th step dissociation				
	Temp 15°C			Temp 20°C	
7.39	−2.927	4.268	7.43	−3.172	4.775
	Temp 25°C			Temp 30°C	
7.44	−3.231	4.920	7.41	−2.811	3.946
	Temp 35°C				
7.43	−2.095	4.204			

In Eqs (1) and (2) m and γ denote molality and molal activity coefficient of the species subscripted. The standard state is so chosen that at infinite dilution in a given solvent γ_i of any species i is equal to unity. The required $(E^0_m)_{Ag\text{-}AgCl}$ values in water at different temperatures were taken from literature[7].

The involved activity coefficient factor in water could be obtained by use of the limiting (L) or more preferably the extended (E) form of Debye-Huckel (DH) equation as given by[3] Eq. (3)

$$-\log \gamma_i = \frac{S_f Z_i^2 I^{1/2}}{1 + a_0 B I^{1/2}} \quad \ldots (3)$$

In Eq. (3) the DH constants $S_f = \frac{1.824 \times 10^6}{(\varepsilon_s T)^{3/2}}$ and $B = \frac{35.46}{(\varepsilon_s T)^{1/2}}$, I is the ionic strength of the cell solution, a_0 is the apparent ionic diameter (which is equal to zero in the case of limiting form of DH equation), ε_s is the dielectric constant of the solvent and the Z_i is the charge of the species involved. In view of the involved uncertainties in a_0 values of the species H_2A^{-2}, HA^{-3} or A^{-4} the activity coefficient factors based on EDH equation might be somewhat uncertain. However, as the activity coefficient factor could be expressed[8] as a polynomial function of $I^{1/2}$, we have obtained pK_3 at different temperatures in water by solving polynomial functions of the form (4)

$$pK_3 = \frac{E - (E^0_m)_{Ag\text{-}AgCl}}{2.303\, R\, T/F} + \log \frac{m_{H_2A^{-2}}\, m_{Cl^-}}{m_{HA^{-3}}}$$

$$= pK_3 + A_1 I^{1/2} + A_2 (I^{1/2})^2 \quad \ldots (4)$$

with the help of a B 6700 Computer. Similar is the case for pK_4. The observed pK_3 and pK_4 values and the coefficient A_1 and A_2 are given in Table 3. The standard deviations of pK values lie within ± 0.03 unit. Notably, pK_3 and pK_4 values at 25°C determined by this method and the ones obtained by coupling the activity coefficient factors based on LDH equation and extrapolating the pK'_3 or pK'_4 versus I plots to $I = 0$, compare fairly well and agree within ± 0.02 unit—the average standard deviation involved in the computer-based data.

The observed pK values at different temperatures were then fitted into Harned-Robinson[9] type expression (5)

$$pK = A/T + B + CT \quad \ldots (5)$$

by the method of least squares. The thermodynamic parameters (ΔG^0, ΔS^0 and ΔH^0 changes) accompanying deprotonation of the acids were then evaluated using the standard relations (6-8)[3] comprising the coefficients of Eq. (5)

$$\Delta G^0 = 2.303\, R[A + BT + CT^2] \quad \ldots (6)$$

$$\Delta S^0 = -2.303\, R[B + 2\,CT] \quad \ldots (7)$$

$$\Delta H^0 = 2.303\, R[A - CT^2] \quad \ldots (8)$$

The values of ΔG^0, ΔS^0 and ΔH^0 [molal scale (m)] so obtained and the values of A, B and C for pK_3 and pK_4 are listed in Table 4. The values of ΔG^0, ΔS^0 on mole fraction scale (N) were obtained by the usual relations[3] viz.

$$\Delta G^0_N = \Delta G^0_m + RT \ln 1000/M_s \text{ and } \Delta S^0_N = \Delta S^0_m - R \ln 1000/M_s \quad \ldots (7)$$

where M_s is the molecular weight of the solvent.

Discussion

The observed pK_3 and pK_4 values and the related thermodynamic quantities in water are compared in Table 5 with some relatively recent literature data based on potentiometric methods using glass and calomel electrodes.

Notably, the data 5 reported by the previous workers differ significantly from the corresponding data observed in this study. In the present study thermodynamic parameters, especially ΔS^0 and hence ΔH^0 are based on polynomial fit of the data at five temperatures into Harned-Robinson's[9] pK versus T expression by least squares technique, where as those of other workers the data are at three or four temperatures and the results are based on simple Vant Hoff isochore assuming $\Delta C_p = 0$. This reflects the approximate nature of the previous results. Moreover, strikingly enough, present data on pK_4 and the related thermodynamic quantities are somewhat intermediate to those of Taqui Khan and Martell and Phillips *et al.* The larger magnitude of pK_4 value of Phillips *et al.* are possibly associated with the over emphasis on the data at lower ionic strength, where the plots of pK' versus $I^{1/2}$ are fairly stiff and hence susceptible to uncertainty. pK values in pure water in the present study, however, are

Table 4—Values of A, B and C of Eq (5) at 25°C and Relevant Energetics ΔG^0, ΔS^0 and ΔH^0 (Molal Scale)

A/K	B	C/K^{-1}	ΔG^0 (kJ mol^{-1})	ΔS^0 (JK^{-1} mol^{-1})	ΔH^0 (kJ mol^{-1})
		3rd step dissociation			
−11367.49	84.24	−0.1394	26.00	−21.3	19.7
		4th step dissociation			
−6021.58	47.46	−0.0665	42.43	−149.4	−2.1

Table 5—Comparison of pK_3 and pK_4 Values and Related Thermodynamic Quantities in Water at 25°C

	pK_3	ΔG^0 (kJ mol^{-1})	ΔS^0 (JK^{-1} mol^{-1})	ΔH^0 (kJ mol^{-1})	pK_4	ΔG^0 (kJ mol^{-1})	ΔS^0 (JK^{-1} mol^{-1})	ΔH^0 (kJ mol^{-1})
Present method	4.55	25.9	−21.3	19.7	7.44	42.3	−150.6	−2.1
Taqui Khan and Martell[2]	4.06	23.0	−18.8	17.2	6.53	37.2	−117.2	2.1
Phillips *et al.*[1]	—	—	—	—	7.68	43.9	−171.5	−7.1

based on polynomial fitting and compare fairly well with the values based on extrapolation of the observed linear plots of pK' versus I. So, these are likely to be free from such uncertainties and hence more reliable. The data of Taqui Khan and Martell, on the other hand being not based on activity correction or extrapolation at all, can hardly be taken as true thermodynamic data.

In this case the negative magnitudes of ΔS_3^0 and ΔS_4^0 and that ΔS_4^0 is more negative than ΔS_3^0 conform to what is expected from the nature of the equilibria involved. Thus in the primary phosphate ionization process: $H_2A^{-2} + H_2O \rightleftharpoons H_3O^+ + HA^{-3}$, the ΔS_3^0 is given by Eq. (10).

$$\Delta S_3^0 = (\bar{S}^0_{H_3O^+} - \bar{S}^0_{H_2O}) + (\bar{S}^0_{HA^{-3}} - \bar{S}^0_{H_2A^{-2}}) \quad \ldots (10)$$

while in the secondary phosphate ionization process: $HA^{-3} + H_2O \rightleftharpoons A^{-4} + H_3O^+$, ΔS_4^0 is given by Eq. (11).

$$\Delta S_4^0 = (\bar{S}^0_{H_3O^+} - \bar{S}^0_{H_2O}) + (\bar{S}^0_{A^{-4}} - \bar{S}^0_{HA^{-3}}) \quad \ldots (11)$$

Since H_3O^+ carrying a charge must be solvated resulting in a more orderliness, hence a decrease of entropy relative to H_2O, i.e. $\bar{S}^0_{H_3O^+} < \bar{S}^0_{H_2O}$. And for a similar reason $\bar{S}^0_{HA^{-3}} < \bar{S}^0_{H_2A^{-2}}$ and hence the observed negative magnitudes of ΔS_3^0. Similarly, in the case of the deprotonation of HA^{-3}, since $\bar{S}^0_{A^{-4}} < \bar{S}^0_{HA^{-3}}$ and $\bar{S}^0_{H_3O^+} < \bar{S}^0_{H_2O}$, the resulting ΔS_4^0 must be negative as observed. But as entropy of hydration of any ion is directly proportional to square of ionic charge, it is expected that $(\bar{S}^0_{HA^{-3}} - \bar{S}^0_{HA^{-2}})$ is less negative than $(\bar{S}^0_{A^{-4}} - \bar{S}^0_{HA^{-3}})$. This explains why ΔS_3^0 accompanying the primary phosphate ionization of ATP (H_2A^{-2}) is less negative than that for the secondary phosphate ionization of ATP(HA^{-3}). This again partially explains why free energies of deprotonation of HA^{-3} is largely compensated resulting in near zero enthalpies of deprotonation compared to that of H_2A^{-2}.

Acknowledgement

Thanks are due to the UGC, New Delhi, for financial assistance.

References

1 Phillips R C, Philip G & Rutman R J, *Biochem*, (1963) 2902.
2 Taqui Khan M M & Martell A B, *J Am chem Soc*, **88** (1966) 3037.
3 Harned H S & Ehlers R W, *J Am chem Soc*, **54** (1932) 1350.
4 Bock R M, Ling N, Morell S A & Liplox S H, *Arch Biochem Biophys*, **62** (1956) 253.
5 Basu-Mullick I N & Kundu K K, *Indian J Chem*, **18A** (1979) 1.
6 Das A K & Kundu K K, *J phys Chem*, **79** (1975) 2604.
7 Bates R G & Bower V E, *J Res Nat Stds*, **53** (1954) 283.
8 Sen B, Johnson D A & Roy R N, *J phys Chem*, **7** (1967) 1523.
9 Harned H S & Robinson R A, *Trans Faraday Soc*, **36** (1940) 973.

Indian Journal of Chemistry
Vol. 27A, September 1988, pp. 768-771

Thermodynamics of Electrolyte Solutions: Activity Coefficients of NaCl in $NaCl + MnCl_2 + H_2O$ System at 25°C

CH VENKATESWARLU & J ANANTHASWAMY*
Department of Chemistry, Osmania University, Hyderabad 500 007

Received 6 *April* 1987; *revised and accepted* 10 *December* 1987

The EMF values of a cell consisting of sodium ion-selective electrode and silver-silver chloride electrode have been measured to find the activity coefficients of NaCl in its mixtures with aqueous $MnCl_2$ at 25°C and total ionic strengths of 0.5, 1.0, 2.0 and 3.0. The Harned coefficients have been evaluated by fitting the activity coefficient data to the equation:

$$\log \gamma_A = \log \gamma_A^\circ - \alpha_{AB} y_B - \beta_{AB} y_B^2$$

The data have been also fitted to the Pitzer equations and the corresponding binary and ternary interaction parameters are reported.

Recently, activity coefficients of aqueous electrolyte solutions and mixed electrolyte solutions have been extensively studied[1-5] because such data are useful in the fields of petroleum drilling, industrial processing, water pollution control and oceanography. However, the ternary mixtures of aqueous alkali metal halides with transition metal halides have not received much attention. Roy *et al.*[6] and Downes[7] have estimated the activity coefficients of HCl in the system $HCl + MnCl_2 + H_2O$. But, only isopiestic data are available[8] for the system $NaCl + MnCl_2 + H_2O$. Hence, in the present study the mean ionic activity coefficients of NaCl in the system $NaCl + MnCl_2 + H_2O$ have been estimated by EMF measurements method at 25°C and total ionic strengths 0.5, 1, 2 and 3.

Materials and Methods

Deionised, doubly distilled water was used for preparing all the solutions. Analytical grade sodium chloride (GR, S Merck) and manganous chloride (AR, Glaxo) were used without further purification. The solutions were standardised volumetrically using $AgNO_3$. All the solutions were prepared by weight. Also, all titrations and dilutions were made using weight burettes.

The cell consisted of a Na ion-selective electrode (Elico, India) and an Ag-AgCl electrode in a mixture of NaCl and $MnCl_2$ solutions placed in a double-walled glass vessel whose temperature was maintained constant by circulation of water from a thermostat. The Ag/AgCl electrodes were prepared as described by Ives and Janz[9]. The potentials were measured with a Keithly 5½ digit electrometer/multimeter after processing the signals with a unit gain amplifier of input impedance $\simeq 10^{12}\ \Omega$. The accuracy of the EMF measurements was ± 0.1 mV. The electrodes were allowed to stand in a mixture of 0.01 *M* NaCl while not in use, and were properly conditioned for use in mixed electrolyte solutions. Electrodes were standardised at all the ionic strengths studied.

At each ionic strength, in the first set, the potentials of the Na electrode vs Ag-AgCl electrode were measured and these potentials were plotted against $\log a_{NaCl}$. The activity coefficients of pure NaCl solutions at 25°C were taken from the literature (NBS data)[10]. The *p*H of the solutions were in the range 3.8-5.5 and these *p*H values are well above the *p*H limits suggested by the manufacturer for the Na ion-selective electrode. At every ionic strength the electrodes were allowed to stand in the solutions for about 30-45 min before taking the initial reading, so as to allow attainment of the equilibrium.

The EMF values of Na ion-selective electrode vs Ag/AgCl electrode in NaCl-$MnCl_2$ mixtures are given by the relation:

$$E_{NaCl\text{-}MnCl_2} = E_o + k \log (a_{Na} a_{Cl} + K a_{Mn}^{1/2} a_{Cl}) \quad \ldots (1)$$

where k is the Nernst slope and K is the selectivity coefficient of Na electrode for Mn^{2+} ions.

In pure NaCl solution, i.e., when $a_{Mn} = 0$,

$$E_{NaCl} = E_o + k \log a_{Na} a_{Cl} \quad \ldots (2)$$

In pure $MnCl_2$ solutions $a_{Na} = 0$ and, therefore,

$$E_{MnCl_2} = E_o + k \log K a_{Mn}^{1/2} a_{Cl} \quad \ldots (3)$$

or

$$K^2 = (1/a_{MnCl_2}^3) \exp [4.606 (E_{MnCl_2} - E_o)/k] \quad \ldots (4)$$

At each ionic strength the EMF data obtained in the calibration run (the first set) was fitted to Eq. 2 and E_o and k values were evaluated using least squares

Table 1—Mean Activity Coefficients of NaCl in NaCl + $MnCl_2$ + H_2O System at 25°C

I=0.5		I=1		I=2		I=3	
y_B	$-\log \gamma_{NaCl}$	y_B	$-\log \gamma_{NaCl}$	y_B	$-\log \gamma_{NaCl}$	y_B	$-\log \gamma_{NaCl}$
0.0911	0.1620	0.0923	0.1713	0.0935	0.1719	0.0960	0.1515
0.1670	0.1617	0.1690	0.1652	0.1710	0.1701	0.1752	0.1535
0.2312	0.1581	0.2338	0.1574	0.2363	0.1658	0.2981	0.1571
0.2862	0.1565	0.2891	0.1536	0.2920	0.1702	0.3468	0.1580
0.3338	0.1565	0.3371	0.1514	0.3402	0.1678	0.3892	0.1600
0.3755	0.1578	0.3789	0.1470	0.3822	0.1669	0.4887	0.1625
0.4123	0.1604	0.4486	0.1442	0.4192	0.1672	0.4978	0.1610
0.4450	0.1641	0.5042	0.1455	0.4520	0.1686	0.5272	0.1623
0.5006	0.1647	0.4915	0.1397	0.5077	0.1658	0.5603	0.1675
0.4949	0.1675	0.5178	0.1427	0.5082	0.1655	0.5979	0.1717
0.5505	0.1751	0.5472	0.1433	0.5376	0.1663	0.5979	0.1687
0.5833	0.1745	0.5800	0.1409	0.5706	0.1642	0.6408	0.1657
0.6202	0.1793	0.6591	0.1389	0.6079	0.1663	0.6904	0.1657
0.7101	0.1877	0.7073	0.1433	0.6504	0.1628	0.7483	0.1746
0.8305	0.2011	0.7632	0.1425	0.7561	0.1640	0.8169	0.1680
0.9074	0.2123	0.8286	0.1501	0.9029	0.1626	0.8992	0.1727
		0.9062	0.1458	0.9490	0.1610	0.9469	0.1725
		0.9508	0.1525				

procedure. Next, selectivity coefficient values for $MnCl_2$ were determined by substituting the EMF data obtained in the second set, i.e., with pure $MnCl_2$ solution, in Eq. 4. The activity coefficients of manganous chloride were taken from the literature (NBS data)[11]. The values of the selectivity coefficients (K) at all the ionic strengths were $< 1 \times 10^{-4}$. Therefore, the second term within brackets on the right hand side of Eq. 1 was neglected. The third set consisted of the EMF measurements with aqueous mixtures of NaCl-$MnCl_2$. For this set the potentials were first measured with pure NaCl solutions and then aliquots of $MnCl_2$ solution were added. Next, starting with pure $MnCl_2$ solution, aliquots of NaCl solution were successively added. The overlapping portion between these two experiments was used to test the reproducibility and accuracy of the measurements. Also, all the three sets were repeated at least twice to get consistent and reproducible results.

The cell EMF values for NaCl + $MnCl_2$ + H_2O mixtures are described by the relation,

$$E_{NaCl\text{-}MnCl_2} = E^o + k \log a_{Na} a_{Cl} \quad \ldots (5)$$

But

$$a_{Na} = m_{Na} \gamma_{\pm} = m_A \gamma_{\pm}$$

and

$$a_{Cl} = m_{Cl} \gamma_{\pm} = (m_A + 2m_B) \gamma_{\pm}$$

where $\gamma_{\pm}$ is the mean ionic activity coefficient of NaCl. Substituting these relations in Eq. 5, we get

$$E_{NaCl\text{-}MnCl_2} = E_o + k \log m_A (m_A + 2m_B) \gamma_{\pm}^2$$

or

Table 2—Harned Coefficients of NaCl in NaCl-$MnCl_2$-H_2O System at 25°C

I	$\log \gamma^o_{NaCl}$	α	β	RMSD[a] × 10^3
0.5	−0.1667	−0.0650	0.1298	2.16
1	−0.1823	−0.1304	0.1030	1.80
2	−0.1749	−0.0299	0.0207	1.79
3	−0.1466	0.0438	−0.0176	2.37

[a]Root mean square deviation

$$\gamma_{\pm}^2 = (1/m_{Na} m_{Cl}) \exp \{2.303 (E_{NaCl\text{-}MnCl_2} - E_o)/k\} \quad \ldots (6)$$

Thus, the activity coefficients of NaCl in aqueous NaCl-$MnCl_2$ mixtures were calculated by substituting in Eq. 6 the cell EMF ($E_{NaCl\text{-}MnCl_2}$) values along with the E_o and k values estimated in the calibration set.

Results and Discussion

The experimental mean activity coefficients of NaCl at all the ionic strengths studied are summarised in the Table 1, at different values of y_B where,

$$y_B = 3m_{MnCl_2}/(m_{NaCl} + 3m_{MnCl_2}) \quad \ldots (7)$$

The log $\gamma_{\pm}$ vs y_B plots are shown in Fig. 1. These $\gamma_{\pm}$ values at each ionic strength, were fitted to the Harned equation[12]:

$$\log \gamma_A = \log \gamma_A^o - \alpha_{AB} y_B - \beta_{AB} y_B^2 \quad \ldots (8)$$

where γ_A^o is the activity coefficient of pure NaCl at the same ionic strength as the mixture. The values of Harned coefficients, i.e., α_{AB} and β_{AB} are listed in

Table 3—s_θ and ψ Values Obtained from the Activity Coefficient Data of NaCl in $NaCl + MnCl_2 + H_2O$ at 25°C

I	$s_{\theta_{NaMn}}$	ψ_{NaMnCl}	RMSD × 10^3	RMSD × 10^2 with $s_\theta = 0.9517$ $\psi = -0.6623$	RMSD × 10^2 with $s_\theta = 0.082$ $\psi = -0.017$
0.5	−1.696	5.143	2.29	3.91	1.70
1.0	−0.1177	1.037	1.89	2.28	3.10
2.0	0.0991	0.0089	1.47	3.48	0.60
3.0	0.0288	−0.0274	2.49	6.33	1.76

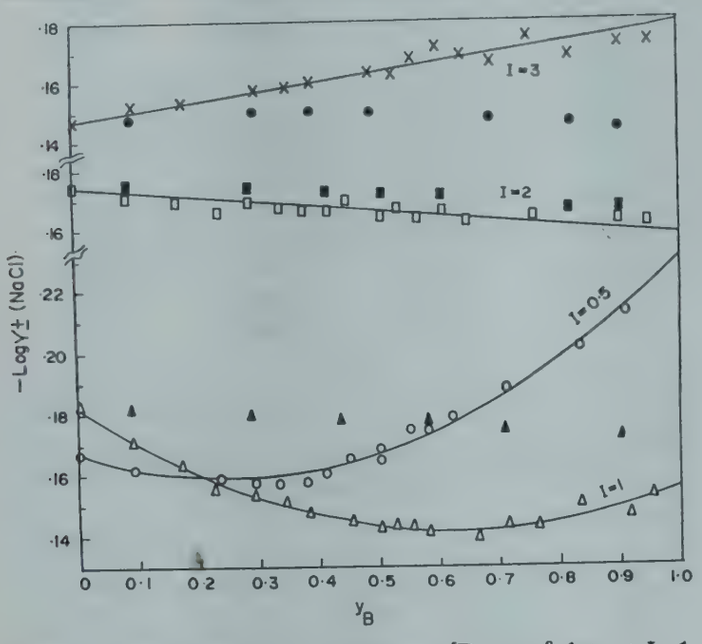

Fig. 1—Plot of log $\gamma_{\pm\ NaCl}$ versus y_{MnCl_2} [Downes[8] data at $I=1$, ▲; $I=2$, ■; at $I=3$. ●]

Table 4—Osmotic Coefficients in the Mixture $NaCl + MnCl_2 + H_2O$ System at 25°C

y_{NaCl}	$I=0.5$	$I=1.0$	$I=2.0$
0	0.853	0.876	0.945
0.1	0.882	0.909	0.946
0.2	0.902	0.930	0.941
0.3	0.919	0.942	0.933
0.4	0.925	0.949	0.925
0.5	0.930	0.959	0.920
0.6	0.932	0.950	0.920
0.7	0.932	0.948	0.925
0.8	0.930	0.944	0.937
0.9	0.926	0.940	0.956
1.0	0.922	0.936	0.984

Table 5—Excess Free Energies of Mixing for the NaCl-$MnCl_2$ System at 25°C

y_{NaCl}	$\Delta_m G^E$ (J kg^{-1} of water)		
	$I=0.5$	$I=1.0$	$I=2.0$
0.2	13.0	52.7	121
0.4	45.3	138	279
0.6	55.0	150	268
0.8	36.2	86.7	129

Table 2. All the calculations were done using a Vax Computer.

The activity coefficient data were also fitted to the recently developed Pitzer equations[13-15]. The NBS data[10,11] on the activity coefficients of pure NaCl and $MnCl_2$ solutions were fitted to the Pitzer equations[13-15]. The values of the Pitzer coefficients are given below:

$\beta^o_{NaCl} = 0.07537$; $\beta^1_{NaCl} = 0.2770$; $C^\phi_{NaCl} = 0.001407$

$\beta^o_{MnCl_2} = 0.3356$; $\beta^1_{MnCl_2} = 1.456$; $C^\phi_{MnCl_2} = -0.02351$

The activity coefficients of aqueous NaCl in constant ionic strength mixtures of NaCl-$MnCl_2$ are also described by the Pitzer equation[16].

From Fig. 1 it is evident that our data are in good agreement with the activity coefficient data of Downes[8] at $I=2$. Also, at $I=1.0$ our data show the same trend as those of Downes[8] eventhough the numerical agreement is not so close. The experimental activity coefficient data were fitted to the Pitzer equation[16] and the binary interaction coefficient ($s_{\theta_{NaMn}}$) and the ternary interaction coefficient (ψ_{NaMnCl}) were evaluated at each ionic strength. These values are listed in Table 3.

Also, the activity coefficient data at all the four ionic strengths were fitted into a single least-squares programme and common s_θ and ψ values were evaluated. These s_θ and ψ values are 0.9517 and −0.6623 respectively. The corresponding RMSD values are also listed in Table 3. Pitzer[16] analysed the isopiestic data reported by Downes[8] and obtained the values of $s_\theta = 0.082$ and $\psi = -0.017$. The RMSD values corresponding to these s_θ and ψ values are also listed in the last column of Table 3. A comparison of the RMSD values listed in the last two columns of Table 3 shows that these two sets of s_θ and ψ values are equally good.

The s_θ and ψ values ($s_\theta = 0.9517$ and $\psi = -0.6623$) were used to calculate the osmotic coefficients of the mixture at various compositions using the Pitzer equations[14] (Table 4). These osmotic coefficients agree within about ± 1.0% with the experimental values reported by Downes[8].

The excess free energies of the mixtures were calculated using the equation,

$$\Delta_m G^E = Y_A[\ln(\gamma_A/\gamma_A^\circ) + (\phi_A - \phi_M)] + Y_B[\ln(\gamma_B/\gamma_B^\circ) + (\phi_B - \phi_M)]$$

where all the symbols have their usual significance[17]. These excess free energies of mixing are listed in Table 5. Thus, these common s_θ and ψ values are able to represent the thermodynamic data of the system up to an ionic strength of 2.0.

Acknowledgement

The authors thank Prof. T. Navaneeth Rao, Prof. B. Sethuram (Osmania University, Hyderabad) and Prof. G. Atkinson (University of Oklahoma, Norman, USA) for constant encouragement and many helpful discussions. One of the authors (Ch V) is thankful to the CSIR, New Delhi for the award of a JRF.

References

1 Ananthaswamy J & Atkinson G, *J chem Engng Data*, **30** (1985) 120.
2 White (Jr) D R, Robinson R A & Bates R G, *J solution Chem*, **9** (1980) 457.
3 Lanier R D, *J phys Chem*, **69** (1965) 3992.
4 Christenson P G, *J chem Engng Data*, **18** (1973) 286.
5 Khoo K H, *J chem Soc Faraday Trans I*, **82** (1986) 1.
6 Roy R N, Gibbons J J, Trower J K & Lee G A, *J solution Chem*, **9** (1980) 535.
7 Downes C J, *J chem Soc Faraday Trans I*, **68** (1972) 1964.
8 Downes C J, *J chem Engng Data*, **18** (1973) 412.
9 Ives D J & Janz G J, *Reference electrodes* (Academic Press, New York, 1961) Chapter 4.
10 Hamer W J & Yung Chi Wu, *J phys Chem Ref Data*, **1** (1972) 1047.
11 Goldberg R N, *J phys Chem Ref Data*, **8** (1979) 1005.
12 Harned H S & Owen B B, *The physical chemistry of electrolyte solutions*, 3rd Edn (Reinhold, New York) 1958, Chapter 14.
13 Pitzer K S, *J phys Chem*, **77** (1973) 268.
14 Pitzer K S & Kim J J, *J Am chem Soc*, **96** (1974) 5701.
15 Ananthaswamy J & Atkinson G, *J chem Engng Data*, **29** (1984) 81.
16 Pitzer K S, *J solution Chem*, **4** (1975) 249.
17 Ananthaswamy J & Atkinson G, *J solution Chem*, **11** (1982) 7.

Indian Journal of Chemistry
Vol. 27A, September 1988, pp. 772-777

Effect of Solvent on Reactions of Coordination Complexes: Part 6 —Kinetics of Solvolysis of *cis*-(Bromo)(2-aminothiazole)-bis(ethylenediamine)cobalt (III) in Acetone + Water Media

ANADI C DASH* & JYOTSNAMAYEE PRADHAN
Department of Chemistry, Utkal University, Bhubaneswar 751004

Received 30 *December* 1987; *accepted* 12 *January* 1988

Rates of solvolysis of *cis*-(bromo)(2-aminothiazole)-bis(ethylenediamine)cobalt (III) have been investigated in acidic acetone + water solvent media (0-80 wt% of acetone) at 30-50°C. The plot of $\log k^s_{obs}$ versus Grunwald Winstein's Y-parameter at 25°C is linear with gradient = 0.14. The plot of $\log k^s_{obs}$ versus $1/D_s$ (D_s = bulk dielectric constant of the mixed solvent) is, however, nonlinear indicating that simple point charge model of the complex ion and dielectric continuum model of the solvent system are inadequate. The plot sof $\log k^s_{obs}$ versus mol fraction of acetone (X_{org}) are linear and biphasic with negative gradients at all temperatures. The dependence of solvolysis rate on X_{org} has been interpreted in terms of solvation of initial and transition states. Solvation is atleast partly controlled by acidity and basicity of mixed solvent media. The activation enthalpy and entropy versus X_{org} plots display multiple maxima and minima indicating that solvent structural changes play significiant role in the activation process. The values of $\Delta S\dagger$ are negative (-16 to -76 KJ mol^{-1} for $0 \leqslant X_{org} \leqslant 0.55$). This discounts the possibility of steric change at cobalt (III) centre during substitution due to the steric effects of the organic solvent component and favours stereoretentive aquation due to rigidity of the initial state and the transition state enforced by the front side solvation involving cooperative hydrogen bonding between Co-Br, N − H dipoles and both the solvent components.

In a preceding paper[1] the rate and activation parameters for the solvolysis of *cis*-$[(en)_2Co(tzNH_2)Br]^{2+}$ ($tzNH_2$ = 2-aminothiazole) in MeOH + water, ethyleneglycol + water and propane-2-ol + water (0-80 wt% of organic solvent component) were reported. The specificity of the solvent effects were evident. It was presumed that the dipolar protic solvents mediate the solvolytic process via hydrogen bonding interactions with the substrate. A front side solvation model involving Co-Br, N − H dipoles, and the tertiary N − of the dangling thiazole ring of the cobalt (III) substrate and the protic-o-solvents was visualized. The coorperativity in hydrogen bonding can be affected if one of the solvent components of aquo-organic solvent systems is a dipolar aprotic solvent. Besides, if the dipolar aprotic solvent is such that it can undergo hydrophobic association with any hydrophobic moiety adjacent to the reactive Co-Br dipole then this may also lead to the modification of the hydrogen bonded network of the solvent cage around the reacting centre of the complex ion. Consequently these effects will be reflected in the rate and activation parameters of the solvolytic reaction. With this aim in view we report in the present work the kinetics of solvolysis of *cis*-(bromo)(2-aminothiazole)bis(ethylenediamine)cobalt(III) in acetone + water media.

Materials and Methods

Cis-(bromo)(2-aminothiazole)bis(ethylenediamine) cobalt (III) diperchlorate was prepared as described earlier[2]. Analysis of Co and Br agreed to 0.3% of the calculated values.

Analytical grade chemicals were used for kinetic runs. Distilled water was redistilled from alkaline $KMnO_4$. Acetone (Glaxo, India, 99.5% pure) was further dried over molecular sieve (4A) and distilled. Solvent mixtures were prepared on wt% basis. Spectral measurements were made using an Elico visible spectrophotometer.

Kinetic measurements

The kinetics of solvolysis of the complex was follwed by potentiometric titration of the liberated bromide. The experimental procedure for rate measurement and calculation of the pseudo-first order rate constant were the same as described earlier[3].

Results and Discussion

Successive spectral scans for the reaction mixture at 45°C (see Fig. 1) in 50 wt% acetone + water medium exhibited isosbestic points at 445 and 520 nm. After long time intervals the isosbestic points are lost with concomitent reduction in intensity of the absorption band over a wide wavelength range. This may be due to some secondary reactions of the primary aquo product *cis*$[(en)_2Co(tzNH_2)OH_2]^{3+}$. This aspect was not persued. However, pseudo-first order kinetics was

observed for the release of bromide over at least two half-lives.

The primary solvolytic reaction may be represented by Eq. (1)

$$cis[Co(en)_2(tzNH_2)Br]^{2+} \xrightarrow{k^s_{obs}} cis[Co(en)_2(tzNH_2)S]^{3+} + Br^- \quad \ldots (1)$$

where $S = H_2O$. Earlier studies from this laboratory[1,2] indicated that k_{obs} in fully aqueous medium is independent of the acidity of the medium at $[H^+]_T \geq 0.002$ mol dm^{-3} (35°C-50°C). Hence all rate studies were made maintaining $[HClO_4] = 0.01$ mol dm^{-3} to avoid complication due to base hydrolysis reaction. The values of the pseudo-first order rate constants are collected in Table 1. The activation parameters calculated by a weighted least square procedure are collected in Table 2.

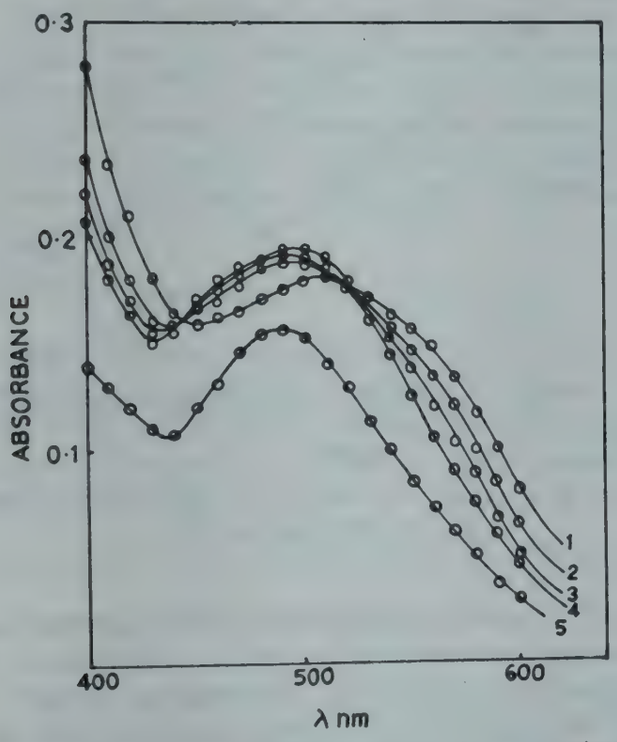

Fig. 1—Successive spectral scans for aquation of *cis*-$[(en)_2Co(NH_2tz)Br]^{2+}$ in 50 wt% acetone + water at 45°C ($[complex] = 1.9 \times 10^{-3}$ mol dm^{-3} cell path = 1 cm (1) 1 min (2) 40 min (3) 115 (115 min, (4) 220 min and (5) 1660 min)

Variation of rate and activation parameters with solvent composition

The pseudo-first order rate constant (k^s_{obs}) decreases with increase in acetone content of the reaction medium. The plots of $\log k^s_{obs}$ versus (D_s^{-1}) (D_s = bulk dielectric constant of the solvent[4]) is, however nonlinear. Similar observation has been recorded in MeOH + water, ethylene glycol + water, and propane-2-ol + water media[1]. The point charge model for the substrate and the dielectric continuum model for the solvent mixture fail and the solvent specificity on the solvolysis rates is clearly evident (Fig. 2). The correlation between $\log k^s_{obs}$ and the Grunwald-Winstein's 'Y'-parameter[5] is excellently linear with gradient = 0.14 (see Fig. 3). Such a correlation supports that the ionising power of the solvent grossly controls the solvolytic process and that organic solvent component does not change the intimate mechanism of the reaction.

Table 2—Activation Enthalpy, and Entropy Data for solvolysis of *cis*-$[Co(en)_2(2\text{-aminothiazole})Br]^{2+}$ in Acetone + Water Medium

Acetone (wt %)	$\Delta H^{\neq}$ (kJ mol^{-1})	$\Delta S^{\neq}$ (JK^{-1} mol^{-1})
0	95 ± 3	−16 ± 11
5	91 ± 5	−31 ± 15
10	90 ± 4	−33 ± 12
20	89 ± 1	−38 ± 2
30	91 ± 3	−32 ± 9
40	84 ± 1	−56 ± 2
50	90 ± 4	−40 ± 12
60	90 ± 3	−40 ± 10
70	85 ± 5	−62 ± 16
80	81 ± 5	−76 ± 16

Table 1—Pseudo-first Order Rate Constants for Solvolysis of *cis*-$[Co(en)_2(2\text{-aminothiazole})Br]^{2+}$ in Acetone + Water Mixtures

$[Complex]_t = 2 \times 10^{-3}$ mol dm^{-3}; $[HClO_4] = 0.01$ mol dm^{-3}

Acetone (wt %)	$X_{Acetone}$	$k^s_{obs} \times 10^5$ (s^{-1}) at			
		30.0 ± 0.1°	35.0 ± 0.1°	39.0 ± 0.1°	50.0 ± 0.1°
0	0	4.21 ± 0.04	7.47 ± 0.87	14.1 ± 1.1	47.9 ± 3.9
5	0.0161	4.54 ± 0.16	7.32 ± 0.15	13.8 ± 0.6	42.3 ± 1.7
10	0.0333	3.92 ± 0.19	6.65 ± 0.17	11.4 ± 1.0	38.1 ± 2.7
20	0.0719	3.19 ± 0.12	5.79 ± 0.23	10.3 ± 0.7	29.9 ± 1.5
30	0.1173	2.54 ± 0.08	4.92 ± 0.22	8.46 ± 0.21	23.9 ± 2.0
40	0.1712	2.21 ± 0.08	3.89 ± 0.21	6.52 ± 0.19	18.8 ± 1.0
50	0.2366	1.80 ± 0.08	2.96 ± 0.09	5.86 ± 0.19	16.6 ± 0.5
60	0.3174	1.49 ± 0.07	2.53 ± 0.07	4.71 ± 0.15	13.9 ± 0.8
70	0.4197	1.04 ± 0.08	1.72 ± 0.09	3.05 ± 0.15	—
80	0.5535	0.69 ± 0.08	1.22 ± 0.05	1.93 ± 0.17	—

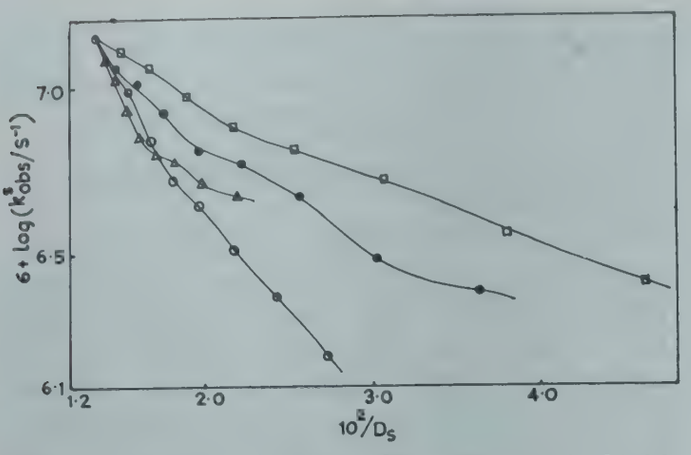

Fig. 2– 6+log k^s_{obs} (s^{-1} versus $10^2/D_s$ plots at 40°C [⊙-MeOH + water, △-EG + water, ⊡-propane-2-ol + water, ●-acetone + water. Data for solvent systems other than Acetone + water are taken from Ref. 1]

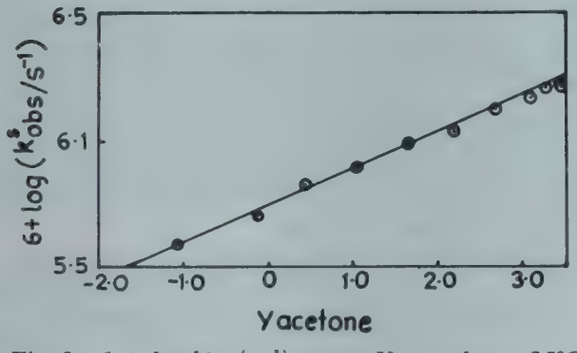

Fig. 3– 6 + log k^s_{obs} (s^{-1}) versus $Y_{acetone}$ plot at 25°C

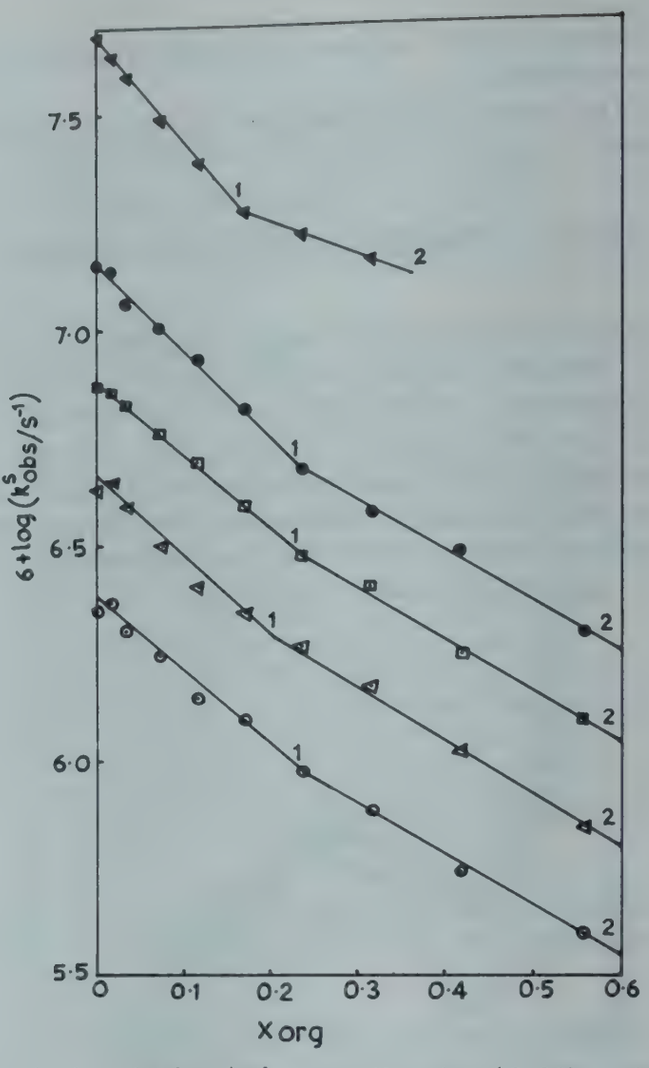

Fig. 4– 6 + log k^s_{obs} (s^{-1} versus X_{org} plots (⊙-25°, △-30°, ⊡-35°, ●-40° and ▲-50°C)

The plots of log k^s_{obs} versus X_{org} (X_{org} = mol fraction of acetone) are clearly biphasic (Fig. 4). A linear relationship between log k^s_{obs} and X_{org} is expected if the acidity (As) and basicity (Bs) of the mixed solvent vary linearly with X_{org} and if the ion-solvent interaction is predominantly governed by these dual solvent vectors[6] (see Eq. 7 of Ref. 3). In this context it is worth mentioning that MeOH-water system behaves most satisfactorily as the rate data fit to the linear relationship (2)

$$\log k^s_{obs} = l_1 X_{org} + C \qquad \ldots (2)$$

(l_1 and C are constants) over the composition range $0 \leq X_{MeOH} \leq 0.6923$ particularly at higher temperatures irrespective of the cobalt (III) substrate used[1,3,7]. The biphasic plots with sharp breaks around $X_{org} \simeq 0.2$ (Fig. 4) indicate that l_1 and C can be treated as constants within a narrow range of X_{org}. We believe that the structural properties of the solvent appear to control the reactivity of the substrate which is not taken care of in the solvent effect relationship stated in Eq. (2). The structural difference between water and acetone might result in preferential solvation of both the initial state (i.s) and the transition state (t.s) of the reactant by any of the solvent components. While acetone can undergo favourable hydrophobic association as well as NH...O=C(CH$_3$)$_2$ H−bonding interaction with the cobalt (III) substrate, water will have the advantage of solvating it via H−bonding interaction with N−H and Co-Br dipoles. Nevertheless, the solvent cospheres of the initial and transition states appear to play dominant role in modulating the reactivity of substrates.

The familiar dissociative interchange mechanism (I_d)[8] in which the Co-Br bond is believed to be stretched to the limit of breaking in the transition state leads to Eq. (3)[3]

$$\log k^s_{obs} = \log k^w_{obs} - \left(\frac{1}{2.303RT}\right)[\Delta G_t(\text{t.s}) - \Delta G_t(\text{i.s})]_{(s-w)} \qquad \ldots (3)$$

where $k^w_{obs} = k^s_{obs}$ at $X_{org} = 0$,

and $[\Delta G_t(\text{t.s}) - \Delta G_t(\text{i.s})]_{(s-w)}$ denotes the transfer free energy of the transition state relative to the initial state for the transfer of species occurring

from water to the mixed solvent. The linear variation of $\log k^s_{obs}$ with X_{org} is expected if the relative transfer free energy function varies linearly with X_{org}. The biphasic natrue of $\log k^s_{obs}$ versus X_{org} plots (Fig. 4), therefore, reveals the effects of appreciable solvent structural perturbations in the solvent cospheres of the transition state as well as the initial state on the relative free energy function. The calculated values of the relative transfer free energy function indicate that $[\Delta G_t(t.s)_{(s\leftarrow w)}$ is more positive than $[\Delta G_t(i.s)]_{(s\leftarrow w)}$ at all solvent compositions (except at $X_{org}=0.016$, 25°C). Hence the I_d transition state is more destablised than the initial state when transfer occurs from water to the mixed solvent.

The interpretation of the biphasic plots of $\log k^s_{obs}$ versus X_{org} can be advanced by ion-solvation model defining an excess molar Gibbs free energy of transfer as proposed by Marcus[9]. Expressing the excess molar Gibbs free energy of transfer for a species, 'i' at a given mol fraction X_{org} by Eq. (4)

$$[\Delta G^E_t(i)]_{X_{org}}=[\Delta G_t(i)]_{(s\leftarrow w)}-X_{org}[\Delta G_t(i)]_{(org\leftarrow w)} \quad \ldots (4)$$

where 'i' denotes the initial state (i.s) or the transition state (t.s), and the subscripts 's', 'w' and 'org' stand for mixed solvent, water and pure organic cosolvent respectively, it can be easily shown that Eq. (4) yields Eq. (5)

$$[\Delta G_t(t.s)-\Delta G_t(i.s)]_{(s\leftarrow w)}=[\Delta G^E_t(t.s)-\Delta G^E_t(i.s)]_{X_{org}} + X_{org}[\Delta G_t(t.s)-\Delta G_t(i.s)]_{(org\leftarrow w)} \quad \ldots (5)$$

Marcus[9] defines a dimensionless reduced quantity called preferential solvation parameter, g, in terms of ΔG^E_t and composition of the medium. Accordingly it is possible to get the relationship (6)

$$[\Delta G^E_t(t.s)-\Delta G^E_t(i.s)]_{X_{org}}=\Delta g RT X_{org}(1-X_{org}) \ldots (6)$$

where $\Delta g = g(t.s)-g(i.s)$ = the difference of the preferential solvation parameter for the transition state and the initial state. Assuming that Δg is independent of the solvent composition and combining Eqs (3), (5) and (6) we obtain

$$\log k^s_{obs}=\log k^w_{obs}-aX_{org}+bX^2_{org} \quad \ldots (7)$$

where $a=(\Delta g+c/RT)/2.303$, $b=\Delta g/2.303$ and $c=[\Delta G_t(t.s)-\Delta G_t(i.s)]_{(org\leftarrow w)}$.

Fitting of the rate data to Eq. (7) by a weighted least squares program adopted to an IBM 1130 computer yields the values of a and b. The values of Δg and c are collected in Table 3. Thus this analysis helps us to estimate the value of the relative transfer free energy term $[\Delta G_t(t.s)-\Delta G_t(i.s)]_{(org\leftarrow w)}$ which otherwise is not amenable to measurement. The values of Δg are low positive in the temperature range of 30-39.9°C, but increase significantly at 50°C. This reflects higher degree of preferential solvation of the transition state relative to the initial state and this effect becomes much more significant at 50°C. The sudden change in the value of $c(=[\Delta G_t(t.s)-\Delta G_t(i.s)]_{(org\leftarrow w)}$ from $+7 kJ mol^{-1}$ to $-8 kJ mol^{-1}$ around 40-50°C, also reflects profound thermal effect on the solvent structural perturbations in the cospheres of the transition state and the initial state when these are transferred from pure water to pure acetone.

The volume profile analysis for the aquation of several cobalt (III) complexes had led to the conclusion that the leaving group in the transition state is fully solvated[10]. A constant value for the molar valume of the five-coordinate intermediate, $(NH_3)_5Co^{3+}$ irrespective of the leaving group in the aquation of $(NH_3)_5CoX^{n+}$ is consistent with the fact that the molar volume of lthe transition state obeys the additivity principle, $\bar{V}[(NH_3)_5CoX^*]^{(3-n)+}_{aq}=\bar{V}[(NH_3)_5Co^{3+}]_{aq}+\bar{V}[X]^{n-}_{aq}$. If the same additivity principle is assumed for thermodynamic transfer function of the product like transition state then we obtain

$$[\Delta G_t(C^{3+})]_{(s\leftarrow w)}=[\Delta G_t(t.s)]_{(s\leftarrow w)}+[\Delta G_t(Br^-)]_{(s\leftarrow w)} \quad \ldots (8)$$

where C^{3+} is the reactive five-coordinate tripositive intermediate, *cis*$[Co(en)_2(tzNH_2)^{3+}]$, of the dis-

Table 3—Calculated Values of Parameters a, b, c and Δg of Eq. (7)

Temp (°C)	a	b	Δg	c (kJ mol^{-1})*
30.0	1.72 ± 0.14	0.67 ± 0.42	1.5 ± 1.0	6.1 ± 2.6
35.0	1.70 ± 0.08	0.50 ± 0.18	1.1 ± 0.4	7.1 ± 1.2
39.9	1.87 ± 0.12	0.75 ± 0.18	1.7 ± 0.4	6.7 ± 1.3
50.0	3.03 ± 0.11	4.40 ± 0.44	10.1 ± 1.0	−8.4 ± 2.8

* $c=[\Delta G_t(t.s)-\Delta G_t(i.s)]_{(org\leftarrow w)}$

sociative transition state. The relative transfer free energy $[\Delta G_t(C^{3+}) - \Delta G_t(i.s)]_{(s\leftarrow w)}$ is then calculated at 25°C using the $\Delta G_t(Br^-)$ data. The values of $\Delta G_t(Br^-)$ for acetone water media are obtained by intrapolation and extrapolation from the available data tabulated by Wells upto 44.3 wt% of acetone[11]. Figure 5 depicts the variation of $[\Delta G_t(C^{3+}) - \Delta G_t(i.s)]_{(s\leftarrow w)}$ with X_{org} upto 50 wt% of acetone from which it is evident that the values of $[\Delta G_t(C^{3+})]_{(s\leftarrow w)}$ are less positive than the same for $[\Delta G_t(i.s)]_{(s\leftarrow w)}$. This might indicate that the tripositive moiety C^{3+} is more stabilised in acetone-water media than the corresponding dipositive initial state. Similar behaviour, but less pronounced, is also exhibited by this complex in propane-2-ol + water media[2]. For example, the values of $[\Delta G(C^{3+}) - \Delta G_t(i.s)]_{(s\leftarrow w)}$ at 25°C vary from 0 to < -3kJ mole^{-1} for propane-2-ol + water in the range of $X_{org} = 0$-0.25 as against much wider variation (0 to -12KJ mol^{-1}) for $0 \leqslant X$ acetone $\leqslant 0.2$ for acetone + water. However, the solvolysis rate is slowed down in the mixed solvent due to the fact that $[\Delta G_t(Br^-)]_{(s\leftarrow w)}$ tends to be more and more positive with increasing X_{org}, which over compensates the favourable solvent effect on $[\Delta G_t(C^{3+}) - \Delta G_t(i.s)]_{(s\leftarrow w)}$ to facilitate the reaction in the mixed solvent. The inflexion in the region of $X_{org} = 0.12$-0.17 in the plot of $[\Delta G_t(C^{3+}) - \Delta G_t(i.s)]_{(s\leftarrow w)}$ versus X_{org} (see Fig. 5) is attributable to possible solvent structural changes occurring around this composition. It is worth noting that the excess volume of mixing V_2^E versus wt% of acetone plot for acetone water mixtures displays a sharp break around $X_{acetone} = 0.1$, V_2^E increases linearly beyond $X_{acetone} = 0.1$ indicating onset of breakdown of the solvent structure as pointed out by Wells[11]. Thus it is evident that the structural perturbations in the bulk of the solvent mixture is effectively transmitted to the solvent cosphere of the initial state and presumably transmitted to the solvent cosphere of the initial state and presumably the transition state. Cooperative hydrogen bonding involving Co-Br, N−H and the solvent dipoles (see structure I) may be visualised in the front side solvation (FSS) model. Besides, hydrophobic interaction between the methyl groups of acetone and the thiazole ring may result in favourable solvation of the initial state and transition state at high percentage of acetone. This may be a reason for which $[\Delta G_t(C^{3+}) - \Delta G_t(i.s)]_{(s\leftarrow w)}$ versus X_{org} plot shows a downward trend beyond $X_{org} \equiv 0.17$ (see Fig. 5).

Figures 6 and 7 and data collected in Table 2 depict the variation of activation parameters with solvent components. Well defined maxima and minima are displayed in the plot of $\Delta H^{\neq}$ or $\Delta S^{\neq}$ versus X_{org}. The mutual compensation effect of $\Delta H^{\neq}$ and $\Delta S^{\neq}$ on the rate is also reflected in the $\Delta H^{\neq}$ versus $\Delta S^{\neq}$ plots for MeOH + water, ethylene glycol + water, propane-2-ol + water and acetone + water media (Fig. 8). Overall $\Delta H^{\neq}$ and $\Delta S^{\neq}$ may be taken to be a composite of the reaction component and the solvation component, $\Delta X^{\neq}_{overall} = \Delta X^{\neq}_R + \Delta X^{\neq}_S$ (Ref. 12). The validity of the compensation law is, therefore, consistent with the fact that perturbations of reaction zone and

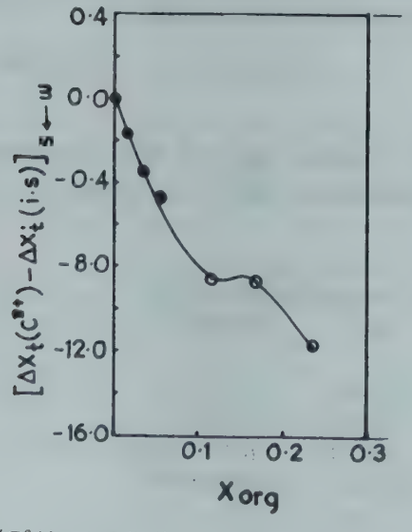

Fig. 5—$[\Delta G_t(C^{3+}) - \Delta G_t(i.s)]_{(s\leftarrow w)}$ (kJ mol^{-1}) versus X_{org} plot at 25°C

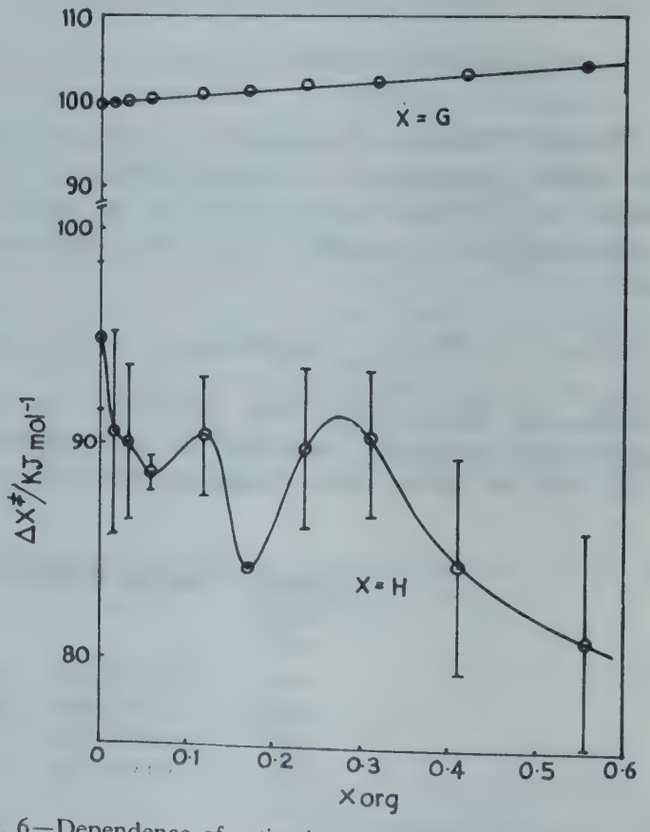

Fig. 6—Dependence of activation Gibbs free energy and activation enthalpy on X_{org} ($\Delta G^{\neq}$ at 298.2K)

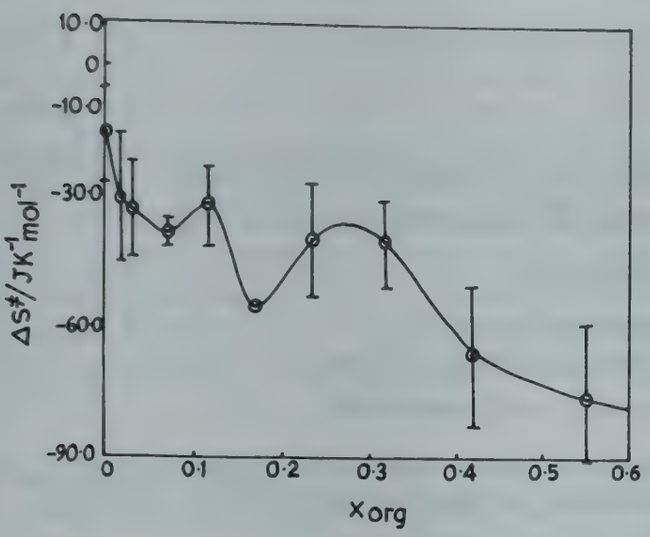

Fig. 7—Dependence of $\Delta S^{\neq}$ ($JK^{-1}\ mol^{-1}$) on X_{org}

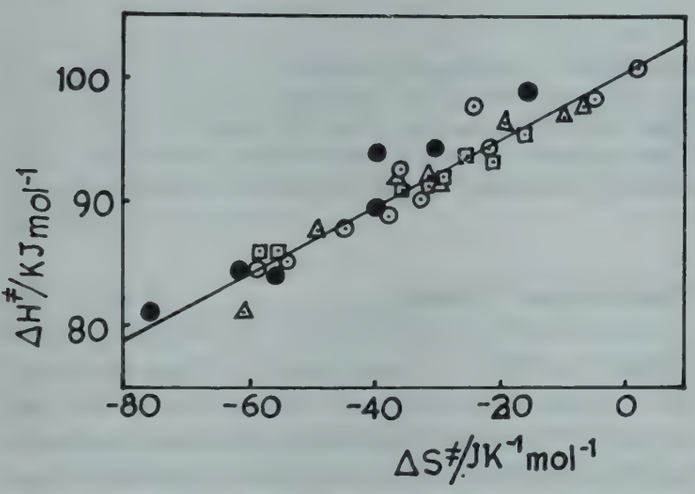

Fig. 8—$\Delta H^{\neq}$ ($kJmol^{-1}$) versus $\Delta S^{\neq}$ ($JK^{-1}mol^{-1}$) plot. (⊙-MeOH + water, △-EG + water, □-propane-2-ol + water and ●-acetone + water)

solvent network remain proportional to each other so that the isodelphic and lyodelphic components of $\Delta H^{\neq}$ and $\Delta S^{\neq}$ correlate well with each other[13].

It is interesting to note that the values of $\Delta S^{\neq}$ are negative in the entire range of solvent composition which further suggest higher degree of ordering in the solvent cosphere of the dissociative interchange (I_d) transition state as compared to the initial state. Similar effects are also evident from the relevant data for the solvolysis of this complex and other related complexes in MeOH + water ethylene glycol + water and propane-2-ol + water mixed solvent media[1,3,7].

It is evident that steric effect of the organic cosolvent does not lead to rearrangement at the cobalt (III) centre. Presumably the front side solvation (see structure I) makes the system rigid in both initial state and transition state and disfavours structural rearrangement at the cobalt (III) centre.

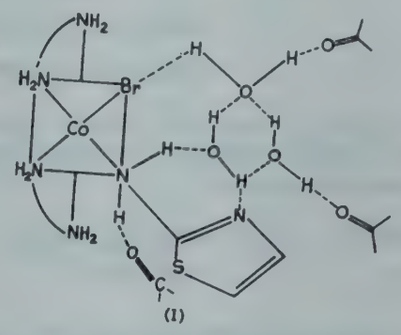

Acknowledgement

This work was partly supported by a grant from the CSIR, New Delhi (to ACD), Miss J P is thankful to the UGC, New Delhi for the award of a junior research fellowship.

References

1 Dash A C & Pradhan J, *J Chem Soc Faraday Trans* 1, **84** (1988) In Press.
2 Dash A C & Mohapatra S K, *Indian J Chem*, **15A** (1977) 871.
3 Dash A C & Dash N, *J chem Soc Faraday* 1, **83** (1987) 2505.
4 Akerlof G, *J Am chem Soc*, **54** (1932) 4125.
5 Leffler J E & Grunwald E, *Rates and equilibria of organic reactions*, (Wiley, New York) 1963, pp 298.
6 Swain C G, Powell A L & Alunni S, *J Am chem Soc*, **105** (1983) 502.
7 Dash A C & Dash N, *J chem Soc Faraday* 1, 84 (1988) 75.
8 Langford C H & Gray H B, *Ligand substitution processes* (Benjamin W A, New York) 1965.
9 Marcus Y, *Ion solvation* (John Wiley, New York) 1985, Chap 7, pp 206.
10 Palmer D A & Kelm H, *Coord Chem Rev*, **36** (1981) 89.
11 Wells C F, *J chem Soc Faraday Trans* 1, **70** (1974) 694.
12 Blandamer M J, *Advances in physical organic chemistry*, Vol 14, edited by V Gold & B Bethel (Academic Press, New York) 1977, pp 247.
13 Grunwald E, *J Am chem Soc*, **106** (1984) 5414.

Indian Journal of Chemistry
Vol. 27A, September 1988, pp. 778-782

Kinetic & Mechanistic Studies on Substitution Reaction of Aquo-ligands from *cis*-Diaquo-bis(biguanide)cobalt(III)/chromium(III) Ions in Aqueous Medium

ASHIS KUMAR GANGOPADHYAY & G S DE*

Department of Chemistry, University of Burdwan, Burdwan 713 104

Received 21 *September* 1987; *revised and accepted* 15 *December* 1987

The kinetics of substitution of aquo ligands from *cis*-diaquo-bis-(biguanide)chromium(III)/cobalt(III) ions by L-histidine in aqueous medium have been studied spectrophotometrically. The following rate law has been established in *p*H range of 3.85 to 5.57

$$\frac{d[\text{Complex-II}]}{dt} = \frac{k_a K_E [\text{Complex-I}]_{total} [\text{Ligand}]}{1 + K_E [\text{Ligand}]}$$

[where, Complex-II = $[M(BigH)_2(Hist)]^{2+}$; Complex-I = $[M(BigH)_2(H_2O)_2]^{3+}$ and ligand = L-histidine; M = Co^{III}, Cr^{III}]. In this equation K_E is the ion-pair equilibrium constant and k_a the rate constant for interchange of outer-sphere complex to inner-sphere complex. The reaction rates are found to be *p*H dependent in the *p*H range of 3.85 to 5.57. Values of activation parameters, $\Delta H^{\ddagger}$ and $\Delta S^{\ddagger}$ have been evaluated. The results are consistent with a mechanism involving outer-sphere association of reactants followed by associative interchange of this outer-sphere complex into the product.

The earlier works[1-5] on ligand substitution reactions in octahedral complexes indicate that the reactions of Co(III) and Cr(III) systems proceed through I_d and I_a path respectively. However, exceptions[6-11] are not rare and experimental evidences have been adduced which point out that depending on the nature of the system, I_a or I_d mechanism may operate both for Co(III) and Cr(III). Banerjea and coworkers[8] studied base hydrolyses of $[M(NH_3)_5(NCS)]^{2+}$ [M = Co(III), Cr(III) and Rh(III)] in aquo-organic mixed solvents and observed a significant difference in relative degree of M − NCS bond cleavage [significantly higher for Cr(III)] and M − OH bond making considerably more pronounced for Co(III) and Rh(III) in the three different cases studied. Chatterjee and coworkers[10] studied base hydrolysis of $[Cr(NH_3)_5N_3]^{2+}$ and suggested dissociative mechanism whereas Banerjea and coworkers[11] studied base hydrolysis of $[Co(NH_3)_5(S_2O_3)]^{+}$ and suggested associative character of the reaction. It was therefore thought worthwhile to study the anation reactions of similar aquo complexes of Co(III) and Cr(III), and therefore selected systems like *cis*-$[M(BigH)_2(H_2O)_2]^{3+}$ [where M = Co(III), Cr(III)] and incoming ligands, such as pyridine carboxylic acids and a series of amino acids for anation reactions.

The present paper relates to the reaction:

cis-$[M(BigH)_2(H_2O)_2]^{3+} + Hist.H_2^{+}$
$\rightarrow [M(BigH)_2(Hist.H)]^{3+} + H_2O + H_3O^{+}$

where M = Co(III), Cr(III).

Materials and Methods

cis-$[Co(BigH)_2(H_2O)_2](ClO_4)_3$ (Complex-I) was prepared as follows: hydroxoaquobis(biguanide)cobalt (III) sulphate was prepared by the method of Ray and Ghose[12]. The perchlorate salt was prepared *in situ* by metathesis of the complex sulphate with barium perchlorate in solution. *cis*-$[Cr(BigH)_2(H_2O)_2](ClO_4)_3$ (Complex-I) was prepared *in situ* by the methods described in literatures[13-15]. Absorption spectra of 0.005 mol dm^{-3} solutions of these complexes, recorded on a UVISPEK spectrophotometer, exhibited λ_{max} at 490 nm, similar to that reported in literatures[16,17]. The absorption spectra of 1:1, 1:2 and 1:3 mixtures (complex: incoming ligand; complex concentration being 0.005 mol dm^{-3}) for both the systems thermostated at 45°C for 48 hr at *p*H 4.0 exhibited λ_{max} at 490 nm. The products of the reactions of $[Co(BigH)_2(H_2O)_2](ClO_4)_3$ and $[Cr(BigH)_2(H_2O)_2](ClO_4)_3$ with histidine were prepared by mixing the reactants in 1:1 molar ratio and the reaction mixtures refluxed for 48 hr on a water-bath. Solid products separated out on concentration of reaction mixtures. The elemental analyses of isolated products revealed the compositions $[Co(BigH)_2(Hist)]^{3+}$ and $[Cr(BigH)_2(Hist)]^{3+}$ (Complex-II). Further these complexes exhibited λ_{max} at 490 nm.

In all experiments AR grade chemicals were used and doubly distilled water was used for preparing solution. All measurements were made on a Hilger UVISPEK spectrophotometer at 460 nm where the absorptions of the reacting complexes and the com-

plexes formed as products differ appreciably. Temperature equilibrated solutions of histidine and the Complex-I were mixed and the concentrations of the reactants in the experimental solutions were such that the first order rate law were applicable and the pseudo-first order rate constants, k_{obs}, for each experiment were evaluated graphically by plotting $\log[(D_\alpha - D_o)/(D_\alpha - D_t)]$ versus time t, where D_α, D_0 and D_t are the absorbances at infinite time, in the beginning and after time, t, respectively. Rates are reproducible within ± 3%.

Results and Discussion

(i) *Effect of varying [Complex-I] on rate constants*

In the set of experiments performed at 45°C the [Complex-I] was varied from 0.005 mol dm^{-3} to 0.0075 mol dm^{-3} at fixed [histidine] of 0.1 mol dm^{-3}, pH = 4 and ionic strength = 0.5 mol dm^{-3}. The pseudo-first order rate constant (k_{obs}) for anation of $[Co(BigH)_2(H_2O)_2]^{3+}$ was $(1.4 \pm 0.04) \times 10^{-4}$ s^{-1} that for $[Cr(BigH)_2(H_2O)_2]^{3+}$ it was $(4.0 \pm 0.2) \times 10^{-4}$ s^{-1}. The k_{obs} values were found to be in good agreement with the first order rate law:

$$\frac{d[\text{Complex-II}]}{dt} = k_{obs}[\text{Complex-I}]$$

(ii) *Effect of varying [histidine] on rate constant*

The [histidine] was varied in the range of 0.05 to 0.15 mol dm^{-3} at fixed [Complex-I] = 0.005 mol dm^{-3}, pH = 4.0 and ionic strength (μ) = 0.5 mol dm^{-3} for both the systems. The results presented in (Table 1) show that the rates increase with increase in $[Hist.H_2^+]$ and approach a limiting rate at higher $[Hist.H_2^+]$ (Figs. 1a, 1b) for both the systems. This behaviour may be due to completion of ion-pair formation at higher $[Hist.H_2^+]$ (ref. 18).

The above results lead to Scheme 1 as a plausible mechanism for anation at different concentrations of the incoming ligand. Scheme 1 leads to rate law (1)

$$cis\text{-}[M(BigH)_2(H_2O)_2]^{3+} + Hist.H_2^+ \overset{K_\epsilon}{\rightleftharpoons} cis\text{-}[M(BigH)_2(H_2O)_2]^{3+}.Hist.H_2^+$$

$[M = Co(III) \text{ and } Cr(III)]$ (I.P)

$$[M(BigH)_2(H_2O)_2]^{3+}.Hist.H_2^+ \xrightarrow[k_a]{Slow} [M(BigH)_2(Hist.H)]^{3+} + H_3O^+ + H_2O$$

Scheme 1

$$\frac{d[M(BigH)_2(Hist.H)^{3+}]}{dt} = \frac{k_a K_\epsilon [M(BigH)_2(H_2O)^{3+}]_{total}[Hist.H_2^+]}{1 + K_\epsilon[Hist.H_2^+]} \quad \ldots(1)$$

$$= k_{obs}[M(BigH)_2(H_2O)^{3+}]_{total} \quad \ldots(2)$$

Table 1 – Variation of Rate Constant (k_{obs}) with $[Hist.H_2^+]$ at Different Temperatures

$[M(BigH)_2(H_2O)_2^{3+}] = 0.005$ mol dm^{-3}; pH = 4.0; μ = 0.5 mol dm^{-3}

	$[Hist.H_2^+]$ mol dm^{-3}	$k_{obs} \times 10^4$ s^{-1}				
		30°	35°	40°	45°	50°C
	Anation of *cis*-$[Co(BigH)_2(H_2O)_2](ClO_4)_3$					
	0.05	—	0.41	0.64	0.80	1.02
	0.075	—	0.57	0.88	1.09	1.32
a	0.100	—	0.72	1.09	1.42	1.76
	0.125	—	0.84	1.26	1.59	1.93
	0.150	—	0.95	1.36	1.76	2.13
	Anation of *cis*-$[Cr(BigH)_2CH_2O)_2](ClO_4)_3$					
	0.05	0.69	1.02	1.53	2.17	—
	0.075	1.02	1.43	2.17	3.07	—
b	0.100	1.27	1.79	2.81	3.80	—
	0.125	1.53	2.17	3.32	4.29	—
	0.150	1.79	2.30	3.58	4.60	—

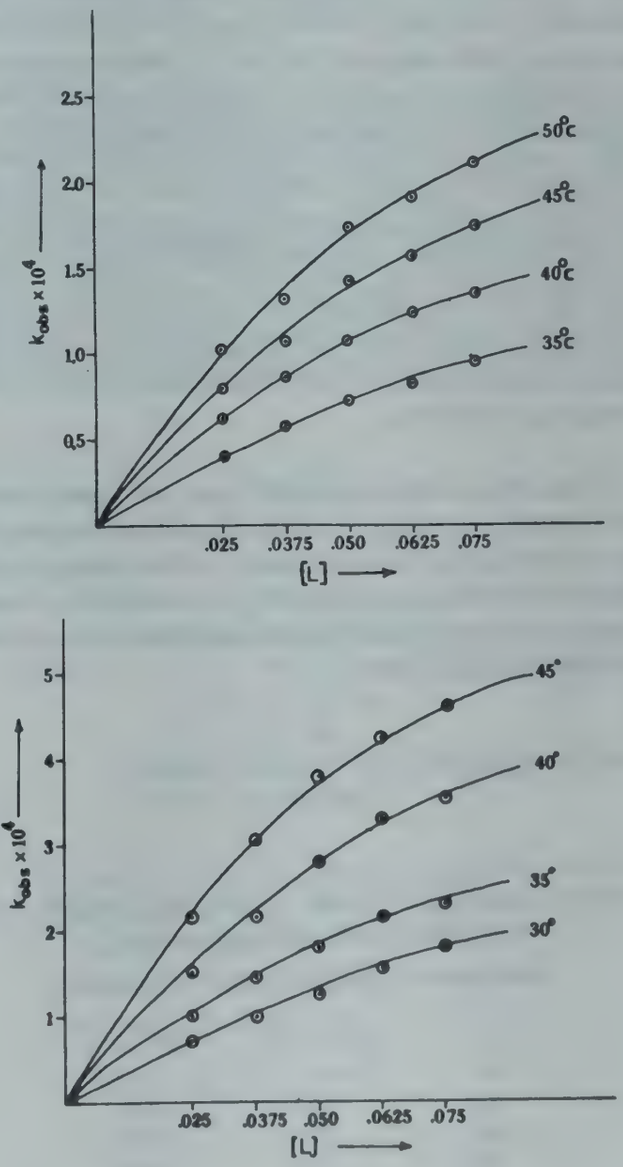

Fig. 1 – Plot of k_{obs} versus [ligand] at different temperatures [(a) Co^{III} system and (b) Cr^{III} system]

Therefore,

$$k_{obs} = \frac{k_a K_E [Hist.H_2^+]}{1 + K_E [Hist.H_2^+]} \quad \ldots (3)$$

$$\frac{1}{k_{obs}} = \frac{1}{k_a} + \frac{1}{k_a K_E [Hist.H_2^+]} \quad \ldots (4)$$

Equation (4) implies that the plot of $1/k_{obs}$ versus $1/[Hist.H_2^+]$ should be linear. This actually found to be so in both the cases (Figs. 2a, 2b). From such linear plots k_a values (Table 2) and K_E values were obtained from the intercept $(1/k_a)$ and slope $(1/k_a K_E)$ respectively. The K_E values of *cis*-$[Co(BigH)_2(H_2O)_2]^{3+}$ and *cis*-$[Cr(BigH)_2(H_2O)_2]^{3+}$ are almost constants and are in the range of 5.2 to 7.1 and 4.5 to 8.0 respectively.

(iii) *Effect of varying pH on rate constant*

Under the condition; [Complex-I] = 0.005 mol dm^{-3}; $[Hist.H_2^+] = 0.1$ mol dm^{-3}, ionic strength = 0.5 mol dm^{-3}; and temp. = 45°C the *p*H of the medium was varied in the range of 3.85 to 5.57 [*p*H were adjusted by adding NaOH or $HClO_4$] in both the cases. It was observed that, k_{obs} values for the anation of $[Co(BigH)_2(H_2O)_2]^{3+}$ were 1.32×10^{-4}, 1.42×10^{-4}, 1.63×10^{-4}, 1.92×10^{-4}, 2.20×10^{-4}, 2.8×10^{-4} s^{-1} and for $[Cr(BigH)_2(H_2O)_2]^{3+}$ the k_{obs} values were 3.6×10^{-4}, 3.8×10^{-4}, 4.1×10^{-4}, 4.6×10^{-4}, 5.5×10^{-4} and 5.9×10^{-4} s^{-1} at *p*H 3.85, 4.0, 4.47, 4.89, 5.32 and 5.57 respectively. Here we find that the k_{obs} values increase with increase the *p*H of the medium. This can be explained as follows:

In the above mentioned *p*H range the ligand histidine comes as a positive charge in solution because it dissociates as shown in Scheme 2. So the change in *p*H does not alter the ligand reactivity considerably. Let us consider the acid dissociation equilibria of both the complexes (Eqs 5 and 6).

$$cis\text{-}[Co(BigH)_2(H_2O)_2]^{3+} \overset{K_1}{\rightleftharpoons} cis\text{-}[Co(BigH)_2(OH)(H_2O)]^{2+} + H^+ \quad \ldots (5)$$

Table 2 – Values of k_a for the Anation of [Complex-I] by Histidine at Different Temperatures

Temperature (°C)	$[M(BigH)_2(H_2O)_2]^{3+}$ + Histidine	
	M = Co^{III}	M = Cr^{III}
30	—	8.33
35	3.03	9.52
40	3.92	10.70
45	5.13	12.12
50	6.50	—

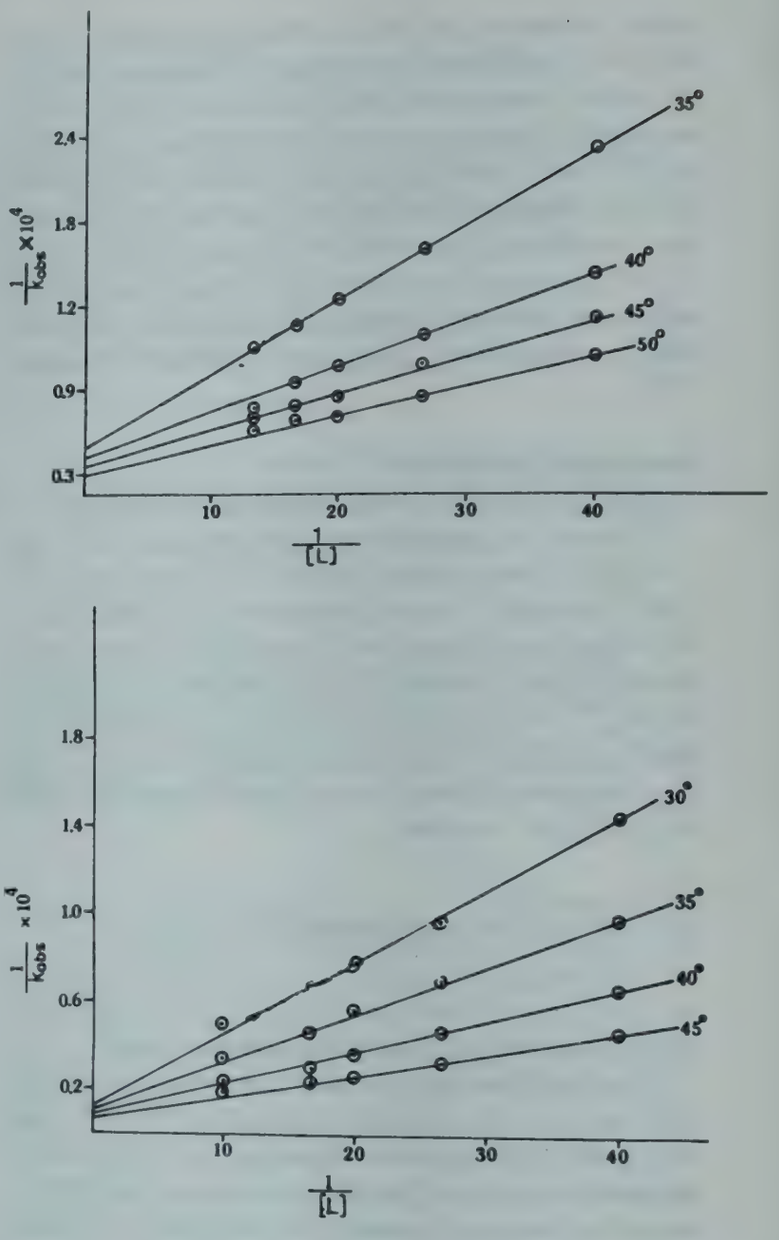

Fig. 2 – Plot of $1/k_{obs}$ versus 1/[ligand] at different temperatures [(a) Co^{III} system and (b) Cr^{III} system]

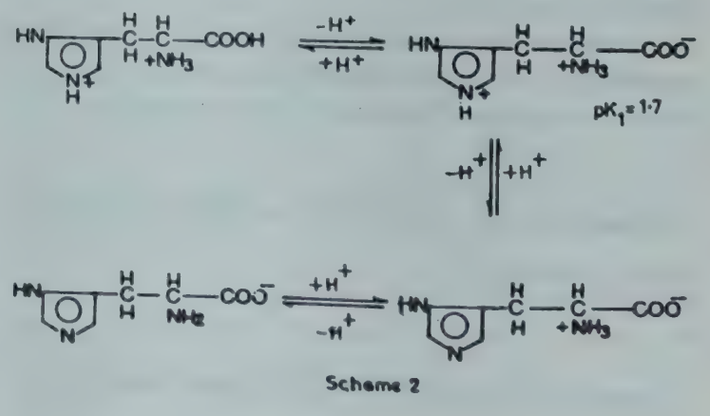

Scheme 2

$$cis\text{-}[Co(BigH)_2(H_2O)_2]^{3+} \overset{K_1}{\rightleftharpoons} cis\text{-}[Co(BigH)_2(OH)(H_2O)]^{2+} + H^+ \quad \ldots (6)$$

The pK_1 value for the first case is observed[16] to be 6. But for second case the pK_1 value, determined *p*H-

metrically in our laboratory comes out to be 8. So at $\leq$ *p*H 4 both the complexes remain mainly in diaquo form and no appreciable change in reaction rates is observed within that *p*H range. But as the *p*H is increased the percentage of hydroxoaquo species increases. The increase in rate is due to the well known labilising effect of hydroxide ion adjacent to water ligand by virtue of its lone pair capable of exerting strong electromeric effect. Hydroxide ion is also a π-donor which facilitates the formation of hydroxo intermediate species and increases the rate.

(iv) *Effect of temperature on reaction rate*

The reactions for both the cases were studied at four different temperatures at different [ligand] and the values of the rate constants for interchange processes are given in Table 1. Activation parameters ($\Delta H^{\ddagger}$ and $\Delta S^{\ddagger}$) of the two systems were evaluated from the linear Eyring plots of log k_a versus 1/T. For *cis*-$[Co(BigH)_2(H_2O)_2]^{3+}$ the $\Delta H^{\ddagger}$ value is found to be (43.41 ± 2.09) kJ mol^{-1} and $\Delta S^{\ddagger}$ value is (-171.24 ± 2.09) JK^{-1} mol^{-1} and for *cis*-$[Cr(BigH)_2(H_2O)_2]^{3+}$ the corresponding values are (26.37 ± 2.303) kJ mol^{-1} and (-215.78 ± 2.09) JK^{-1} mol^{-1}. In both the cases we obtain low $\Delta H^{\ddagger}$ values and large negative $\Delta S^{\ddagger}$ values. The activation parameters thus determined are presented in Table 3.

The activation parameters for $[Co(BigH)_2(H_2O)_2]^{3+}$ + histidine system are compared with activation parameters for substitution of aquo ligands of the Co^{III} system by phenylbiguanide as given by Chakravorty and Sil[16]. The authors observed low activation energy for the system showed by them and suggested I_a mechanism. These activation parameter values obtain by us have also been compared with activation parameters for substitution of aquo ligands of the Cr^{III} system by phenylalanine[19] where also a low $\Delta H^{\ddagger}$ value and a large negative $\Delta S^{\ddagger}$ value were observed and an I_a mechanism was suggested. For this case also $\Delta H^{\ddagger}$ value is quite low and a large negative $\Delta S^{\ddagger}$ is noticed indicating a significant ligand participation in the transition state. Considering all the results an associative interchange (I_a) mechanism is suggested for the replacement reaction of aquo ligands of *cis*-$[Co(BigH)_2(H_2O)_2]^{3+}$ by histidine.

The activation parameters for $[Cr(BigH)_2(H_2O)_2]^{3+}$ + histidine have been compared with the activation parameters for the substitution of aquo ligands of this complex by neutral ligands like 2,2′-dipyridyl and 1,10-phenanthroline[17]. Earlier authors[17] observed high activation energy for such systems and suggested an I_d mechanism. But in the present system the $\Delta H^{\ddagger}$ value is quite low while $\Delta S^{\ddagger}$ is large and negative. This indicates significant ligand participation in the transition state. Considering all the results an associative interchange (I_a) mechanism is suggested for the replacement reaction of aquo ligands of *cis*-$[Cr(BigH)_2(H_2O)_2]^{3+}$ by histidine.

Table 3 – Activation Parameters

System	$\Delta H^{\ddagger}$ (kJ mol^{-1})	$\Delta S^{\ddagger}$ (JK^{-1} mol^{-1})	Ref.
cis-$[Co(BigH)_2(H_2O)_2]^{3+}$ + Histidine	43.41 ± 2.09	-171.24 ± 2.09	This work
cis-$[Co(BigH)_2(H_2O)_2]^{3+}$ + Phenylbiguanide	57.78	−83.74	16
cis-$[Co(BigH)_2(H_2O)_2]^{3+}$ + Phenylalanine	45.97 ± 2.09	-162.03 ± 2.09	19
cis-$[Cr(BigH)_2(H_2O)_2]^{3+}$ + Histidine	26.37 ± 2.303	-215.78 ± 2.09	This work
cis-$[Cr(BigH)_2(H_2O)_2]^{3+}$ + 2,2′-dipyridyl	85.82	2.93	17
cis-$[Cr(BigH)_2(H_2O)_2]^{3+}$ + 1,10-phenanthroline	82.89	−3.34	17

Conclusion

The results obtained in the present study suggest that the reactions between $[M(BigH)_2(H_2O)_2]^{3+}$ with histidine involve outersphere association between the two reacting species followed by an associative interchange process where both bond breaking and bond making occur in a concerted manner. Generally substitution of aquo ligands from Co(III) aquo complexes proceed through dissociative pathway. But in the ana-

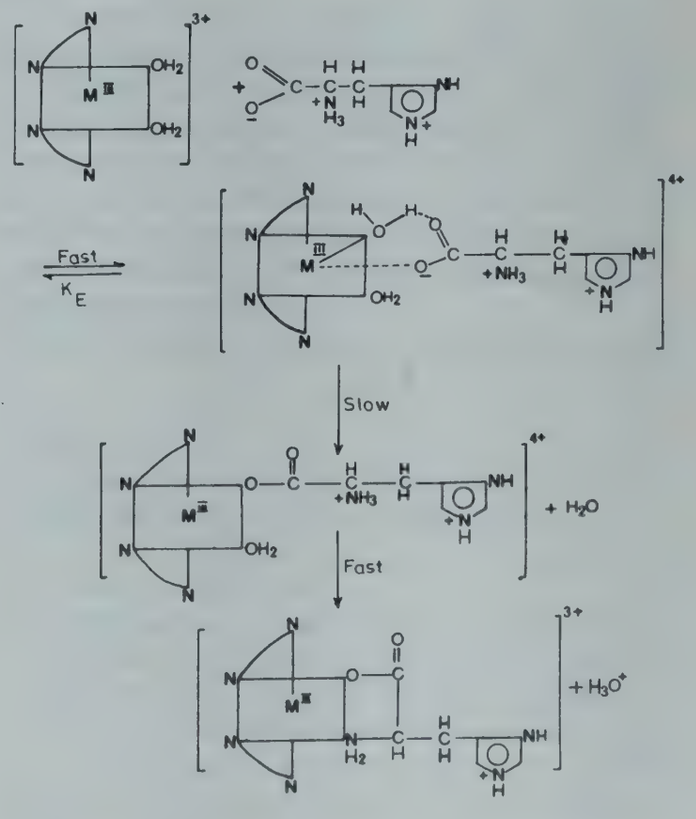

Scheme 3 – Probable mechanism for anation process

tion of $[Co(BigH)_2(H_2O)_2]^{3+}$ by histidine, a low $\Delta H\ddagger$ and a negative $\Delta S\ddagger$ prompted us to invoke an associative interchange mechanism. The following argument can be given as an explanation for such observation. Biguanide itself is an unsaturated ligand and has a π-back bonding tendency. It is likely that the π-bonding of the bischelate ligand removes electron cloud around cobalt and chromium centres from t_{2g} orbitals, thereby increasing the tendency of these orbitals to accept the incoming ligand. Therefore, significant bond formation takes place before any bond breakage in the transition state. In the present systems such a mechanism is supported by the low $\Delta H\ddagger$ values, because the energy of the bond breaking is partially compensated by the energy released due to the bond formation by the incoming ligand. The probable scheme of the reaction is drawn in Scheme 3. A compact associated transition state is produced by the ion-pair formation between Complex-I and ligand by H-bonding as shown in Scheme 3.

References

1 Hamm R E, Johnson R L, Perkins R H & Davis R E, *J Am chem Soc*, **80** (1958) 4469.

2 Banerjea D & Duttachaudhury S, *J inorg nucl Chem*, **32** (1970) 1617.

3 Mandal J N & De G S, *Indian J Chem*, **16A** (1978) 580.

4 Pearson R G & Moore J W, *Inorg Chem*, **3** (1964) 1334.

5 Pal M & De G S, *Indian J Chem*, **14A** (1976) 763.

6 Dhar A, Das S, Banerjee R N & Banerjea D, *Trans met Chem*, **7** (1982) 125.

7 Basak A K & Chatterjee C, *Trans met Chem*, **5** (1980) 212.

8 Bishnu M N, Chakravorty B, Banerjee R N & Banerjea D, *J coord Chem*, **13** (1983) 63.

9 Swaddle T W, *Coord Chem Rev*, **14** (1974) 217.

10 Chatterjee C & Chaudhury P, *Indian J Chem*, **9** (1971) 1132.

11 Banerjea D & Dasgupta T P, *J inorg nucl Chem*, **27** (1965) 2617.

12 Ray P & Ghosh S P, *J Indian chem Soc*, **19** (1942) 1.

13 Ray P, *J Indian chem Soc*, **14** (1937) 675.

14 Ray P, *J Indian chem Soc*, **15** (1938) 355.

15 Banerjea D & Chakravorty B, *J inorg nucl Chem*, **26** (1964) 1233.

16 Chakravorty B & Sil A K, *Indian J Chem*, **15A** (1977) 502.

17 Sengupta S & Banerjea D, *Z anorg alleg Chem*, **93-96** (1976) 424.

18 Basolo F & Pearson R G, *Mechanism of inorganic reactions* (Wiley Eastern, New Delhi) 1977, pp. 154.

19 De G S & Gangopadhyay A K, *Indian J Chem*, **26A** (1987) 824.

Indian Journal of Chemistry
Vol. 27A, September 1988, pp. 783-785

Kinetics of Oxidation of Triethylenetetraamine by Hexacyanoferrate(III)

(Miss) PRATIMA MISHRA & PREM C NIGAM*

Department of Chemistry, Indian Institute of Technology, Kanpur 208 016

Received 6 *October* 1987; *revised* 23 *December* 1987; *accepted* 15 *January* 1988

The kinetics of the title reaction has been investigated spectrophotometrically at 410 nm, *p*H = 10.5, $I = 0.13$ mol dm^{-3} (KNO_3) and temp. = 30 ± 0.1°C. The reaction exhibits first order dependence each in [hexacyanoferrate(III)] and [trien] and overall second order. The rate constant increases in the *p*H range of 8.5 to 11.85. The reactive species of trien (abbrev. P) in the above *p*H region are H_2P^{2+}, HP^{+1} and P. From the *p*H dependence data it has been possible to resolve the rate constants due to reactions of $Fe(CN)_6^{3-}$ with P ($k_1 = 1.9 \times 10^{-1}$ dm^3 mol^{-1} s^{-1}) and HP^+ ($k_2 = 1.6 \times 10^{-1}$ dm^3 mol^{-1} s^{-1}). The rate of reaction between $Fe(CN)_6^{3-}$ and H_2P^{2+} is extremely slow. The effect of ionic strength is found to be negligible. The activation parameters evaluated are: $\Delta H^{\neq} = 39 \pm 2.8$ kJ mol^{-1} and $\Delta S^{\neq} = -298 \pm 2$ JK^{-1} mol^{-1}. An electron transfer from $Fe(CN)_6^{3-}$ to the substrate during decomposition of the latter is proposed.

During investigation of ligand exchange reactions between polyaminocarboxylato complexes of Fe(III) and cyanide, we observed[1,2] that the reaction product, hexacyanoferrate(III) further oxidises the released ligands and in turn gets converted into hexacyanoferrate(II). We have also reported our results on the kinetics of oxidation of diethylenetriaminepentaacetic acid by hexacyanoferrate(III)[3]. We also noticed that hexacyanoferrate(III) oxidises polyamines. It was considered worthwhile to study the kinetics and mechanism of oxidation of a typical polyamine, viz. triethylenetetraamine (trien) by the same oxidant.

Materials and Methods

Potassium hexacyanoferrate(II) (AR, Sarabhai M) potassium hexacyanoferrate(III) (AR, SDS) and triethylenetetraamine (AR, Fluka) were used as such. *p*H was maintained at any desired value by the addition of either sodium hydroxide or perchloric acid. The *p*H meter was standardized with standard BDH buffers. Potassium nitrate (AR) was used to maintain ionic strength.

A Toshniwal spectrophotometer RL-02 model, fitted with a circulatory arrangement for thermostating the cell compartment, was used for kinetic study. The temperature could be controlled within ±0.1°C. A Shimadzu double beam spectrophotometer UV-240 model was used for recording the spectral changes and for the kinetic study also. All *p*H measurements were made on an Elico digital *p*H meter LI-120 model.

Kinetic measurements

The reaction between trien and hexacyanoferrate(III) was followed at 420 nm (λ_{max} of $[Fe(CN)_6]^{3-}$, $\varepsilon = 1020$ dm^3 mol^{-1} cm^{-1}), *p*H = 10.5, $I = 0.134$ mol dm^{-3} (KNO_3) and temp. = 30 ± 0.1°C. The kinetics of reaction was studied under pseudo-first order conditions, viz. [trien] ≫ [oxidant]. Solutions of hexacyanoferrate(III) and trien were equilibrated at the desired temperature for 30 min before mixing. The ionic strength and *p*H were adjusted each time before mixing the reactants.

The pseudo-first order rate constants were calculated from plots of log C_A versus time, where C_A refers to $[K_3Fe(CN)_6]$ remaining at any time t. The absorbance c! nges were observed for at least 70% of the reaction.

Results

Stoichiometry

A known excess of $Fe(CN)_6^{3-}$ was added to a known quantity of trien and the absorbance change at 410 nm was determined after no appreciable changes in absorbance were observed (≈ 4 days). The ratio of mol of hexacyanoferrate(III) per mol of trien was 1.07 ± 0.04 (average of four values). The *p*H of the reaction mixtures was kept at 10.5 and temperature at 30 ± 1.0°C. The reaction may, therefore, be expressed by Eq. (1)

$$Fe(CN)_6^{3-} + \text{trien} \rightarrow Fe(CN)_6^{4-} + \text{oxidation products} \quad \ldots (1)$$

Kinetics

In Table 1 are given the pseudo-first order rate constants and the second order rate constants.

Dependence of rate on pH

The reaction was studied in the *p*H range of 8.5-11.85 and the rate constants at various *p*H values are reported in Table 2. The species distribution of trien at various *p*H values, shown in Fig. 1, were calculated on a Dectane-10 computer using a programme developed by Perrin and Sayce[4]. The predominant species of trien in the *p*H range of interest are H_2P^{2+}

Table 1—Evaluation of Pseudo-first Order Rate Constants and Second Order Rate Constants

$[Fe(CN)_6^{3-}] = 5.0 \times 10^{-4}$ mol dm^{-3}; pH = 10.5, temp. = 30 ± 0.1°C; I = 0.13 mol dm^{-3} (KNO_3)

$10^3 \times [\text{trien}]_T$ (mol dm^{-3})	$k_{obs} \times 10^3$ (s^{-1})	$k_f = k_{obs}/[\text{trien}]_T \times 10^1$ (dm^3 mol^{-1} s^{-1})
5.0	0.9	1.8
7.5	1.3	1.7
10.0	1.8	1.8
12.5	2.2	1.8
15.0	2.6	1.7
		Av (1.76 ± 0.05)

Table 2—Effect of Varying pH on Reaction of $Fe(CN)_6^{3-}$ with trien, $[Fe(CN)_6^{3-}] = 5 \times 10^{-4}$ mol dm^{-3}; $[\text{trien}]_T = 10^{-2}$ mol dm^{-3}; temp. = 30 ± 0.1°C; and I = 0.13 mol dm^{-3} (KNO_3)

pH	$k_{obs} \times 10^3$ (s^{-1})	pH	$k_{obs} \times 10^3$ (s^{-1})
8.5	1.35	10.5	1.79
9.0	1.45	11.0	1.86
9.5	1.58	11.85	1.88
10.0	1.66		

($K_2 = 10^{9.08}$), HP^+ ($K_1 = 10^{9.80}$)[5] and P in varying proportions. It is observed that between pH 8.5 and 10.0, the reaction rate increases linearly with increase in pH and levels off at pH > 9.5. Below pH 8.5 the rate is extremely slow. The rate can be expressed by Eq. (2).

$$\text{Rate} = k_f[Fe(CN)_6^{3-}][P]_T \quad \ldots (2)$$

In Eq. (2) the concentration term $[P]_T$ includes all protonated and unprotonated forms of trien. The rate of oxidation of trien by $[Fe(CN)_6]^{3-}$ can also be given by Eq. (3).

$$\begin{aligned}\text{Rate} &= [Fe(CN)_6^{3-}]\{k_1[P] + k_2[HP^+] + k_3[H_2P^{2+}]\} \\ &= [Fe(CN)_6^{3-}]\{k_1[P] + k_2K_1[H^+][P] \\ &\quad + k_3K_1K_2[H^+]^2[P]\} \\ &= [Fe(CN)_6^{3-}]\{k_1 + k_2K_1[H^+] + k_3K_1K_2[H^+]^2\}[P]\end{aligned} \quad \ldots (3)$$

where k_1, k_2 and k_3 are the rate constants for the species P, HP^+ and H_2P^{2+} respectively; and K_1 and K_2 are the first and second protonation constants of trien.

Comparing Eqs (2) and (3) we get

$$k_f\frac{[P]_T}{[P]} = k_1 + k_2K_1[H^+] + k_3K_1K_2[H^+]^2 \quad \ldots (4)$$

$$\text{where } \frac{[P_T]}{[P]} = 1 + K_1[H^+] + K_1K_2[H^+]^2$$

At pH above 10.0 the terms containing $[H^+]^2$ can be neglected. So Eq. (4) is simplified to Eq. (5).

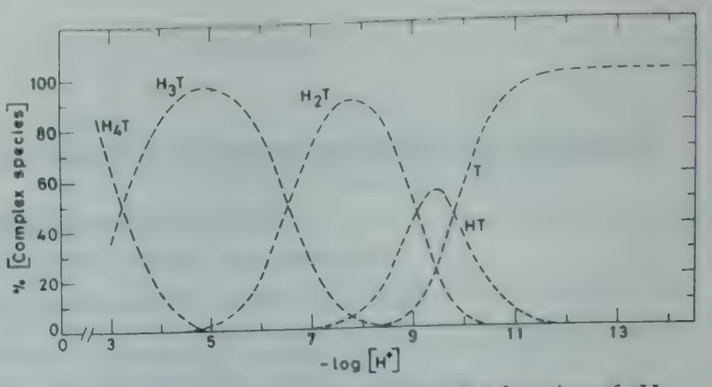

Fig. 1—Species distribution of trien as a function of pH

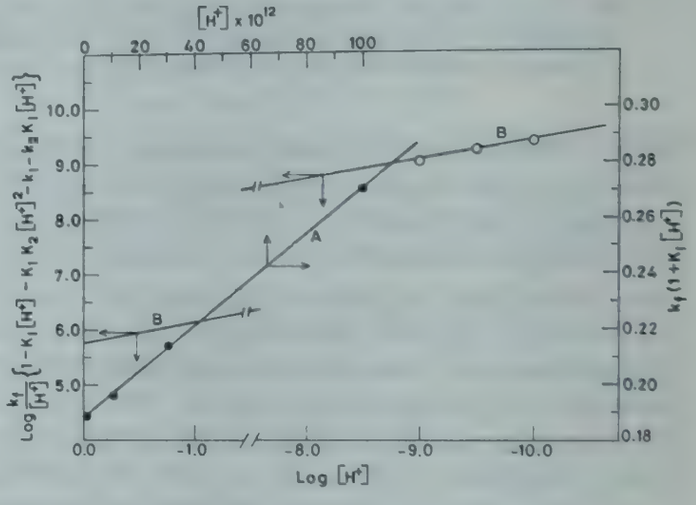

Fig. 2—Resolution of rate constants due to reaction of $Fe(CN)_6^{3-}$ with P and HP^+ (A); and with HP^+ and H_2P^{2+} (B).

$$k_f\{1 + K_1[H^+]\} = k_1 + k_2K_1[H^+] \quad \ldots (5)$$

In higher pH region a plot of left hand side of Eq. (5) versus $[H^+]$ is linear (Fig. 2), the slope of which gives the value of k_2 (i.e. reaction rate between $Fe(CN)_6^{3-}$ and HP^+) equal to $(1.7 \pm 0.05) \times 10^{-1}$ dm^3 mol^{-1} s^{-1}. The intercept of the linear plot gives k_1 (i.e. rate constant for reaction between P and $Fe(CN)_6^{3-}$ equal to $(1.9 \pm 0.05) \times 10^{-1}$ dm^3 mol^{-1} s^{-1}. Further transforming expression (4) and taking logarithm, we get

$$\log\frac{k_f}{[H^+]}\{1 + K_1[H^+] + K_1K_2[H^+]^2 - k_1 - k_2K_1[H^+]\}$$

$$= \log(k_3K_1K_2) + \log[H^+] \quad \ldots (6)$$

A plot of left hand side of Eq. (6) versus $\log[H^+]$ is linear (Fig. 2), the slope of which is close to one and the intercept gives an estimated value of k_3 equal to $(7.4 \pm 0.5) \times 10^{-14}$ dm^3 mol^{-1} s^{-1}. This is consistent with the observation that the rate below pH 8.5 is extremely slow.

Activation parameters

Activation parameters for this reaction have been calculated from Arrhenius plot in the temperature

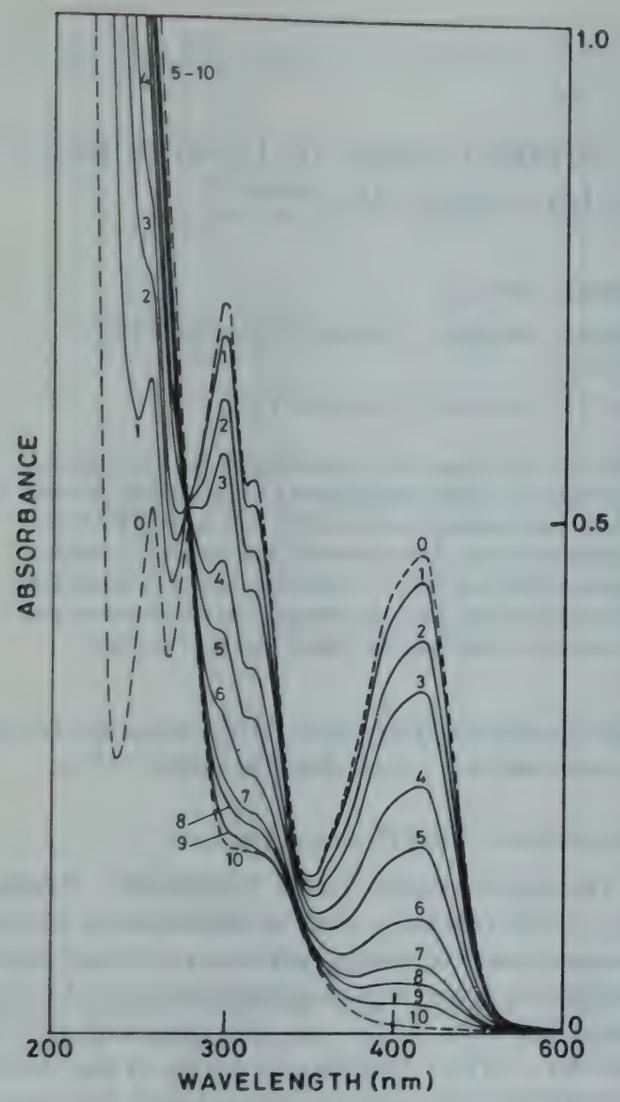

Fig. 3—Repetitive scan of the reaction mixture during a kinetic run ($[Fe(CN)_6^{3-}] = 5 \times 10^{-4}$ mol dm^{-3}; [trien] = 10^{-2} mol dm^{-3}; *p*H = 10.5; I = 0.13 mol dm^{-3} (KNO_3); temp. = 27° ± 0.1°C (curves 1-10 were obtained after time intervals of 1, 2, 3.75, 7.5, 11.0, 18.5, 26.5, 34.0, 48.0 min and 16 hr respectively)

range of 25°-37°C and values are: $\Delta H^{\neq} = 39 \pm 2.8$ KJ mol^{-1}, and $\Delta S^{\neq} = 298 \pm 2$ JK^{-1} mol^{-1}.

Effect of ionic strength on rate

There is negligible effect of ionic strength on the rate in the range $I = (0.1 - 1.35)$ mol dm^{-3} at *p*H = 10.5.

Discussion

The kinetic data given in Table 1 are consistent with the interaction of P with hexacyanoferrate(III) in a bimolecular step. The presence of cyanide in the concentration range of 2.5×10^{-2} to 5.5×10^{-2} mol dm^{-3} also does not materially affect the forward rate ruling out the possibility of prior dissociation of the hexacyanoferrate(III).

As the reaction is mainly between a charged $Fe(CN)_6^{3-}$ and an uncharged trien, we do expect the rate to be independent of ionic strength. This is consistent with the observation recorded above for the ionic strength effect at *p*H = 10.5.

The spectral changes occurring during a typical kinetic run are shown in Fig. 3. There is a continuous decrease in the peak heights of the peaks at 410 nm and 303 nm due to hexacyanoferrate(III). Hexacyanoferrate(II) exhibits weak absorption bands at 322 and 260 nm, but these could not be observed because they were lost in the shoulder and peaks of hexacyanoferrate(III) at 325 and 262 nm respectively. An isosbestic point at 281 nm indicates the coexistence of two species, viz. $Fe(CN)_6^{3-}$ and $Fe(CN)_6^{4-}$ in the reaction mixture. Two specific tests for hexacyanoferrate(II), viz. ammonium molybdate and thorium nitrate[6] tests confirm the formation of $Fe(CN)_6^{4-}$ as one of the reaction products. The absence of any new peak points to the fact that no reaction intermediate is possibly present in any appreciable concentration. The absorption peaks of other products may be in the UV region where trien absorbs strongly. Their existence in the reaction mixture cannot, therefore, be observed in the given spectrum (Fig. 3). The identification of the oxidation products of trien has not been possible because their separation and isolation, though attempted, were not successful. Oxidation of primary amines by Pd^{II} and Au^{III} are reported to lead to ketones, aldehydes or carboxylic acids depending upon reaction *p*H and structure of amine. The oxidation of indoline on the other hand gave indole[7].

Results presented above point to an outer sphere electron transfer from hexacyanoferrate(III) to trien in a bimolecular step. Under the present conditions of the reaction, the reactants were $Fe(CN)_6^{3-}$ on the one hand and trien and $Htrien^+$ on the other depending on the *p*H of the medium. The respective rate constants have been resolved (vide infra). The highly negative value of $\Delta S^{\neq}$ shows that the activated complex obtained in the bimolecular process is highly charged. The low E_a is also understandable because no bond breaking takes place during the course of reaction.

References

1 Naik R M & Nigam P C, *Transition Met Chem*, **10** (1985) 227.
2 Mishra Pratima, Naik R M & Nigam P C, *Inorg Chim Acta*, **127** (1987) 71.
3 Gupta Nishi, Nigam P C & Naik R M, *Indian J Chem*, **25A** (1986) 39.
4 Perrin D D & Sayce I G, *Talanta*, **14** (1967) 833.
5 Margerum D W, Rorabacher D B & Clarkejun J F G, *Inorg Chem*, **2** (1983) 667.
6 Vogel A I, '*Text book of macro and micro quantitative inorganic analysis*' (Orient Longman, New Delhi) 1982, 321.
7 Kuehne M E & Hall T C, *J Org Chem*, **41** (1976) 77.

Indian Journal of Chemistry
Vol. 27A, September 1988, pp. 786-789

Kinetics & Mechanism of Oxidation of Semicarbazide by Chloramine-B Bromamine-B & Dichloramine-B

B THIMME GOWDA* & J ISHWARA BHAT†

Department of Post-graduate Studies and Research in Chemistry, Mangalore University, Mangalagangothri, Mangalore 574199

Received 10 *August* 1987; *revised* 6 *November* 1987; *accepted* 21 *December* 1987

Kinetics of oxidation of semicarbazide (SC) by chloramine-B (CAB) in acid medium, bromamine-B (BAB) in acid and alkaline media and dichloramine-B (DCB) in 50% (v/v) aqueous methanol have been investigated. Oxidations by CAB and DCB show first order dependence in [oxidant], fractional order in [SC] and fractional order in $[H^+]$. In the case of BAB oxidation in acid medium the reaction orders in [BAB] and [SC] are unity and fractional, but inverse fractional in $[H^+]$. In alkaline medium the oxidation is first order in [BAB] and zero order each in [SC] and $[OH^-]$. Variations in ionic strength and dielectric constant of the reaction medium and added reaction products do not have any significant effect on the rates of oxidations. Mechanisms consistent with the observed kinetics have been proposed and the related rate laws derived.

The title investigation is a part of our kinetic and mechanistic studies on the oxidations of organic substrates by positive halogens in general and N-halo-N-metallo aromatic sulphonamides in particular[1-3].

Materials and Methods

The oxidants chloramine-B (CAB), bromamine-B (BAB) and dichloramine-B (DCB) were prepared by literature methods and their purity checked by recording their spectra and estimating the amount of active halogen present in them. Stock solutions (0.1 mol dm^{-3}) of CAB and BAB (aqueous) and DCB (in methanol) were prepared, standardised and stored in dark coloured bottles. Aqueous stock solution ($\sim$ 0.1 mol dm^{-3}) of semicarbazide (SC; E. Merck) was used. The ionic strength of the reaction medium was kept at 0.3 mol dm^{-3} by adding concentrated solution of sodium perchlorate (E. Merck). All other reagents used were of AR grade.

Kinetic Measurements

The kinetic studies were made under pseudo-first order conditions with [SC] $\gg$ [oxidant] (5 to 20 fold excess). The reactions were initiated by the rapid addition of requisite amounts of oxidant solutions, thermally pre-equilibrated at a desired temperature, to a mixture containing known amounts of SC, perchloric acid (or sodium hydroxide with BAB) and sodium perchlorate solution and water (and methanol in the case of DCB to maintain 1:1 (v/v) aqueous methanol), pre-equilibrated at the same temperature. The progress of the reactions was monitored for at least two half-lives by iodometric estimation of unreacted [oxidant] at regular time intervals. The pseudo-first order rate constants were computed by the method of least squares and were reproducible within $\pm$ 3%.

Stoichiometry and Product Analysis

The stoichiometries of SC – CAB, SC – BAB and SC – DCB reactions were determined by allowing the reactions (containing mixtures of SC and oxidant in different ratios) to go to completion at 303 K at different $[H^+]$ or $[OH^-]$ in the range of 0.02-0.2 mol dm^{-3}. The presence of cyanate in the reaction mixtures was detected by standard tests. Benzenesulphonamide (BSA), the reduced product of the oxidants was detected by TLC. The observed stoichiometries may be represented by Eq. (1).

$$NH_2NHCONH_2 + 2RNHX\ (\text{or } RNX_2) \rightarrow 2RNH_2\ (\text{or } RNH_2) + N_2 + CNO^- + 2X^- + 3H^+ \quad \ldots(1)$$

where $R = C_6H_5SO_2$ and X = Cl or Br.

Although the observed 1:4 stoichiometry may also be represented by Eq. (2),

$$NH_2NHCONH_2 + 2RNHX\ (\text{or } RNX_2) + H_2O \rightarrow 2RNH_2\ (\text{or } RNH_2) + N_2 + CO_2 + NH_4^+ + 2X^- + H^+ \quad \ldots(2)$$

corresponding to the formation of CO_2 and ammonia as products instead of CNO^-, the former products are formed in negligible proportions.

Results and Discussion

Kinetics of oxidations of semicarbazide (SC) by CAB, in aqueous perchloric acid medium, by BAB in

†Govinda Dasa College, Surathkal 574158

Table 1—Pseudo-first Order Rate Constants (k_{obs}) for Oxidation of Semicarbazide by Chloramine-B, Bromamine-B and Dichloramine-B

(Temp. = 303 K; μ = 0.3 mol dm^{-3})

10^3[oxidant]$_0$ (mol dm^{-3})	10^2[SC]$_0$ (mol dm^{-3})	10 [H$^+$] (mol dm^{-3})	10^4 k_{obs} (s^{-1})		
			CAB	BAB[a]	DCB[b]
0.2	2.0	0.5	8.5	—	—
0.3	2.0	0.5	—	7.9	8.8
0.5	2.0	0.5	8.5	7.8	8.9
1.0	2.0	0.5	8.5	7.8	8.9
2.0	2.0	0.5	8.6	7.8	8.9
3.0	2.0	0.5	—	7.7	8.8
4.0	2.0	0.5	8.6	—	—
1.0	0.5	0.5	5.8	3.6	4.9
1.0	1.0	0.5	6.9	5.2	6.6
1.0	2.0	0.5	8.5	7.8	8.9
1.0	4.0	0.5	—	11.6	10.7
1.0	5.0	0.5	10.5	13.8	—
1.0	10.0	0.5	12.3	17.4	18.2
1.0	2.0	0.1	5.9	—	7.7
1.0	2.0	0.2	7.2	11.2	8.5
1.0	2.0	0.5	8.5	9.3	8.9
1.0	2.0	1.0	9.8	7.8	9.8
1.0	2.0	1.5	10.5	7.1	—
1.0	2.0	2.0	10.7	6.3	10.0

(a) 10 [H$^+$] = 1.0 mol dm^{-3}
(b) 50% (v/v) aq. methanol medium.

Table 2—Pseudo-first Order Rate Constants (k_{obs}) for Oxidation of Semicarbazide by Bromamine-B in Alkaline Medium at 303 K.

(μ = 0.3 mol dm^{-3})

10^3[oxidant]$_0$ (mol dm^{-3})	10^2[SC]$_0$ (mol dm^{-3})	10^2[OH$^-$] (mol dm^{-3})	10^4 k_{obs} (s^{-1})
0.2	2.0	5.0	8.2
0.5	2.0	5.0	8.2
1.0	2.0	5.0	8.1
2.0	2.0	5.0	8.1
3.0	2.0	5.0	8.0
1.0	0.5	5.0	8.0
1.0	1.0	5.0	8.1
1.0	2.0	5.0	8.1
1.0	5.0	5.0	8.2
1.0	10.0	5.0	8.4
1.0	2.0	2.0	8.3
1.0	2.0	5.0	8.1
1.0	2.0	10.0	8.0
1.0	2.0	15.0	8.1
1.0	2.0	20.0	7.9

Table 3—Kinetic Orders in [oxidant], [S], [H$^+$] and [OH$^-$] and Activation Parameters for Oxidation of Semicarbazide by Chloramine-B, Bromamine-B and Dichloramine-B[a]

Orders observed in	CAB	BAB	DCB	BAB[(b)]
[Oxidant]	1	1	1	1
[S]	0.28	0.57	0.42	0
[H$^+$] or [OH$^-$]	0.2	−0.27	0.10	0
Activation parameters				
log A	6.17	6.7	6.84	5.15
Ea (kJ mol^{-1})	53.6	54.6	57.4	48.0
$\Delta H^{\ddagger}$ (kJ mol^{-1})	51.1	52.1	54.9	45.5
$\Delta S^{\ddagger}$ (JK^{-1})	−30.3	−31.0	−27.3	−34.9
$\Delta G^{\ddagger}$ (kJ mol^{-1})	60.3	61.5	63.2	56.1

(a) Activation parameters of BAB oxidations in acid medium are for the rate-determining step. In all other cases the values correspond to overall reactions.
(b) Alkaline medium.

acid and alkaline media and DCB in 1:1 aqueous methanol were investigated at several initial concentrations of the reactants, $HClO_4$ or OH^- (0.02-0.2 mol dm^{-3}, Tables 1-3). At constant [$HClO_4$] or [NaOH] with several fold (15 to 20 times) excess of the substrate, the plots of log ([oxidant]$_0$/[oxidant]) versus time were linear for two half-lives with all the oxidants and the pseudo-first order rate constants were unaffected by changes in [oxidant]$_0$, establishing first order in [oxidant]. At constant [oxidant]$_0$ and [$HClO_4$] the rates increased with increase in [SC] and the plots of log k_{obs} versus log [SC] (Table 1) were linear with varying fractional slopes indicating fractional order kinetics in [SC] with all the oxidants (Table 3). But the

rate was independent of [SC] in BAB oxidation in alkaline medium. At constant $[oxidant]_0$ and $[SC]_0$ the rates slightly increased with increase in $[HClO_4]$ giving fractional order dependence in CAB and DCB oxidations. In the case of BAB as oxidant the rate decreased with increase in $[HClO_4]$ and showed inverse fractional order in $[H^+]$ and the rate was independent of $[OH^-]$ in alkaline solutions.

The rates varied slightly with change in ionic strength of the medium in all the cases. Decrease in dielectric constant of the medium by changing the solvent composition by adding methanol slightly increased the rate in all the cases. The plots of log k versus 1/D were linear with positive slopes. Addition of reaction products benzenesulphonamide (BSA) and Cl^-/Br^- had negligible effect on the rates of oxidations with all the oxidants in both acid and alkaline media.

The substrate concentrations were varied at different temperatures and the rate constants of the rate limiting steps were computed, which in turn were used to compute the activation parameters from the Arrhenius plots (Table 3).

In acid solutions of the oxidants, the probable reactive species[4] are RNHX, RNH_2X^+, HOX and H_2OX^+. In alkaline solutions the likely oxidising species are RNHX, HOX and OX^-.

Mechanisms

(i) *With chloramine-B*

The first order dependence in [CAB], fractional order in [S] and fractional order in $[H^+]$ may be explained by the mechanism shown in Scheme 1.

$$RNHCl + H^+ \overset{K_1}{\rightleftharpoons} RNH_2Cl^+ \quad \text{(fast)}$$

$$RNH_2Cl^+ + S \overset{K_2}{\rightleftharpoons} Y \quad \text{(fast)}$$

$$Y \overset{k_3}{\rightarrow} Y' + RNH_3^+ \quad \text{(slow)}$$

$$Y' + RNH_2Cl^+ \overset{k_4}{\rightarrow} \text{products} \quad \text{(fast)}$$

Scheme 1

Based on Scheme 1, the rate laws (3 and 4) have been deduced.

$$\frac{-d[CAB]}{dt} = \frac{K_1K_2k_3[CAB]_t\,[S][H^+]}{1 + K_1[H^+] + K_1K_2[H^+][S]} \quad \ldots(3)$$

or

$$k_{obs} = \frac{K_1K_2k_3[S][H^+]}{1 + K_1[H^+] + K_1K_2[H^+][S]} \quad \ldots(4)$$

(ii) *With dichloramine-B*

Here again the first order dependence in [DCB], and fraction order each in [S] and $[H^+]$ could be explained by a mechanism similar to that shown in Scheme 1.

(iii) *With bromamine-B*: (a) *In acid medium*

The first order dependence in [BAB], fractional order in [S] and inverse fractional order in $[H^+]$ observed in acid medium may be accounted for by a Michaelis-Menten type mechanism shown in Scheme 2.

$$SH^+ \overset{K_5}{\rightleftharpoons} S + H^+ \quad \text{(fast)}$$

$$RNHBr + S \overset{K_6}{\rightleftharpoons} Z \quad \text{(fast)}$$

$$Z \overset{k_7}{\rightarrow} Z' + RNH_2 \quad \text{(slow)}$$

$$Z' + RNHBr \overset{k_8}{\rightarrow} \text{products} \quad \text{(fast)}$$

Scheme 2

Applying steady state hypothesis to the intermediate (Z), the rate laws (5-7) have been deduced.

$$\frac{-d[BAB]}{dt} = \frac{K_6k_7[RNHBr]_0[S]}{1 + K_6[S]}$$

$$= \frac{K_5K_6k_7[RNHBr]_0[SH^+]}{[H^+] + K_5K_6[SH^+]} \quad \ldots(5)$$

$$k_{obs} = \frac{K_6k_7[S]}{1 + K_6[S]}$$

$$= \frac{K_5K_6k_7[SH^+]}{[H^+] + K_5K_6[SH^+]} \quad \ldots(6)$$

$$\frac{1}{k_{obs}} = \frac{1}{K_6k_7[S]} + \frac{1}{k_7}$$

$$= \frac{[H^+]}{K_5K_6k_7[SH^+]} + \frac{1}{k_7} \quad \ldots(7)$$

Plots of $1/k_{obs}$ versus $1/[S]$ and $1/k_{obs}$ versus $[H^+]$ were linear with finite intercepts (Fig. 1) in accordance with rate law (7). From the slope and intercept of the former plot values of k_7 and K_6 were calculated. The constants were also computed at different temperatures by varying [S] at each temperature (K_6 ($mol^{-1}\,dm^{-3}\,s^{-1}$): 31.9, 32.8 and 31.8 respectively and k_7 (s^{-1}): 11.2, 22.2 and 46.7 respectively at 293, 303 and 313 K). k_7 values at different temperatures were used to calculate the activation parameters from the Arrhenius plots (Table 3).

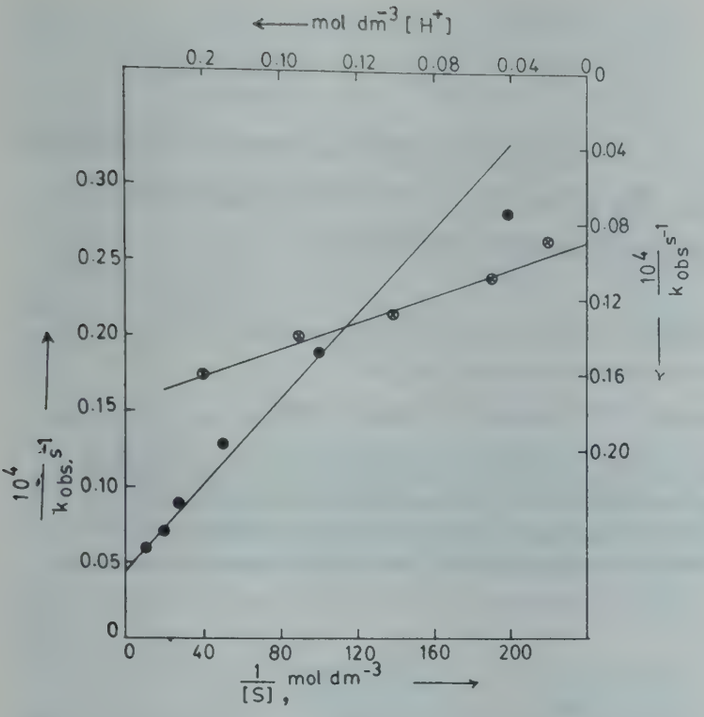

Fig. 1—(A) Plot of $1/k_{obs}$ versus $1/[S]$ ($10^3\,[BAB]_0 = 10\,[HClO_4]$ $= 1.0$ mol dm^{-3}; temp. = 303 K; $\mu = 0.3$ mol dm^{-3})

(B) Plot of $1/k_{obs}$ versus $[H^+]$ ($10^3\,[BAB]_0 = 1.0$ mol dm^{-3}; $10^2\,[SC] = 2.0$ mol dm^{-3}; temp. = 303 K; $\mu = 0.3$ mol dm^{-3}).

(b) *In alkaline medium*

The first order dependence in [BAB] and zero order each in [S] and $[OH^-]$ may be explained by a mechanism shown in Scheme 3.

$$RNBr^- + H_2O \xrightarrow{k_9} RNH_2 + OBr^- \quad \text{(slow)}$$

$$OBr^- + S \xrightarrow{k_{10}} \text{products} \quad \text{(fast)}$$

Scheme 3

Scheme 3 leads to rate laws (8 and 9).

$$\frac{-d[BAB]}{dt} = k_9[BAB][H_2O] \qquad \ldots(8)$$

$$k_{obs} = k_9[H_2O] \qquad \ldots(9)$$

The proposed mechanisms are also supported by moderate values of the activation parameters. The formation of more ordered activated complexes is evident from the negative $\Delta S^{\ddagger}$ values.

References

1 Gowda B T & Bhat J I, (a) *React Kinet Catal Lett*, **31** (1986) 461; *Indian J Chem*, **25A** (1986) 1129, 1149; **26A** (1987) 215; (b) *J Indian chem Soc*, **63** (1986) 665; **64** (1987) 150; (c) *Tetrahedron*, **43** (1987) 2119.

2 Gowda B T & Mrs Rao R V, (a) *Indian J Chem*, **24A** (1985) 1021; **25A** (1986) 578, 968; (b) *Oxidn Commn*, **10** (1987) 31; (c) *J chem Soc Perkin Trans* 2 (1988) 355.

3 Gowda B T & Sherigara B S, (a) *Oxidn Commn*, **9** (1986) 165; (b) *Indian J Chem*, **25A** (1986) 960; **26A** (1987) 930; (c) *J Indian chem Soc*, **64** (1987) 158.

4 Campbell M M & Johnson G, *Chem Rev*, **78** (1978) 65.

Indian Journal of Chemistry
Vol. 27A, September 1988, pp. 790-793

Reactions of N-(2,4-Dinitrophenoxy)-9,10-dihydroanthracene-9,10-*endo*-α,β-succinimide with Hydroxide Ion, Piperidine, Cyclohexylamine & Morpholine: Evidence for Base Catalysis

RANJUMONI SAIKIA, ASHOK KUMAR SINGH & GURUDAS BHATTACHARJEE*
Department of Chemistry, University of Roorkee, Roorkee 247 667

Received 29 *September* 1987; *revised* 4 *December* 1987; *accepted* 14 *January* 1988

Kinetics of hydrolysis of N-(2,4-dinitrophenoxy)-9,10-dihydroanthracene-9,10-endo-α,β-succinimide with hydroxide ion, piperidine, cyclohexylamine and morpholine has been studied in 1:4 aqueous acetonitrile at 35 ± 0.1°C. Evidence for base catalysis has been obtained for reactions with hydroxide ion and piperidine. Relative ease of detachment of the nucleofuge from the intermediate complex seems to account for the absence of base catalysis in the case of morpholine and cyclohexylamine.

Substitution reactions on various nitro-activated halobenzenes, ethers and related compounds have been intensively studied[1-6] in the presence of amines and other bases. Evidence for base catalysis has been obtained in many cases[7,8] and in others either no base catalysis or negligible catalysis has been observed[9-14]. Occurrence of base catalysis seems to be dependent on the structural and electronic nature of the amine, the nucleofuge and the solvent[15-19]. But dependence of catalysis on electronic and structural nature of the leaving group is yet a subject of study. Simple leaving groups like halogen, alkoxy and aryloxy on nitro activated benzene nucleus have already been studied. It is worthwhile, studying a case where the leaving group is bulky and sterically hindered.

N-Hydroxy compounds derived from various Diels-Alder adducts have found extensive use in peptide synthesis[20-22]. In view of their importance, results of kinetic studies on N-(2,4-dinitrophenoxy)-9,10-dihydroanthracene-9,10-*endo*-α,β-succinimide (**2**) with hydroxide ion, piperidine, cyclohexylamine and morpholine in aqueous acetonitrile (1:4, v/v) at 35 ± 0.1°C are presented and discussed in this paper.

Materials and Methods

N-(2,4-Dinitrophenoxy)-9,10-dihydroanthracene-9,10-endo-α,β-succinimide (**2**): (a) *Anthracene-maleic anhydride adduct*

The adduct was prepared as per method given elsewhere[23] and recrystallized from xylene, m.p. 261° (lit.[23] 261-62°).

(b) *N-Hydroxy 9,10-dihydroanthracene-9,10-endo-α,β-succinimide* (**1**)

The above adduct (5 g, 0.018 mol) was converted into **1** by refluxing with hydroxylamine hydrochloride (1.25 g, 0.018 mol) in ethanol (2 hr) in the presence of a trace of pyridine in the light of procedure described elsewhere[24], m.p. 278°; PMR ($CDCl_3$; 100 MHz; TMS internal reference: δ, 3.30 (*m*, 2H, C-11 and C-12), 3.40 (*m*, 1H, OH), 4.86 (*m*, 2H, C-9 and C-10), 7.30 (*m*, 8H, aromatic protons).

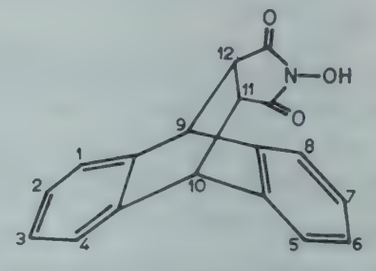

(1)

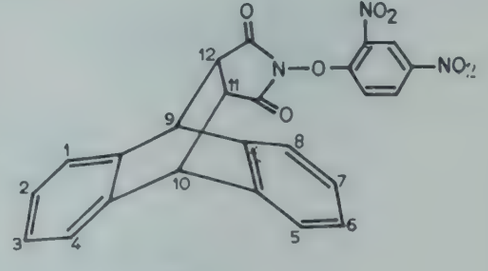

(2)

(c) *Compound* (**2**)

Compound **1** (3 g, 0.01 mol) dissolved in methanol was mixed with a methanolic solution of 1-chloro-2,4-dinitrobenzene (2 g, 0.01 mol) in the presence of equimolecular amount of sodium methoxide. The mixture was warmed for a few minutes and allowed to cool to obtain a colourless crystalline product, which was recrystallized from absolute ethanol to afford pure **2**, m.p. 282°; IR (KBr): 1750 (νCO), 1600, 1525 and 1350 (NO) cm^{-1}; UV (acetonitrile):

235 nm (log ε 4.98); PMR ($CDCl_3$; 100 MHz; TMS internal reference): δ 3.35 (*m*, 2H, C-11 and C-12), 4.87 (*m*, 2H, C-9 and C-10), 7.23-8.45 (*m*, 11H aromatic protons).

Reagents

Cyclohexylamine (Reidal), morpholine (Reidel), piperidine (Fluka, purum), acetonitrile (GR, E Merck), sodium hydroxide (GR, E Merck) were used as such.

Kinetic measurements

Reactions were carried out in aqueous acetonitrile (1:4, v/v) under pseudo-first order conditions at 35 ± 0.1°C. Kinetics were followed spectrophotometrically at 235 nm employing a Unicam SP 500 spectrophotometer fitted with thermostatted cell holders.

The rate constants were obtained from the plot of $\log[(A_\alpha - A_o)/(A_\alpha - A_t)]$ versus t (A_α, A_o and A_t represent the absorbances of the reaction mixture at infinity, zero time and at time t respectively), and were analysed by least square curve fitting method using a DEC 2050 computer. Every kinetic reading was an average of minimum of three runs. All *p*H measurements were made using a Global digital D-*p*H 500 *p*H meter.

The *pK*a values of different amines in 1:4 aqueous acetonitrile were determined *p*H-metrically (against NaOH solution in 1:4 aq acetonitrile). The effective concentration of amine was calculated from the measured *p*H of the solution and the added salt concentration.

Product analysis

The reaction products of base hydrolysis of **2** with OH^- ions, morpholine, cyclohexylamine and piperidine were 2,4-dinitrophenol, N-(2,4-dinitrophenyl)morpholine, N-(2,4-dinitrophenyl)cyclohexylamine and N-(2,4-dinitrophenyl)piperidine respectively, alongwith the parent adduct (**1**). These products were fully characterised by direct comparison with authentic samples.

Results and Discussion

In the case of hydroxide ion and piperidine, the second order rate constant, k_A ($= k_o/[\text{base}]$) steadily increased with increase in [base] (Table 1). However, in the case of morpholine and cyclohexylamine only negligible variation occurred in k_A values. Plots of k_A versus $[OH^-]$ and [piperidine] were linear with slopes and intercepts characteristic of base catalysis as proposed by Bunnett and coworkers[1,12]. In the case of morpholine and cyclohexylamine such plots were also linear with very small slopes. The well established mechanism for such base-catalysed reaction is shown in Scheme 1.

Table 1—Second Order Rate Constants (k_A) for Hydrolysis of Compound (**2**) by Various Nucleophiles at 35 ± 0.1°C in 1:4 Aqueous Acetonitrile

([Substrate] = 4×10^{-5} mol dm^{-3})

Nucleophile	*pKa	$10^4[Nu]_{eff}$ (mol dm^{-3})	$10^2 k_A$ (dm^{3}mol^{-1} s^{-1})
OH^-	—	3.0	66.6
		4.0	79.5
		4.5	81.1
		5.0	86.8
		5.5	97.6
Piperidine	10.15	4.92	205.2
		5.54	227.6
		6.15	239.8
		6.76	268.5
		7.38	276.4
		8.61	308.9
Morpholine	8.16	11.0	10.9
		22.0	10.4
		27.5	9.96
		33.0	11.1
		38.5	11.7
		44.0	11.1
Cyclohexylamine	9.56	14.7	13.9
		29.5	14.2
		44.3	14.5
		59.0	14.5
		73.7	14.2

*In 1:4 aqueous acetonitrile at room temperature.

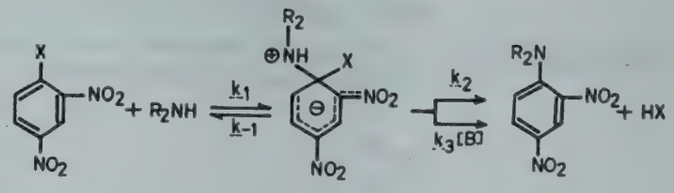

Scheme 1

On the basis of steady state hypothesis, Scheme 1 leads to the rate law (1)

$$k_A = \frac{k_1 k_2 + k_1 k_3[B]}{k_{-1} + k_3[B]} \quad \ldots (1)$$

where [B] represents any base present in the system. If $k_2 + k_3[B] \gg k_{-1}$, Eq. (1) simplifies to Eq. (2).

$$k_A = k_1 \quad \ldots (2)$$

When $k_{-1} \gg k_2 + k_3[B]$, Eq. (1) reduces to Eq. (3)

$$k_A = \frac{k_1 k_2}{k_{-1}} + \frac{k_1 k_3[B]}{k_{-1}} \quad \ldots (3)$$

or,

$$k_A = k' + k''[B] \quad \ldots (4)$$

A linear dependence of k_A with [B] is observed with an intercept $k_1k_2/k_{-1} = k'$ and slope $k_1k_3/k_{-1} = k''$. It has also been proposed[12] that when $k''/k' > 50$, the reaction is truly base catalysed and when $k''/k' < 50$ the reaction is not truly base-catalysed and the first step of the reaction is rate-limiting.

An analysis of rate data of the present study suggests that rate Eq. (4) is applicable in the case of morpholine ($k''/k' = 12.1$) and cyclohexylamine ($k''/k' = 7.9$). But a very high catalytic rate coefficient k'' is observed in the case of piperidine ($k''/k' = 2558$) and hydroxide ion ($k''/k' = 2361$). Absence of catalysis in the case of morpholine and cyclohexylamine can be interpreted in the light of Jenck's proposal[25] and consideration of stability of the intermediate complex formed in each case. It may be mentioned here that the leaving group in the present case is a relatively poor one.

A comparative study of stability of the intermediates (**3-6**) suggests that hydroxide ion and piperidine form comparatively stable intermediates than those obtained with morpholine and cyclohexylamine (Scheme 2).

After the transfer of electron from the attacking base, the electron density in the phenyl ring increases. This somewhat saturates the electron demand of nitro group and the latter now only weakly assists in the deprotonation of the intermediate complex. The protonation of oxygen on the nucleofuge moiety at this stage helps in its detachment. An examination of the intermediates (**5**) and (**6**) suggests that these are comparatively stronger acids and proton transfer to the nucleofuge moiety can occur relatively easily. The reverse reaction becomes unimportant ($k_2 + k_3[B] \gg k_{-1}$). The nucleofuge gets detached, and the reaction proceeds via the uncatalysed path.

Intermediates (**3**) and (**4**), being comparatively weaker acids, do not deprotonate easily and consequently reverse pathway assumes importance ($k_{-1} \gg k_2 + k_3[B]$). This necessitates the participation of the second base molecule for deprotonation and subsequent removal of the nucleofuge.

It may be mentioned here that rate constant for OH^- ion is lower than that of piperidine. The OH^- ion is a comparatively hard base than piperidine and

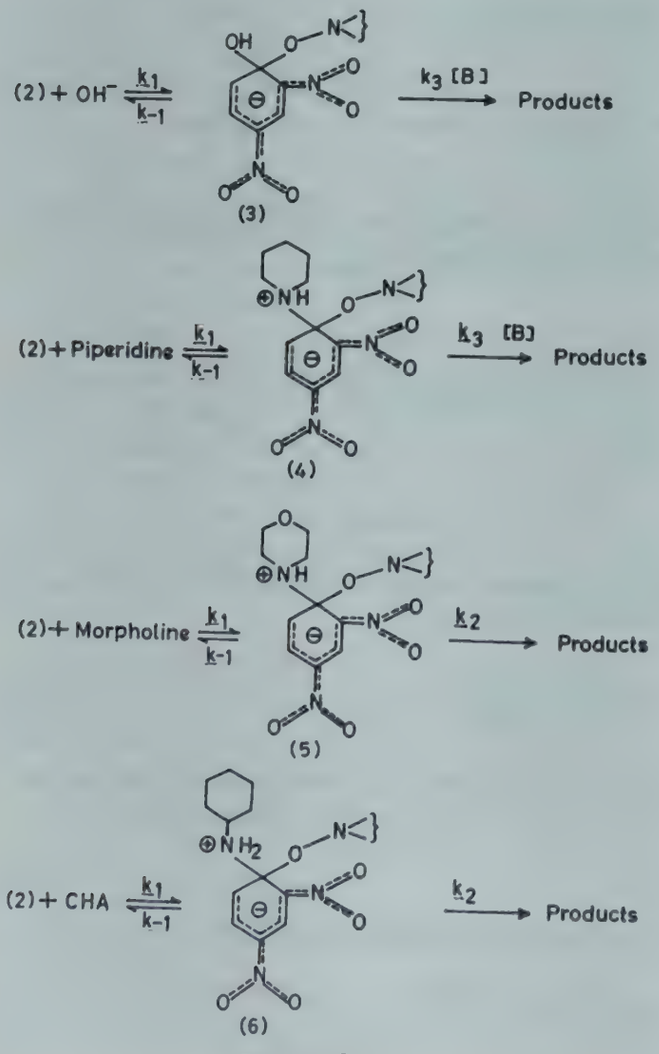

Scheme 2

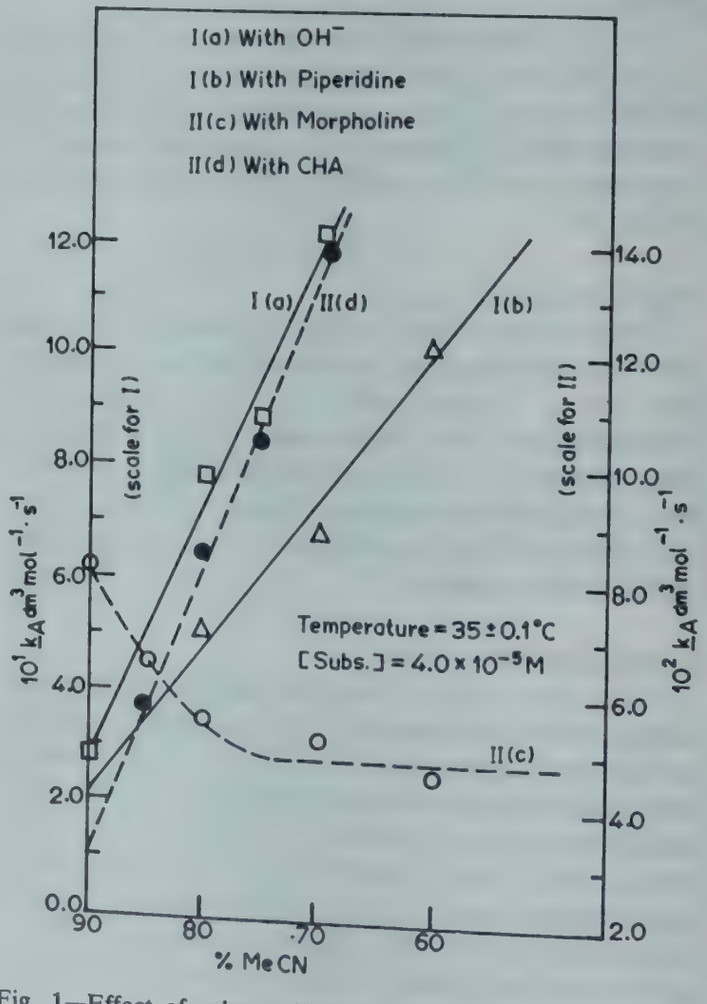

Fig. 1—Effect of solvent dielectric constant on second order rate constant (k_A) for the reaction of **2** with different bases

the site of attack (aromatic carbon) is relatively soft, hence in the light of HSAB principle piperidine is expected to react faster.

Further, it is worth mentioning here that recently Nudelman *et al.*[26] have observed the absence of base-catalysis in acetonitrile medium for the reaction of piperidine with 1-fluoro-2,4-dinitrobenzene. This is not at all surprising in view of the fact that base catalysis depends very much on the nature of the nucleofuge as well.

Solvent dependence

The reactions were studied in various acetonitrile-water mixtures. A sharp increase in rate with increase in dielectric constant of the medium was observed in the case of hydrolysis by OH^- ion, piperidine and cyclohexylamine in support of a polar transition state in these cases. But in the case of morpholine when the percentage of MeCN dropped from 90 to 80%, a sharp decrease in rate occurred, but further decrease in acetonitrile (i.e. increase in water percentage) beyond 75% did not bring about any appreciable change in the rate (Fig. 1). This indicates that solvation of the ground state of the nucleophile is relatively more in the case of morpholine due perhaps to the presence of a second electronegative atom in the molecule.

Temperature dependence

All the reactions were found to obey Arrhenius relationship. In each case a high negative value of entropy of activation was obtained indicating the crowded nature of the transition state.

Acknowledgement

One of the authors (RS) is grateful to the Govt. of India for the award of a fellowship under QIP scheme.

References

1 Bunnett J F & Randall J J, *J Am chem Soc*, **80** (1958) 6020.
2 Bernasconi C F & Rossi R H, *J org chem*, **41** (1976) 44.
3 Nudelman N S & Palleros D, *J chem Soc Perkin Trans* 2, (1984) 1277.
4 Bamkole T O, Hirst J & Onyido I, *J chem Soc Perkin Trans* 2, (1982) 889.
5 Bunnett J F & Cartano A V, *J Am chem Soc*, **103** (1981) 4861.
6 Banjoko O & Ezeani C, *J chem Soc Perkin Trans* 2, (1986) 531.
7 Bunnett J F & Garst R H, *J org chem*, **33** (1968) 2320.
8 Nudelman N S & Cerdeira S, *J chem Soc Perkin Trans* 2, (1986) 695.
9 Bunnett J F, Tetsugokato & Nudelman N S, *J org chem*, **34** (1969) 785.
10 Hirst J, Hussain G & Onyido I, *J chem Soc Perkin Trans* 2, (1986) 397.
11 Mancini P M E, Martinez R D, Vottero L R & Nudelman N S, *J chem Soc Perkin Trans* 2, (1984) 1133.
12 Bunnett J F & Garst R H, *J Am chem Soc*, **87** (1965) 3895.
13 Lee H H & Main L, *Aust J chem*, **28** (1975) 2521.
14 Nudelman N S & Palleros D, *J chem Soc Perkin Trans* 2, (1981) 995.
15 Bernasconi C F, *J org chem*, **32** (1967) 2947.
16 Bunnett J F & Bernasconi C F, *J org chem*, **35** (1970) 70.
17 Ayediran D, Bamkole T O, Hirst J & Onyido I, *J chem Soc Perkin Trans* 2, (1977) 597.
18 Banjoko O & Otiono P, *J chem Soc Perkin Trans* 2, (1981) 399.
19 Bamkole T O, Hirst J & Onyido I, *J chem Soc Perkin Trans* 2, (1979) 1317.
20 Fujino Masahiko & Kitada Chieko, *Chem Abstr*, **93** (1980) 47214h.
21 Paul K & Mitchell T A, *Chem Abstr*, **85** (1977) 39849e.
22 Kitada Chieko & Fujino Masahiko, *Chem Pharm Bull*, **26** (1978) 585.
23 Bansal R K, *Indian J chem Educ*, **6** (1972) 36.
24 Vogel A I, *A text book of practical organic chemistry*, (longmans, London) 1978, 1113.
25 Jenks W P, *J Am chem Soc*, **94** (1972) 4731.
26 Nudelman N S, Mancini P M E, Martinez R D & Vottero LR, *J chem Soc Perkin Trans* 2, (1987) 951.

Indian Journal of Chemistry
Vol. 27A, September 1988, pp. 794-796

Notes

Anion Hydration & Hydrogen Isotope Effects in Dehydration of Chloride Form of Anion Exchange Resins

DEOKI NANDAN & A R GUPTA*
Chemistry Division, Bhabha Atomic Research Centre,
Trombay, Bombay 400 085

Received 7 *March* 1988; *revised and accepted* 11 *May* 1988

Chloride ion hydration in resin phase (Dowex 1, Cl^--form) has been studied using hydrogen isotope effect in dehydration of the exchangers at 353 K. Separation factors have been determined as a function of n_w (moles of water per equivalent resin). When primary hydration shell of chloride ion is being formed ($n_w = 2$ to 6) the data show that chloride ion-water interactions are much weaker than water-water interactions in pure water, indicating that chloride ions are not hydrated in the chemical sense. Chloride ions disturb the water structure marginally, as indicated by the slight strengthening of H-bonding amongst water molecules at $n_w = 10 - 12$.

Recently, hydrogen isotope effect in the dehydration of crosslinked cation exchangers (Dowex 50W) in alkali metal forms has been used as a probe to investigate ion-water and water-water interactions in the resin phase[1,2]. These studies revealed that (i) a second hydration shell exists around Li^+ and Na^+ ions and (ii) the hydrogen bonds amongst the water molecules of the first and the second hydration shells were stronger than those in the bulk water. Presently the authors have studied the hydrogen isotope effect in the dehydration of anion exchange resin with a view to determining anion-water and water-water interactions in the exchanger phase of variously crosslinked polystyrene-DVB quaternary ammonium type anion exchange resins (Dowex 1) in the Cl^- form.

Dowex 1 (Cl^-) resins of 4% (100-200 mesh) and 8% (100-200 mesh) crosslinkings (J T Baker, USA) were treated in the usual manner[3] and converted into Cl^- form. Their ion exchange capacities on the dry weight basis were 4.161 (4%) and 4.013 (8%) meq/g. The air-dried (AD) resins were equilibrated either with liquid water of natural deuterium (D) concentration to obtain surface dried (SD) resins, or vacuum-dried and then isopiestically equilibrated (IE) with varying water activity (a_W) as described earlier[4]. A Rayleigh distillation type apparatus was used to determine H/D separation factors in the dehydration of these SD and IE resins at 353 ± 0.5 K under reduced pressure. The procedure[1,2] involved removing water from a larger aliquot of a particular resin in steps ensuring that each stage was characterised by the liquid-vapour equilibrium. A smaller aliquot was completely dehydrated and total water collected in one step to determine the quantity of water and its H/D ratio. The H/D ratios of various water samples collected were determined using a mass spectrometer model 660[1,5].

The results obtained in various experiments performed are summarised in Table 1. The isotope effect (single stage separation factor, α) is defined by Eq. (1)

$$\alpha = \frac{[H/D]\text{ water vapor}}{[H/D]\text{ pore liquid water}} \quad \ldots (1)$$

was calculated from the Rayleigh formula (Eq. 2)

Table 1—Data on Hydrogen/Deuterium Isotope Effects in Dehydration of Dowex 1 (Cl^--form) Resins at 353 K

Resin sample No.	Sample wt (g) (larger aliquot)	Cross-linking (%)	a_W	n_w	Total water(g) in resin sample and its D-content (ppm)		Last water fraction(g) and	$\alpha(\pm 0.003)$
					Collected	Expected		
1	4.5580	4	0.430	2.44	0.6838(151.0)	0.6938(151.1)	0.1487(153.9)	1.012
2	3.5008	8	0.575	3.20	0.6591(152.1)	0.6600(152.4)	0.1425(155.3)	1.014
3	3.4397	8	0.695	4.24	0.8036(152.5)	0.8153(152.9)	0.2478(155.1)	1.015
4	2.8016	8	0.945	7.35	1.0530(151.3)	1.0807(152.3)	0.4340(154.6)	1.021
5	2.2238	4	0.965	8.2	0.8400(151.8)	0.8113(152.2)	0.1688(157.9)	1.025
6	1.5644	8	0.990	11.3	0.7049(158.0)	0.7010(—)	0.0842(171.1)	1.039
7*	1.6757	8	1.000	11.6	0.7632(3885)	0.7473(—)	0.2382(4052)	1.037
8	1.1105	4	0.985	16.3	0.6463(153.0)	0.6247(153.5)	0.2487(157.6)	1.032
9	1.6143	4	1.000	20.1	0.9700(153.3)	0.9750(153.0)	0.0495(169.6)	1.035
10†	0.9039	Pure water	1.000	—	0.8967(152.7)	0.9039(153.0)	0.0262(171.5)	1.034

*This experiment was done with enriched water. Smaller aliquot was dried in oven for water content.
†Data on distillation of pure water (ref. 1)

$$\left(\frac{N}{N_0}\right)^{\alpha\,\alpha-1} = \frac{W_0}{W} \qquad \ldots (2)$$

where N and N_0 are respectively the D/H ratios of the last fraction and the total water initially present in the resin, and W_0 and W are the weights of the total and the last fraction of water. The α-values thus obtained are listed in Table 1. The agreement between the quantity of water collected from the isotope effect experiment and the expected amount based on single step distillation indicates that in multistep distillation experiments, water losses are not significant. This is further supported by the agreement in the composition of initial water in the resin (N_0) obtained from the single step and the mass balance in the multistep experiment. The values of α-1 i.e. ε have been plotted as a function of n_w in Fig. 1.

The sorption of water by strong acid or strong base type ion exchange resins based on polystyrene-DVB copolymers is governed by counterion-water interactions provided there are no specific ionogenic group-counter ion interactions. Ionogenic groups (sulphonate in cation exchangers or quaternary ammonium groups in anion exchangers) are essentially unhydrated[1,6,7]. Under these conditions, the resin phase resembles a single ion solution and this is also valid for Cl^--form of Dowex 1 resins. Thus, in the present study, we are looking at chloride ion-water interactions, unperturbed by cation-water interactions, which are invariably present in aqueous electrolyte solutions.

Figure 1 shows that α has a low value of 1.012 at $n_w \sim 2$, which increases with increasing n_w reaching a maximum value of 1.038 at $n_w \sim 11$. Subsequently α approaches α_W with further increase in n_w. As hydrogen isotope effect is a measure of the overall binding of hydrogen atoms involved in H-bonded structures, like liquid water having a separation factor (α_W) at a given temperature, the above data at low n_w values clearly show that the interactions of chloride ion-nearest neighbour water molecules, as indicated by α (even when no water-water interactions are involved) are much weaker than water-water interactions in pure water (α_W). The isotope effects at higher n_w^* values, taking into account the fact that α at $n_w \sim 11$ is somewhat greater than α_W, imply that water molecules in the cluster around chloride ion are H-bonded slightly more strongly than that in pure water.

Most of the studies on chloride ion hydration (like quantum mechanical[8], molecular dynamics (MD)[9], neutron or X-ray diffraction[10], NMR[11], IR[12] etc.) indicate that chloride ions are hydrated through H-bonding with the nearest neighbour water molecules. The preferential orientation is approximately a linear H-bond. Such a hydrogen bond should be fairly strong but most of the dynamical parameters[9,11] e.g. residence times etc. indicate the opposite.

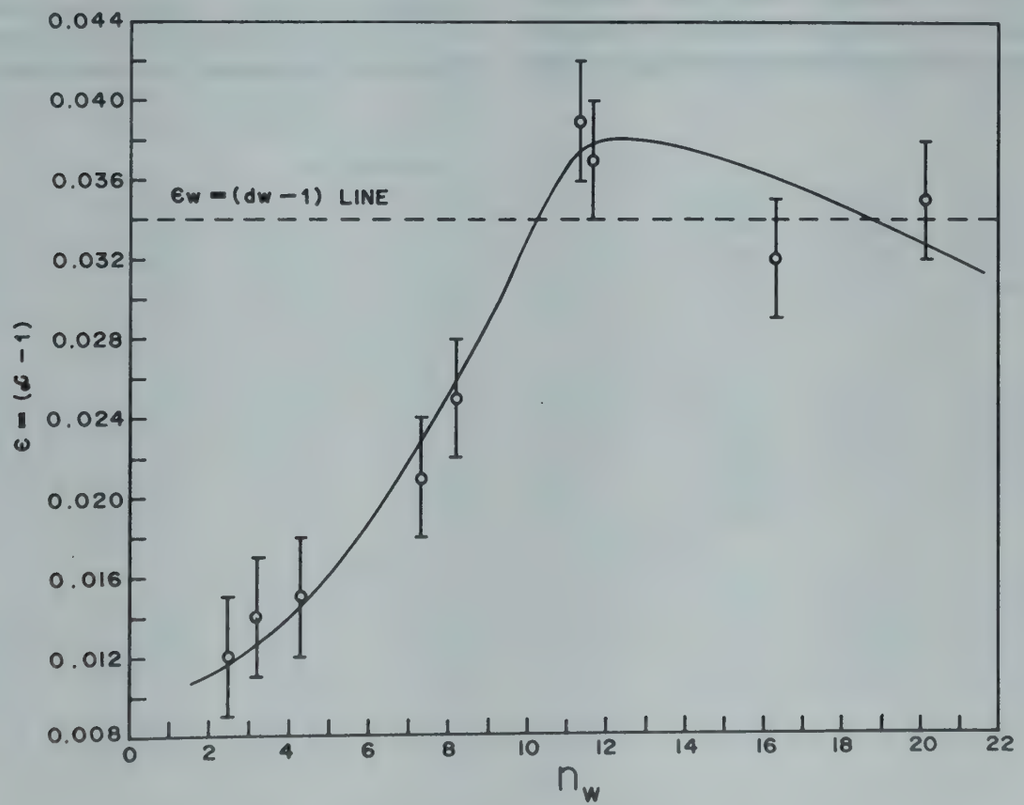

Fig. 1—Variation of ε (= α − 1) as a function of n_w for Cl^- forms of Dowex-1 resins at 353K.

Accordingly it has been assumed that anions in general (exceptions are anions like F^- or OH^-) are weakly hydrated and H-bonds in the primary hydration shell are weak. These interactions decrease as anion size increases. The present study provides the first direct evidence that H-bonds involved in the chloride ion hydration are much weaker than those in pure water. This raises the important question; if water-water interactions are stronger than chloride ion-water interactions, are we justified in talking of hydrated chloride ions?

The picture that emerges for chloride ion hydration on the basis of present data and other known facts is as follows. When only 2 or 3 water molecules per chloride ions are present, theoretical calculations[13] show that preferred orientation is symmetri

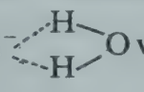

cal, i.e. Cl^- ···H—O—H which permits no H-bond formation among the water molecules (very low α at low n_w). As more water molecules are addedc, immediate neighbour water molecules reorient themselves to form distorted H-bonds among themselves (increase in α with η_W). Eventually, water molecules form a three-dimensional H-bonded cluster around the chloride ion. The polarising effect of the chloride ion on water molecules in this cluster could presumably be responsible for a slight increase in H-bond strength and observed maximum in α. Thus chloride ions are not hydrated in the conventional sense (i.e. no primary hydration shell with strongly attached water molecules) but just sit in the cavity within the H-bonded water cluster without disturbing it. The number of nearest neighbour water molecules, i.e. hydration number, is therefore, primarily dictated by water-water interactions and not chloride ion-water interactions. In that sense, the hydration numbers for chloride ions determined by various techniques like MD[9], X-ray or neutron diffraction[10] arise as a consequence of their geometrical definition rather than due to chemical consequences. These observations should apply to anion hydration in general except for specific anions like F^- and OH^- which interact with water molecules very strongly. The results of a detailed study of anion hydration involving other anions like Br^- or I^- will be published later.

References

1 Gupta A R, Nandan D & Sarpal S K, *J phys Chem*, **86** (1982) 3257.
2 Gupta A R & Nandan D, *J phys Chem*, **89** (1985) 4329.
3 Nandan D & Gupta A R, *J chem Soc Faraday Trans* (1982) 971.
4 Nandan D & Gupta A R, *Indian J Chem*, **12** (1974) 868.
5 Murthy M S, Prahallada Rao B S, Handu V K & Satam J V, *Report BARC*-1026, 1979.
6 Boyd G E & Soldano B A, *Z Electrochem*, **57** (1953) 162.
7 Nandan D & Gupta A R, *Indian J Chem*, **20A** (1981) 974.
8 Shuster P, Jakubetz W & Marius W, '*Topics in current chemistry*', Vol. 60 (1975) pp 1-107.
9 Heinzinger K, Bopp Philippe & Jancso G, *Acta Chim Hung*, **121** (1986) 27.
10 Enderby J E, *Sci Prog Oxf*, **67** (1981) 553.
11 Hertz H G, '*Water—A comprehensive treatise*', edited by F Franks (Plenum Press, New York), Vol. 3 (1973) chapter 7.
12 Verral R E, '*Water—A comprehensive treatise*', edited by F Franks (Plenum Press, New York), Vol. 3, Chapter 5.
13 Gowda B T & Benson S W, *J Comp Chem*, **4** (1983) 283.

Indian Journal of Chemistry
Vol. 27A, September 1988, pp. 797-798

Excess Molar Volumes of Binaries of Ethylbenzene with Chlorobenzene, Nitrobenzene, Aniline & Benzyl Alcohol†

S K CHAUDHARI & S S KATTI*
Physical Chemistry Division, National Chemical Laboratory, Pune 411 008

Received 13 *August* 1987; *revised and accepted* 20 *January* 1988

Excess molar volumes, V_m^E for binary systems of ethylbenzene with chlorobenzene, nitrobenzene, aniline and benzyl alcohol have been measured at 298.15 K using a continuous dilution dilatometer. V_m^E values are negative over the entire composition range for all the systems except for ethylbenzene (1) + aniline (2) system, wherein V_m^E are slightly positive at lower concentrations of aniline ($x > 0.8$). The maximum values V_m^E(max) follow the trend: aniline < chlorobenzene < benzyl alcohol < nitrobenzene.

In our earlier work[1] we evaluated excess molar volumes, V_m^E of binary mixtures of *n*-octane with isomeric butanols with a view to studying the effect of branching in the alcoholic component on V_m^E. Presently we have measured excess volumes of binary mixtures of title binaries, with a view to understanding the effect of different functional groups of polar aromatic compounds on excess volumes.

Ethylbenzene (Fluka, pure) was rendered thiophene free and fractionally distilled over sodium metal. Chlorobenzene, nitrobenzene, aniline and benzyl alcohol (S D Fine Chemicals, India, AR) were purified by fractional distillation under reduced pressures. All the compounds were stored over 4-A molecular sieves. The densities of these purified compounds measured at 298.15 K agreed well with those reported in the literature[2,3].

Excess volumes were measured in a continuous dilution dilatometer basically similar to the design of Kumaran and McGlashan[4]. Temperature was maintained at 298.15 ± 0.005 K. Excess volumes are reproducible within ± 0.002 $cm^3\ mol^{-1}$.

Table 1—Experimental Excess Molar Volumes V_m^E at 298.15 K

x	V_m^E ($cm^3.mol^{-1}$)	x	V_m^E ($cm^3.mol^{-1}$)	x	V_m^E ($cm^3.mol^{-1}$)	x	V_m^E ($cm^3.mol^{-1}$)
ethylbenzene(1) + chlorobenzene(2)							
0.0632	−0.0305	0.3991	−0.1262	0.4873	−0.1337	0.6360	−0.1239
0.1385	−0.0620	0.4125	−0.1285	0.5146	−0.1342	0.7107	−0.1117
0.2204	−0.0896	0.4405	−0.1304	0.5162	−0.1335	0.8138	−0.0819
0.2740	−0.1046	0.4477	−0.1334	0.5477	−0.1332	0.9071	−0.0456
0.3381	−0.1196	0.4668	−0.1323	0.5593	−0.1331	—	—
ethylbenzene (1) + nitrobenzene (2)							
0.0289	−0.0338	0.3447	−0.2442	0.5187	−0.2927	0.7639	−0.2447
0.0954	−0.0853	0.4063	−0.2705	0.5214	−0.2949	0.8318	−0.1970
0.1810	−0.1451	0.4396	−0.2796	0.5789	−0.2966	0.9284	−0.0977
0.2464	−0.1893	0.4572	−0.2863	0.6282	−0.2925	0.9372	−0.0832
0.3030	−0.2223	0.4782	−0.2874	0.7114	−0.2690	—	—
ethylbenzene (1) + aniline (2)							
0.0498	−0.0218	0.3570	−0.0708	0.4547	−0.0637	0.6925	−0.0198
0.1182	−0.0426	0.3912	−0.0700	0.4635	−0.0634	0.8012	0.0013
0.1869	−0.0620	0.3947	−0.0694	0.5075	−0.0574	0.9081	0.0097
0.2601	−0.0687	0.4225	−0.0666	0.5343	−0.0510	—	—
0.3223	−0.0716	0.4272	−0.0661	0.6069	−0.0390	—	—
ethybenzene (1) + benzyl alcohol (2)							
0.0688	−0.0576	0.4095	−0.1620	0.5520	−0.1426	0.8149	−0.0562
0.1448	−0.1025	0.4453	−0.1590	0.5980	−0.1312	0.8203	−0.0524
0.2317	−0.1371	0.4481	−0.1587	0.6484	−0.1167	0.9234	−0.0138
0.2919	−0.1494	0.4714	−0.1557	0.6571	−0.1125	0.9424	−0.0089
0.3722	−0.1602	0.4876	−0.1539	0.7077	−0.0949	—	—
0.4048	−0.1616	0.4993	−0.1540	0.7418	−0.0867	—	—

†NCL Communication No. 4200

Table 2—Coefficients a_0, a_1 and a_2 of Eq (1) and Standard Deviation σ

a_0	a_1	a_2	σ
Ethylbenzene (1) + chlorobenzene (2)			
−0.53556	−0.01619	0.00958	0.0007
Ethylbenzene (1) + nitrobenzene (2)			
−1.15627	−0.24318	−0.14927	0.0052
Ethylbenzene (1) + aniline (2)			
−0.2278	−0.33177	0.09842	0.0012
Ethylbenzene (1) + benzyl alcohol (2)			
−0.61460	−0.36795	0.09863	0.0034

The V_m^E values for all the systems are given in Table 1 and were fitted by least squares method to Eq (1).

$$V_m^E/(cm^3\,mol^{-1}) = x(1\text{-}x)[a_0 + a_1(2x\text{-}1) + a_2(2x\text{-}1)^2] \quad \ldots(1)$$

The coefficients a_0, a_1 and a_2 along with standard deviation, σ, are given in Table 2.

Our V_m^E values for ethylbenzene (1) + chlorobenzene (2) agreed reasonably well with those of Tanaka and Benson[5]. For the system ethylbenzene (1) + aniline (2), V_m^E values are about 3% lower, at $x = 0.5$ than those of Fried *et al.*[6].

The excess volumes are negative over the entire range of mol fraction for all the systems except for x $C_6H_5C_2H_5 + (1\text{-}x)C_6H_5NH_2$ system, where V_m^E values are slightly positive at lower concentrations of aniline ($x > 0.8$).

The maximum V_m^E values follow the trend: aniline < chlorobenzene < benzyl alcohol < nitrobenzene.

References

1 Chaudhari S K & Katti S S, *J chem Thermodynamics*, **17** (1985) 101.

2 Riddick J A & Bunger W B, *Techniques in chemistry*, Vol 2, *Organic Solvents* (Willey Interscience, New York) 1970.

3 Timmermans J, *Physicochemical constants of pure organic compounds* (Elsevier, New York) 1950.

4 Kumaran M K, McGlashan M L, *J chem Thermodynamics*, **9** (1977) 320.

5 Tanaka R, Benson G C, *J chem Engng Data*, **21** (1977) 320.

6 Fried V, Miller L P, Watcher H N, *Bull chem Soc Japan*, **50** (1977) 497.

Indian Journal of Chemistry
Vol. 27A, September 1988, pp. 799-802

Apparent Molal Volumes & Compressibilities of Electrolytes in Aqueous & Aqueous Urea Solutions

K J PATIL*, A B WAZALWAR & G R MEHTA
Department of Chemistry, Institute of Science, Nagpur 440 001

Received 6 *March* 1987; *revised* 18 *November* 1987; *accepted* 9 *December* 1987

Apparent molal volumes (ϕ_V) and compressibilities (ϕ_K) of NaCl, Me_4NBr, Et_4NBr and Bu_4NBr in the concentration range of 0.1*m* to 1.0*m* at 25°C in water and 6*m* aqueous urea solutions have been computed from measured sound velocities and densities. The limiting values of $\phi_V(\phi_V^0)$ and $\phi_K(\phi_K^0)$ and their concentration variations are explained on the basis of ion-solvent and ion-ion interactions. The magnitudes and trends of transfer functions ($\Delta\phi_V^0$ and $\Delta\phi_K^0$) from water to 6*m* aqueous urea solutions for tetraalkylammonium salts indicate that the structural hydration effects become smaller in aqueous urea solutions as compared to those in aqueous solutions.

The peculiarities exhibited by tetraalkylammonium ions in aqueous solutions are due not only to their large ionic size but also to the significant modification of water structure around the cations because of hydrophobic hydration[1]. The densities and heat capacities of tetraalkylammonium salts have been reported by Desnoyers *et al.*[2] in water and aqueous urea solutions (3*m*) at 25°C. On the basis of sign and magnitude of transfer function, these authors suggested some kind of cooperative effect when two hydrophobic solutes interact with each other without the formation of hydrophobic bond. In this communication we report the apparent molar volumes and compressibilities of NaCl, Me_4NBr, Et_4NBr and Bu_4NBr in water and 6*m* aqueous urea solution at 25°C. The standard transfer functions for volume and compressibility for various salts from water to 6*m* aqueous urea solutions have been computed at infinite dilution employing appropriate thermodynamic equations. The results are discussed in terms of hydrophobic interactions, effect on water structure and urea-water interactions.

Urea, sodium chloride, tetramethylammonium bromide, tetraethylammonium bromide and tetrabutylammonium bromide were of AR (BDH) grade. The salts were stored in a vacuum desiccator for several days before use. All the solutions were prepared afresh in doubly distilled water on molality basis. The densities of solutions were measured at 25°C using (i) a calibrated density bottle having a standard joint thermometer and side capillary for volume adjustment (German made), and (ii) a double-limb pyknometer. The density data for aqueous binary solutions of electrolytes agreed well with the literature data and were reproducible within $\pm 5 \times 10^{-5}$ g/cm^3.

Sound velocities were measured using an ultrasonic interferometer (2 MHz) which was calibrated using water, methanol and benzene at 25°C and also at different temperatures. The measured values of sound velocity for pure liquids agreed within ±1 m/s with best literature values and the reproducibility was of the order of ±0.5 m/s. The temperature of the cell was maintained constant with an accuracy of ±0.02°C.

Adiabatic compressibilities were calculated using the Laplace equation. Apparent molal volumes (ϕ_V) and compressibilities (ϕ_K) of the salts were calculated using the expressions given earlier[3]. The variations in ϕ_V and ϕ_K with change in concentration (molality in binary solutions and aqua molal-

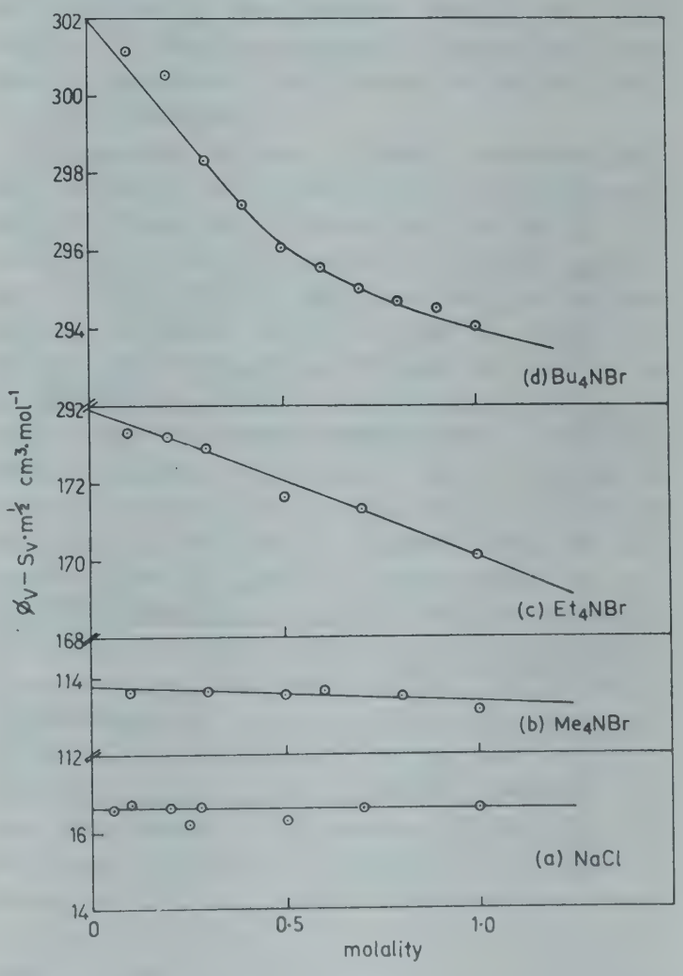

Fig. 1—Variation of apparent molal volumes of NaCl, Me_4NBr, Et_4NBr and Bu_4NBr in water with concentration at 25°C

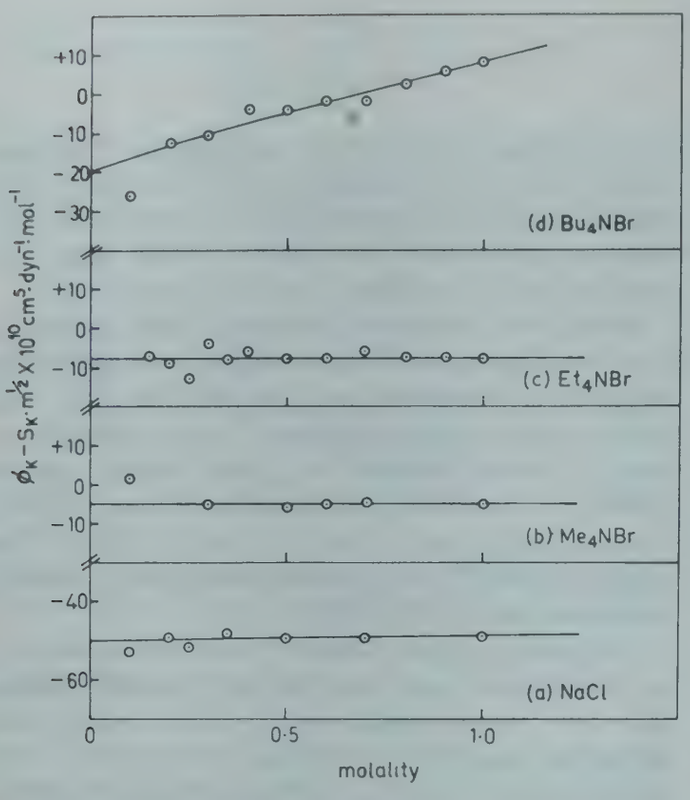

Fig. 2—Variation in apparent molal compressibilities of NaCl, Me_4NBr, Et_4NBr and Bu_4NBr in water with concentration at 25°C

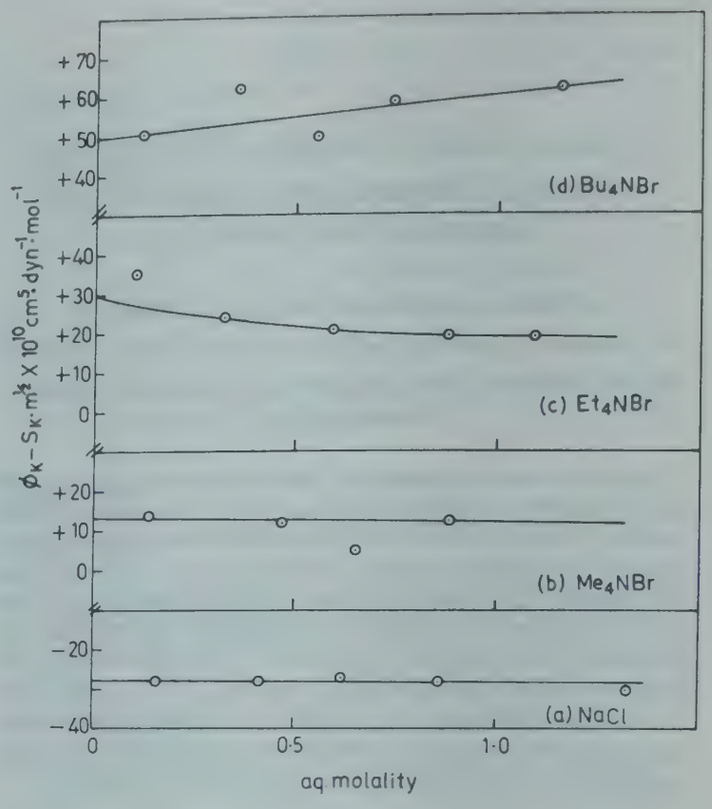

Fig. 4—Variation in apparent molal compressibilities of NaCl, Me_4NBr, Et_4NBr and Bu_4NBr with concentration in urea-water mixture (6*m*) at 25°C

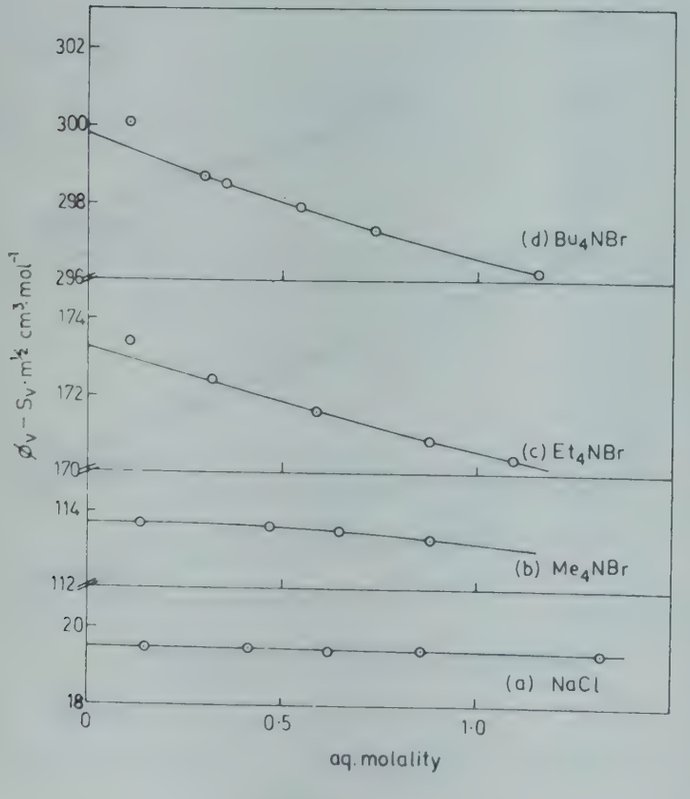

Fig. 3—Variation of apparent molal volumes of NaCl, Me_4NBr, Et_4NBr and Bu_4NBr with concentration in urea-water mixture (6 *m*) at 25°C

ity in ternary solutions) of electrolytes are generally represented by Eqs (1) and (2) respectively.

$$\phi_V = \phi_V^0 + S_V.m^{1/2} + B_V.m \quad \ldots (1)$$

$$\phi_K = \phi_K^0 + S_K.m^{1/2} + B_K.m \quad \ldots (2)$$

where ϕ_V^0 and ϕ_K^0 are the partial molal volume ($\bar{V}_2^0$) and compressibility ($\bar{\beta}_2^0\bar{V}_2^0$) of the solute, S_V and S_K are the appropriate slopes of Debye-Hückel limiting law and B_V and B_K are adjustable parameters signifying deviations due to solute-solute interactions. At 25°C for 1:1 electrolytes in water, $S_V = 1.86$ cm^3 mol^{-1} and $S_K = 6.3 \times 10^{-10}$ cm^5 dyne^{-1} mol^{-1} (see ref. 4). For 6*m* urea solution, we have assumed that S_V and S_K are the same as those in aqueous solution since, the dielectric constants of water and urea-water solutions are nearly the same. The variation of dielectric constants of aqueous urea solutions with pressures, $\left(\frac{dD}{dP}\right)_T$ is not known, it is not possible to calculate exact S_V and S_K values for urea solutions. The variation of $\phi_V - S_V.m^{1/2}$ and $\phi_K - S_K.m^{1/2}$ with molality (aqueous solutions) for NaCl, Me_4NBr, Et_4NBr and Bu_4NBr at 25°C are shown in Figs. 1 and 2 while the variation of these parameters with aqua molality (6*m* urea solution) for the above salts at 25°C

Table 1—Apparent Molal Volumes (ϕ_V^0), Compressibilities (ϕ_K^0) and Variation in These Parameters with Molality in Aqueous and Aqueous Urea Solution

Solvent	ϕ_V^0 cm^3 mol^{-1}	$\phi_K^0 \times 10^{10}$ cm^5 dyne^{-1} mol^{-1}	$\Delta\phi_V^0$ cm^3 mol^{-1}	$\Delta\phi_K^0 \times 10^{10}$ cm^5 dyne^{-1} mol^{-1}
		NaCl		
H_2O	16.6(16.62)[a]	−50 (−50.5)[c]	2.9	22
6*m* urea	19.5	−28		
		Me_4NBr		
H_2O	113.75(114.3)[b]	−5 (−4.1)[c]	−0.05	18
6*m* urea	113.7	+13		
		Et_4NBr		
H_2O	173.9 (173.6)[b]	−7.5(−4,6)[c]	−0.65	36.5
6*m* urea	173.25	+29		
		Bu_4NBr		
H_2O	301.9 (300.4)[b]	−19.5(−17.3)[c]	−2.1	69
6*m* urea	299.8	+49.5		

(a) Millero F J & Drosf-Hansen W, *J chem engng Data*, **13** (1968) 330.
(b) Philip P R, Desnoyers J E & Hade A, *Can J Chem*, **51** (1973) 187.
(c) Mathieson J E & Conway B E, *J soln Chem*, **3** (1974) 455.

are shown in Figs 3 and 4 respectively. The extrapolated values of ϕ_V^0 and ϕ_K^0 are collected in Table 1 and are compared with literature data. The accuracy in ϕ_V and ϕ_K at the measured concentrations is of the order of ± 0.1 cm^3 mol^{-1} and $\pm 0.2 \times 10^{-10}$ cm^5 dyne^{-1} mol^{-1} respectively, but the extrapolated values (ϕ_V^0 and ϕ_K^0 respectively) may be in the error by ± 1.0 cm^3 mol^{-1} and $\pm 2 \times 10^{-10}$ cm^5 dyne^{-1} mol^{-1} as the measurements could not be carried out at very low concentrations of the electrolyte. The values of ϕ_V^0 and ϕ_K^0 are obtained by smooth extrapolation at higher concentration. The transfer values of $\Delta\phi_V^0$ and $\Delta\phi_K^0$ for the salts from water to aqueous urea solutions are also collected in Table 1.

The negative slopes in Figs 1 and 3 in respect of ϕ_V variation signify the effect of solute-solute interactions[5]. However, the magnitude of B_V is greatly reduced in aqueous urea solution. It has been well established that the magnitude of B_V depends upon the hydrophobicity of the molecules or ions[6]. The ϕ_V^0 values in water for the salts showed, considering the uncertainties in the measurement, fair agreement with the literature values[2]. The $\Delta\phi_V^0$ values for Me_4NBr, Et_4NBr and Bu_4NBr are small negative while for NaCl it is positive which confirms that the hydration of alkali metal cations differ from that of alkylammonium ions. The ϕ_K^0 values for electrolytes in water are negative and positive in 6*m* aqueous urea solution. The negative ϕ_K^0 values have been interpreted in terms of immobilisation of solvent molecules around the cations. The positive ϕ_K^0 values in 6*m* aqueous urea solution are the important observations of the present work and these may be due to reduction in charge-dipole interactions. The positive ϕ_K^0 values are generally reported in aqueous-nonelectrolyte[7,8] and nonelectrolyte-non-nonelectrolyte[9] solutions.

Examination of data in Table 1 indicates that $\Delta\phi_K^0$ values are large particularly for Et_4NBr and Bu_4NBr. These large values may be due to decrease in ion-ion interaction (hydrophobic ineraction) in urea solution while ion-water interaction may be of similar nature in both the media, although water structural effects may be different in the two media. Thus, if one postulates that urea mixes with water by substitutional dissolution without affecting the volume and energetics of H-bonded network water appreciably[10] forming a clathrate-like structure in solution, then the accommodation of solute may occur with little volume loss. This may result in a very small change in volume of transfer as observed in present study. The very large $\Delta\phi_K^0$ value for Bu_4NBr probably signifies that the structural effects are more predominant in urea solution for this salt, having a resultant structure which may be dynamic and more fragile against the pressure effects. This interpretation can also be supported on the basis of Franks and Franks[10] model of aqueous urea solution and the tendency of urea to form H-bonded structures particularly around non-polar molecules (hydrocarbons) in well known crystalline clathrates[11]. On the basis of solubility measurements Wen and coworkers[12] have suggested that aqueous

solutions of urea and tetrabutylammonium salts exhibit some specific interactions (molecular complex formation) which is again in harmony with the suggested interpretation.

The authors are thankful to Prof R B Kharat and Prof (Mrs) Sapkal for facilities and encouragement during this work.

References

1 Wen W Y, *Water and aqueous solutions; Structure, thermodynamics and transport properties*, edited by R A Horne (Wiley-Interscience, New York) 1971 Chapter 15.

2 (a) Philip P R, Desnoyers J E & Hade A, *Can J Chem*, **51** (1973) 187.

(b) Leduce P A & Desnoyers J E, *Can J Chem*, **51** (1973) 2993.

(c) Desrosiers N, Perron G & Desnoyers J E, *Can J Chem*, **54** (1976) 2163.

3 Patil K J & Ali S I, *Indian J pure appl Phys*, **19** (1981) 617.

4 Mathieson J E & Conway B E, *J soln Chem*, **3** (1974) 455.

5 Wen W Y & Saito S, *J phys Chem*, **68** (1964) 2639.

6 Franks F, *Water, a comprehensive treatise*, Vol. 4, edited by F Franks (Plenum Press, New York) 1974 Chapter 1.

7 Kaulgud M V & Patil K J, *J phys Chem*, **78** (1974) 714.

8 Kaulgud M V & Patil K J, *J phys Chem*, **80** (1976) 138.

9 Patil K J, Mehta G R & Chandewar R K, *Indian J Chem*, **25A** (1986) 1147.

10 Frank H S & Franks F, *J chem Phys*, **48** (1968) 4746.

11 Fatterly L C, *Non-stoichiometric compounds*, Chapter 8 edited by L Mandelcorn (Academic Press, New York) 1964.

12 Saito S, Lee M & Wen W Y, *J Am chem Soc*, **88** (1966) 5107.

Indian Journal of Chemistry
Vol. 27A, September 1988, pp. 803-805

Mixed Ligand Complexes of Oxotitanium(IV) & Tin(IV) with Dihydrazones

G H HAVANUR, V K REVANKAR & V B MAHALE*
Department of Chemistry, Karnatak University, Dharwad 580 003

Received 29 *July* 1987; *revised and accepted* 23 *November* 1987

Titanyl perchlorate and tin tetrachloride react with dihydrazones (LH_4) derived from dihydrazides of dibasic acids and salicylaldehyde or 3-methoxysalicylaldehyde, in alcoholic medium in presence of pyridine to form the complexes $(TiO)_2(L)(Py)_2$ and $SnCl_2(LH)_2(Py)_2$, respectively. IR spectral studies show that the ligands react in the enol form. Ti(IV) and Sn(IV) react in different manners with the ligands. Thermal stabilities of titanium complexes are also discussed.

The applications of hydrazones in structural[1] and analytical[2] chemistry have been recently reviewed. The hydrazones formed by condensation of dibasic acid hydrazides with *o-hydroxy* aromatic aldehydes are capable of forming a variety of metal complexes[3]. The ligands (structure I) are well suited for producing binuclear metal complexes. A literature survey revealed

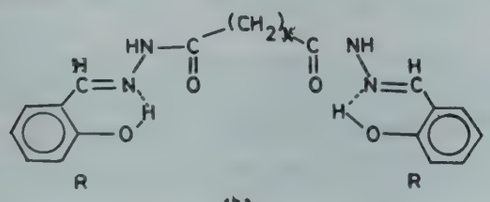

(I)

Ligand No.	X	R	Ligand No.	X	R
1	0	H	6	0	OCH_3
2	1	H	7	1	OCH_3
3	2	H	8	2	OCH_3
4	4	H	9	4	OCH_3
5	8	H	10	8	OCH_3

that complexes of tin with the ligands of type(I) have not been synthesised. Complexes of the type TiL (LH_4 is ligand) have been reported[4] with ligands 2, 3 and 4. In continuation of our earlier interest in this type of ligands[5,6], we have found that mixed ligand complexes of oxotitanium and tin can be synthesised by carrying out reactions in presence of pyridine. In this note we report the preparation and characterisation of complexes of the types $(TiO)_2(L)(Py)_2$ and $SnCl_2(LH_2)(Py)_2$.

All the chemicals used were of A R or reagent quality. Solvents used were purified by standard methods. Titanyl perchlorate was synthesised by the reported method[7]. Anhydrous tin(IV) chloride was a Riedel sample and was used without further purification. Organic ligands were synthesised by reported methods[8] and their purity was checked by elemental analysis.

Preparation of complexes

In the synthesis of oxotitanium complexes, the ligand (0.005 mol) alongwith pyridine (1 ml) was suspended in ethanol (50 ml) and to this was added an aqueous alcoholic solution of titanyl perchlorate (0.01 mol). The mixture was refluxed on a water-bath for about 6 hr when an orange to red crystalline solid separated. It was filtered, washed repeatedly with ethanol and dried *in vacuo* over phosphorus pentoxide. In the synthesis of tin complexes, the ligand (0.005 mol) and pyridine (1 ml) were suspended in dry methanol in a flask equipped with a magnetic stirrer, a water condenser with a guard tube and a nitrogen inlet. Nitrogen atmosphere was maintained during the course of the reaction. Calculated quantity (0.005 mol) of tin tetrachloride, dissolved in dry methanol, was added and the contents were stirred and refluxed for 1 hr. The mixture containing the yellow coloured compound was cooled, filtered, the solid washed with dry methanol and dried over phosphorus pentoxide *in vacuo*. Complexes could not be recrystallised due to their limited solubilities in common organic solvents.

Titanium and tin were estimated gravimetrically as TiO_2 and SnO_2, and C, H and N by microanalytical methods. Chloride was estimated gravimetrically.

Analytical data are given in Table 1. Conductivity measurements were made in DMF at 10^{-3} *M* concentration using ELICO-CM-82 conductivity bridge with a cell having cell constant 0.51. IR spectra were recorded in KBr (4000-400 cm^{-1}) on a Perkin Elmer Instrument. Far IR spectra of tin complexes were recorded by the polyethylene pellet technique at R.S.I.C., Madras. TG, DTA measurements were made at I.I.Sc., Bangalore. UV-Visible spectra were recorded in DMF on a Hitachi 150-20 spectrophotometer.

Analytical data (Table 1) show that titanium forms 2:1 (metal : ligand) complexes while tin forms 1:1 complexes. Preparations were carried out using various proportions of metal salts and ligands. $SnCl_4$ gave complexes with ligands 1 and 2 only. Reaction of $SnCl_4$ with ligands 3, 4 and 5 did not give hydrazone complexes but gave pyridine adducts of $SnCl_4$. The non-reactivity of $SnCl_4$ with ligands 3, 4 and 5 may be due to stereochemical factors as these ligands contain more than one CH_2 groups (structure I).

All the titanium complexes, except for complexes C1 and C6 (see Table 1), contain pyridine, which is

Table 1—Analytical Data of Dihydrazone Complexes of Oxotitanium(IV) and Tin(IV)

S.No.	Complex (colour)	Found (Calc.), %				
		M	N	C	H	Cl
C1	$C_{16}H_{10}N_4O_4(TiO)_2.2H_2O.2C_2H_5OH$ (Brick red)	16.6 (16.6)	9.7 (9.7)	41.6 (41.5)	3.9 (4.4)	—
C2	$C_{17}H_{12}N_4O_4(TiO)_2Py_2.2C_2H_5OH$ (Dark orange)	14.0 (13.4)	11.2 (11.7)	51.7 (52.1)	5.0 (4.7)	—
C3	$C_{18}H_{14}N_4O_4(TiO)_2Py_2.2C_2H_5OH$ (Orange red)	13.2 (13.1)	11.5 (11.5)	52.1 (52.7)	5.2 (4.9)	—
C4	$C_{20}H_{18}N_4O_4(TiO)_2Py_2.2C_2H_5OH$ (Orange red)	12.8 (12.7)	10.9 (11.1)	53.5 (53.9)	5.5 (5.3)	—
C5	$C_{24}H_{26}N_4O_4(TiO)_2Py_2.2C_2H_5OH$ (Orange)	12.2 (11.8)	10.0 (10.3)	55.8 (56.1)	6.1 (5.9)	—
C6	$C_{18}H_{14}N_4O_6(TiO)_2.6H_2O$ (Brick red)	15.8 (15.5)	8.8 (9.0)	34.3 (34.9)	4.1 (4.2)	—
C7	$C_{19}H_{16}N_4O_6(TiO)_2Py_2.2C_2H_5OH$ (Dark red)	12.9 (12.4)	10.5 (10.8)	51.3 (51.1)	4.7 (4.9)	—
C8	$C_{20}H_{18}N_4O_6(TiO)_2Py_2.2C_2H_5OH$ (Red)	11.5 (12.1)	10.2 (10.6)	50.2 (51.7)	4.8 (5.0)	—
C9	$C_{22}H_{22}N_4O_6(TiO)_2Py_2.2C_2H_5OH$ (Red)	11.3 (11.7)	10.0 (10.2)	53.0 (52.9)	5.7 (5.3)	—
C10	$C_{26}H_{30}N_4O_6(TiO)_2Py_2.2C_2H_5OH$ (Blood red)	10.8 (11.0)	9.5 (9.6)	54.5 (55.0)	6.2 (5.9)	—
C11	$C_{16}H_{12}N_4O_4SnCl_2Py_2$ (Yellow)	18.2 (17.7)	12.9 (12.5)	—	—	10.1 (10.6)
C12	$C_{17}H_{14}N_4O_4SnCl_2Py_2$ (Yellow)	17.9 (17.3)	11.8 (12.2)	—	—	10.5 (10.2)

not removed even after thorough drying of the complexes. Pyridine evolved when complexes were boiled with dil. aqueous sodium hydroxide. Bands at 1620 and 620 cm^{-1} in IR spectra of the complexes confirm the presence of pyridine.

IR spectra of ligands show bands at 3200 and 1675 cm^{-1} assignable to ν(NH) and ν(C=O) respectively. In titanium complexes, ν(NH) and ν(C=O) bands are absent. This shows that the hydrazones are present in the enol form in the complexes and the enolic hydrogens are deprotonated. A broad, weak band in the region 2700-2800 cm^{-1} of spectra of ligands, assigned to ν OH of salicylaldehyde, disappears in the complexes. This suggests the replacement of H by metal. The sharp, strong band present at 1610 cm^{-1} in the ligands is assigned to ν(C=N). In the titanium complexes, a strong and broad band is observed around 1620 cm^{-1} with a shoulder on the low frequency side around 1600 cm^{-1}. The band at 1620 cm^{-1} is as signed to coordinated pyridine and the shoulder around 1600 cm^{-1} to ν(C=N); a slight negative shift of ν(C=N) band indicates the coordination of nitrogen of azomethine to titanium.

Titanium complexes are precipitated along with a few molecules of alcohol and/or water as shown by weak, broad bands in the region 3450-3600 cm^{-1} of their IR spectra. These bands are not seen in tin complexes. The absence of strong characteristic band around 1000 cm^{-1} suggests that neither perchlorate nor discrete Ti=O groups are present in the complexes. The medium intensity band around 820-830 cm^{-1} suggests the presence of polymeric (O-Ti-O-Ti-) or 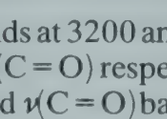 Ti grouping[9].

Electronic spectra of the ligands are characterised by maxima around 320, 290 and 280 nm. These are slightly shifted in the complexes. In addition, complexes exhibit a broad band in around 365 nm. This is attributed to ligand → metal charge-transfer. A similar band is observed in schiff base[10] and dithiocarbamate complexes of titanium[11].

All the complexes begin to decompose exothermally around 300° and decomposition is complete by 430° as shown by a plateau in TG curve above 430°. This must lead to the formation of stable TiO_2. The TG curves below 300° suggest a two-step reaction in complexes C1 and C6 (net mass losses 10% and 28%) but a single-step gradual reaction in complexes C3 and C4 (mass loss 15%). No definite conclusions can be drawn from this data. The difference in the thermal decomposition characteristics of C1 and C6 from that of C3 and C4 may be due to some structural differences in the mode of attachment of ligands to titanium.

The following tentative structure (II) may be proposed for titanium complexes.

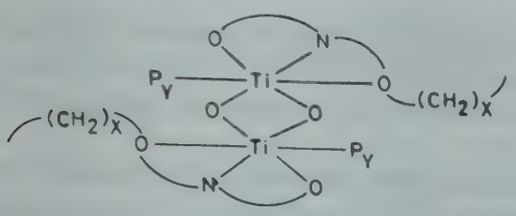

(II)

In the case of tin complexes, ν(C=O) and ν(NH) modes disappear. This means that the ligands act in enol form and the two enolic protons are replaced by metal, linking enolic oxygen to tin. ν(C=N) present at 1610 cm^{-1} in ligands shows little or no shift in the complexes. A new band appears in the region 1615-1625 cm^{-1}. This is assigned to coordinated pyridine[12]. Free pyridine shows a strong band at 1581 cm^{-1}. Thus, N of pyridine is coordinated to Sn but azomethine nitrogen is not linked to Sn. The pattern in the region 1500-1625 cm^{-1} differs in Ti and Sn complexes of the same ligands. This must be due to different modes of attachment of ligands to metal Ti/Sn. Band at 2700-2800 cm^{-1} assignable to hydrogen bonded OH is absent in the tin complexes but a new band appears at 3200-3260 cm^{-1}. This may be due to phenolic OH which is free in the complexes.

ν(Sn-Cl) mode, recorded as a liquid film, is observed[13] at 368 cm^{-1}. This decreases progressively with increase in alkylation or coordination of Sn. In complexes of type $SnCl_2.L$ [H_2L = polydentate ligand] a strong band in the region 307-325 cm^{-1} with a shoulder at low frequency side is assigned to ν(Sn-Cl)[14]. In the hydrazone complexes of tin studied here a strong broad band observed around 320 cm^{-1} is assigned to ν(Sn-Cl). This is in good agreement with the values predicted by several workers[15] for coordination number 6 of Sn. Conductivity measurments (7-9 ohm^{-1} cm^2 mol^{-1}) shows that the complexes are non-electrolytes. Sn in the complexes is hexacoordinated linked to two oxygens, two nitrogens

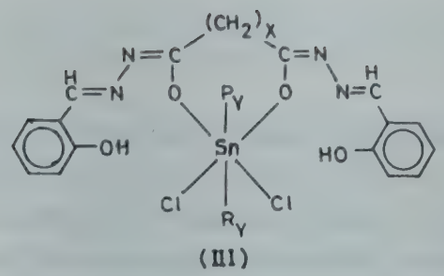

(III)

of pyridine and two chlorines. Structure (III) is proposed for tin complexes. Tin complexes could not be isolated when the value of X in $(CH_2)_x$ was beyond one. This may be due to instability of tin-containing ring when its size increases beyond six members.

The authors thank RSIC, IIT, Bombay for spectral facilities. Financial assistance by UGC and CSIR, New Delhi is acknowledged.

References

1 Dutta R L & Hossain Md M, *J scient ind Res*, **44** (1985) 635.
2 Singh R B, Jain P & Singh R P, *Talanta*, **29** (1982) 77.
3 Iskander M F, Sayed L, Hefney A F M & Zayan S E, *J inorg nucl Chem*, **38** (1976) 2209.
4 Ramesh Chandra & Kapoor R N, *Ann Chim (Roma)*, (1982) 309; *Chem Abstr*, **97** (1982) 103275a.
5 Kulkarni P J, Revankar V K & Mahale V B, *Abstract* **IO-5**, *Presented at the 5th Annual Conference of Indian Council of Chemists, Dhanbad*, 1985.
6 Havanur G H & Mahale V B, *Indian J Chem*, **26A** (1987) 1063.
7 Krishnan V & Patel C C, *Chemy Ind*, (1961) 321.
8 Vogel A I, *A text book of practical organic chemistry* (ELBS, Longmans Green, London).
9 Biradar N S, Mahale V B & Kulkarni V H, *J inorg nucl Chem*, **35** (1973) 2565.
10 Biradar N S, Mahale V B & Kulkarni V H, *Inorg chim Acta*, **7** (1973) 267.
11 Sangari H S, Chhatwal G R, Singh R P & Kaushik N K, *Indian J Chem*, **20A** (1981) 185.
12 Madhok K L, *Indian J Chem*, **24A** (1985) 122.
13 Clark R J H, Davies A G & Puddephatt R J, *J chem Soc*, **A** (1968) 1828.
14 Kulkarni V H, Patil B R & Prabhakar B K, *J inorg nucl Chem*, **43** (1981) 17.
15 Garcia-Vazquez Jose A, Lopez-Becerra Manuel & Masaguer Jose R, *Polyhedron*, **2(10)** (1983) 1081.

Indian Journal of Chemistry
Vol. 27A, September 1988, pp. 806-808

Synthesis & Characterisation of Co(II), Ni(II), Cu(II), Zn(II), Cd(II), UO_2^{2+} & VO^{2+} Chelates of *o*-(N-α-Pyrrolidimino)propanoic Acid & *o*-(N-α-Pyrrolidimino) benzoic Acid

SANTWANA GAUR, S P RANGA, SHOBHA SHARMA & R K MEHTA*

Department of Chemistry, University of Jodhpur, Jodhpur

Received 7 *July* 1987; *revised and accepted* 1 *February* 1988

The stability constants of the chelates of Co(II), Ni(II), Cu(II), Zn(II), Cd(II), UO_2^{2+} and VO^{2+} with *o*-(N-α-pyrrolidimino)propanoic acid (H_2PP) and *o*-(N-α-pyrrolidimino) benzoic acid (H_2PB) have been determined potentiometrically using Calvin's extension of Bjerrum's method in aqueous medium ($\mu = 0.1, 0.05$ and $0.01\,M$ $NaClO_4$) at 25°, 35° and 45°C, respectively. The thermodynamic parameters ($\Delta G°$, $\Delta H°$ and $\Delta S°$) have also been evaluated. Metal chelates have been isolated in the solid state also and characterised on the basis of elemental analyses, magnetic, UV and IR spectral, molar conductance and thermal studies.

The dissociation constants of *o*-(N-α-pyrrolidimino)propanoic acid (H_2PP) and *o*-(N-α-pyrrolidimino)benzoic acid (H_2PB) and stability constants of their chelates with Co(II), Ni(II), Cu(II), Zn(II), Cd(II), UO_2^{2+} and VO^{2+} have been determined by Calvin's extension of Bjerrum's method[1,2]. The results obtained are represented in the present note.

The ligands H_2PP and H_2PB were synthesised by the condensation of 2-pyrrolidone with β-alanine and anthranilic acid separately in presence of piperidine as the condensing agent. On refluxing equimolar ethanolic solutions of the reactants for 2-3 hr, light yellow solutions were obtained which were filtered hot, concentrated and cooled when yellow crystals separated out. These were recrystallised from ethanol. H_2PP and H_2PB were obtained in quantitative yields; M.P.: 121°C (H_2PP) and 86°C (H_2PB). [Found: C, 53.80; H, 7.60; N, 17.89. $C_7H_{12}N_2O_2$ (H_2PP) requires: C, 53.84; H, 7.69; N, 17.94%; and Found: C, 64.61; H, 5.82; N, 13.68. $C_{11}H_{12}N_2O_2$ (H_2PB) requires: C, 64.70; H, 5.88; N, 13.72%]. The purity of the ligands was checked by TLC and spectral data.

The following solutions (A—C) (total volume 40 ml) were prepared and titrated potentiometrically against carbonate-free sodium hydroxide solution ($0.1\,M$) at 25°, 35° and 45°C and ionic strengths of 0.1, 0.05 and $0.01\,M$ ($NaClO_4$): (A) 10.0 ml of $0.01\,M$ H_2PP/H_2PB + 4.0 ml $1.0\,M$ $NaClO_4$ + 26.0 ml water; (B) 10.0 ml of $0.01\,M$ H_2PP/H_2PB + 4.0 ml $1.0\,M$ $NaClO_4$ + 10.0 ml $0.01\,M$ metal ion solution + 16.0 ml water; (C) 20.0 ml of $0.01\,M$ H_2PP/H_2PB + 4.0 ml $1.0\,M$ $NaClO_4$ + 10.0 ml $0.01\,M$ metal ion solution + 6.0 ml water.

The values of pK_1 and pK_2 of H_2PP and H_2PB, as determined by interpolation at half $\bar{n}$ values method and algebraic method were found to be 5.20, 9.50 and 5.03, 8.77 at 25°C; 5.04, 9.34 and 4.74, 8.55 at 35°C; 4.82, 8.95 and 4.57, 8.29 at 45°C, respectively at $\mu = 0.1\,M$ $NaClO_4$, revealing the biprotic nature of the ligands. With decreasing ionic strength the *pK* values increase in accordance with Hückel rule[12]. The *pK* values fall with the rise of temperature. The formation curves for metal-ligand systems drawn by plotting $\bar{n}$ vs $-[\log A^{2-}]$ attain maxima at $\bar{n} > 1.5$ indicating the formation of 1:1 and 1:2 chelates. The refinement of the stability values was done by various computational methods[3], e.g., correction term, convergence formula, successive approximation and interpolation at various $\bar{n}$ values. The average values of stabilities follow the order: $VO^{2+} > UO_2^{2+} >$ Cu(II) > Ni(II) > Co(II) > Zn(II) > Cd(II), in agreement with Irving-Williams rule[4] (Table 1).

The values of overall changes in free energy ($\Delta G°$) enthalpy ($\Delta H°$) and entropy ($\Delta S°$) were evaluated using Gibbs-Helmholtz equation. The positive $\Delta H°$ values reveal the existence of some steric strain around the metal ion in the complexes due to fused rings. The positive entropy ($\Delta S°$) term is favourable for the formation of chelates.

On incorporating the data in Harned's equation[5], values of θ, pK_m^H and ΔH^* were found to be 500.84, 3.42, 84.61 and 515.57, 1.75, 87.29 for H_2PP and H_2PB respectively.

The solid metal chelates[6-8] were obtained by refluxing an ethanolic solution of H_2PP/H_2PB ($0.02\,M$) with metal nitrate ($0.02\,M$) solution in 75% ethanol. During reflux, mixture was stirred, a few drops of dil. ammonia were added till solid mass separated out which was then filtered, washed and dried *in vacuo*.

Microanalysis of the metal chelates display 1:1 (metal-ligand) stoichiometry. Pyrolysis (TGA) thermograms of the hydrated chelates revealed that on gradual heating from room temperature the hydrated salts were completely dehydrated and decomposed in the temperature range 190-800°. From the mass-loss curves of the metal chelates it is observed that no change occurs around 80-190° indicating the absence of crystal-held water in them. TGA of these chelates revealed mass-loss corresponding to three water molecules (n = 3) when M = Co(II), Ni(II) and Cu(II), two water molecules (n = 2) when M = VO^{2+}, and one

Table 1—Stability Constants and Thermodynamic Parameters at 35°C of Bivalent Metal Chelates of *o*-(N—α-Pyrrolidimino)propanoic Acid (H_2PP) and *o*-(N—α-Pyrrolidimino)benzoic Acid (H_2PB)

Metal ion	log β°			$-\Delta G°$ (kJmol^{-1})	$\Delta H°$ (kJmol^{-1})	$\Delta S°$ (J deg^{-1} mol^{-1})
	25°	35°	45°			
Co(II)	17.40	17.56	17.72	103.56	29.03	430.48
	(19.25)	(19.32)	(19.45)	(113.94)	(19.95)	(434.70)
Ni(II)	20.20	20.32	20.45	119.83	22.68	462.69
	(20.92)	(21.05)	(21.15)	(124.14)	(20.86)	(470.77)
Cu(II)	21.35	21.41	21.50	126.26	13.60	454.09
	(22.51)	(22.63)	(22.75)	(133.46)	(21.77)	(503.99)
Zn(II)	9.64	9.70	9.79	57.20	13.60	229.87
	(9.65)	(9.78)	(9.90)	(57.67)	(22.68)	(260.87)
Cd(II)	9.28	9.35	9.45	55.14	15.42	229.09
	(8.46)	(8.54)	(8.69)	(50.36)	(20.86)	(231.23)
UO_2^{2+}	22.72	22.82	22.92	134.58	18.14	495.84
	(23.55)	(23.63)	(23.72)	(139.35)	(15.42)	(502.90)
VO^{2+}	22.40	24.52	24.61	144.60	19.05	531.33
	(24.99)	(25.10)	(25.25)	(148.02)	(23.58)	(557.14)

The values in the parantheses are those of the H_2PB-chelates.

Table 2—Electronic Spectral Data of Co(II), Ni(II), Cu(II) and VO^{2+} Complexes of H_2PP and H_2PB

Complex	Band maxima (cm^{-1})			Assignments
	ν_1	ν_2	ν_3	
H_2PP				
$Co(C_7H_{10}N_2O_2)(H_2O)_3$	8483	18000	21950	$^4T_{1g}(F) \rightarrow {}^4T_{2g}(F)$; $^4T_{1g}(F) \rightarrow {}^4A_{2g}(F)$; $^4T_{1g}(F) \rightarrow {}^4T_{1g}(P)$;
$Ni(C_7H_{10}N_2O_2)(H_2O)_3$		14970	26980	$^3A_{2g} \rightarrow {}^3T_{1g}(F)$; $^3A_{2g} \rightarrow {}^3T_{1g}(P)$
$Cu(C_7H_{10}N_2O_2)(H_2O)_3$	12890			$^2E_g \rightarrow {}^2T_{2g}$
$VO(C_7H_{10}N_2O_2)(H_2O)_2$	11880	20680		$d_{xy} \rightarrow d_{xz}, d_{yz}$; $d_{xy} \rightarrow d_{x^2-y^2}$
H_2PB				
$Co(C_{11}H_{10}N_2O_2)(H_2O)_3$	8110	17590	20900	$^4T_{1g}(F) \rightarrow {}^4T_{2g}(F)$; $^4T_{1g}(F) \rightarrow {}^4A_{2g}(F)$; $^4T_{1g}(F) \rightarrow {}^4T_{1g}(P)$;
$Ni(C_{11}H_{10}N_2O_2)(H_2O)_3$		14470	25100	$^3A_{2g} \rightarrow {}^3T_{1g}(F)$; $^3A_{2g} \rightarrow {}^3T_{1g}(P)$;
$Cu(C_{11}H_{10}N_2O_2)(H_2O)_3$	14200			$^2E_g \rightarrow {}^2T_{2g}$
$VO(C_{11}H_{10}N_2O_2)(H_2O)_2$	11850	20400		$d_{xy} \rightarrow d_{xz}, d_{yz}$, $d_{xy} \rightarrow d_{x^2-y^2}$

water molecule (n = 1) when M = Zn(II), Cd(II) and UO_2^{2+}.

The molar conductance values of $10^{-3}M$ solutions of metal chelates in DMF lie in the range 3.1-6.9 and 2.8-5.7 ohm^{-1}cm^{2}mol^{-1}, indicating their non-electrolytic nature. All the metal chelates, except those of Zn(II), Cd(II) and UO_2^{2+} were found to be paramagnetic. The magnetic moments of the hydrated chelates of Co(II), Ni(II), Cu(II) and VO^{2+} with H_2PP/H_2PB are 4.85/4.93, 3.21/3.23, 1.95/1.93, 1.86/1.95 B.M. respectively, indicating the presence of 3, 2, 1 and 1 unpaired electrons. Thus, based on these evidences, an octahedral geometry is suggested for Ni(II), Co(II), UO_2^{2+} and VO^{2+} chelates. Cu(II) chelate appears to have a distorted octahedral geometry. Zn(II) and Cd(II) chelates are expected to be tetrahedral.

Results of electronic spectra of the metal chelates in benzene are shown in Table 2 which suggest an octahedral geometry for the Co(II), Ni(II), Cu(II) and VO^{2+} chelates of both the ligands.

The electronic spectrum of Ni(II) complex exhibited two bands, ν_2 and ν_3, at 14970, 25980 m^{-1} (H_2PP) and 14470, 25100 cm^{-1} (H_2PB) and the band ν_1 at 8970 cm^{-1} (H_2PP) and 8770 cm^{-1} (H_2PB). Values of ν_1, ν_2 and ν_3 were used for calculation of Racah parameters (*B* and *C*) 1001, 4654.6 (for H_2PP) and 833, 3873.0 (for H_2PB). Condon-Shortly parameters (F_2

and F_4) were found to be 1665.5, 132.9 (for H_2PP) and 1386.3, 110.6 (H_2PB) respectively. The value[9] of 'β' 0.92 (H_2PP) and 0.77 (H_2PB) was used to estimate the Sinha's covalency parameter (δ)[10] 0.08 (H_2PP) and 0.29 (H_2PB) 1-β values 0.08 and 0.23 (H_2PP and H_2PB), indicated the nature of bonding between metal and ligand to be more covalent as compared to metal-aquo ion. Value of '*Dq*' was calculated as 897 and 877 cm^{-1} for H_2PP and H_2PB respectively. The ratio ν_2/ν_1 1.66 (H_2PP) and 1.65 (H_2PB) was well within the expected range. The L F S E value was found to be 30.79 (H_2PP) and 30.08 (H_2PB) kcal/mol.

Similarly the spectral parameters for Co(II) complexes were calculated. The values are: Racah parameter (*B* and *C*) 967, 4071.0 (H_2PP) and 944, 3974.2 (H_2PB); Condon-Shortly parameters (F_2 and F_4) 1348.5, 116.3 (H_2PP) and 1511.7, 113.5 (H_2PB) values of (β) 0.78 and 0.76; (δ) 0.28 and 0.31; (1-β) 0.22 and 0.24; (*Dq*) 848 and 811 cm^{-1}; (ν_2/ν_1) ratio 2.12 and 2.17 and L F S E, 14.54 and 13.90 kcal/mol were found for H_2PP and H_2PB complexes respectively.

For Cu(II) complexes, value of *Dq* were calculated as 1289 and 1420 cm^{-1}, and of L F S E as 22.09 and 24.34 kcal/mol for H_2PP and H_2PB respectively.

The IR spectra of the ligands H_2PP and H_2PB in KBr/Nujol mull reveal three bands in the ranges 3330-3350, 1610-1620, 2570-2590 cm^{-1} which are assignable to ν_{N-H}, $\nu > C = N$ and ν_{COOH} respectively. In all the metal chelates under examination the bands in the region 3330-3350 and 2570-2590 cm^{-1} could not be located suggesting their elimination due to chelation. $\nu > C = N$ in the complexes shifted to lower wave numbers indicating participation of azomethine nitrogen in complexation. Hydrated metal chelates displayed additional bands in the regions 500-580 and 370-410 cm^{-1} which are assignable to $\nu M - N$ and $\nu M - O$ modes respectively. All the hydrated chelates show one band in the range 3315-3320 cm^{-1} due to νOH of coordinated water. The pyridine and

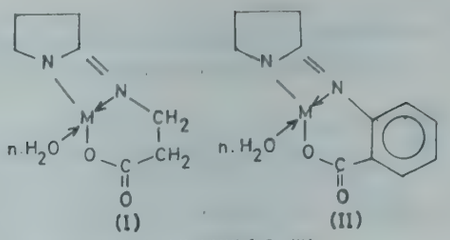

When n=3, M=Co (II), Ni (II) & Cu (II)
n=2, M= VO^{2+}
n=1, M= UO_2^{2+}, Zn (II) & Cd (II)

picoline adducts of these metal chelates indicated no such peak in the range 3200-3400 cm^{-1}. This observation clearly corroborates the coordinated nature of water molecules as indicated by their loss at relatively high temperature (> 180°C). Further, a band in the region 720-755 cm^{-1} in the IR spectra of the chelates indicates that water molecules are coordinated and not latice held.

Based on the above findings the metal chelates may be represented by the structures I and II involving four-membered rings. Metal chelates having four-membered rings are fairly stable[11].

References

1 Bjerrum J, *Metal amine formation in aqueous solution* (P Haase, Copenhagen), (1941) 298.
2 Hodgson D J, *Progr inorg Chem*, **19** (1975) 173.
3 Irving H & Rossotti H S, *J chem Soc*, (1953) 3397.
4 Irving H & William R J P, *J chem Soc*, (1953) 3192; *Nature*, **162** (1948) 746.
5 Harned H S & Kazanijian J, *J Am chem Soc*, **58** (1936) 1912.
6 Gupta C P, Sankhala N K & Mehta R K, *J prakt Chem*, **321** (1979) 691.
7 Mehta P, Bhatia S & Mehta R K, *Z phys Chem, Leinzig*, **267** (1986) 392.
8 Gupta C P, Sankhla N K & Mehta R K, *J inorg nucl Chem*, **41** (1979) 1392.
9 Jorgensen C K, *Progr inorg Chem*, **4** (1962) 73.
10 Sinha S P, *Spectrochim Acta*, **22** (1966) 57.
11 Pandey B D & Rupainwar D C, *Curr Sci*, **49** (1980) 339.
12 Huckel E, *Z Phys*, **26** (1925) 93.

Indian Journal of Chemistry
Vol. 27A, September 1988, pp. 809-811

Uranyl Nitrate Complexes of Some Schiff Bases Derived from Substituted Benzaldehydes & Amino Compounds

G SOBHANA DEVI & P INDRASENAN*
Department of Chemistry, University of Kerala, Trivandrum 695 034

Received 14 *July* 1987; *revised* 18 *January* 1988; *accepted* 1 *February* 1988

Complexes of uranyl nitrate with ten schiff bases have been prepared and characterised on the basis of analytical, conductance, molecular weight and spectral data. The schiff bases used are; N-(3-methoxy-4-hydroxybenzylidene)benzhydrazone (MHBBH), N-(3-methoxy-4-hydroxybenzylidene)salicyloylhydrazone (MHBSH), N-(3-methoxy-4-hydroxybenzylidene)-anthranilic acid (MHBAA), N^2-(3-methoxy-4-hydroxybenzylidene)aminophenol (MHBAP), N^4-(3-methoxy-4-hydroxybenzylidene)aminoantipyrine (MHBAAP), N-(3,4-dimethoxybenzylidene)benzhydrazone (DMBBH), N-(3,4-dimethoxybenzylidene)salicyloylhydrazone (DMBSH), N-(3,4-dimethoxybenzylidene)anthranilic acid (DMBAA), N^2- 3, 4-dimethoxybenzylidene)aminophenol (DMBAP) and N^4-(3,4-dimethoxybenzylidene)aminoantipyrine (DMBAAP).

As a part of our programme for the synthesis and characterisation of solid actinide complexes[1,2], presently we have prepared and characterised hitherto unknown uranyl nitrate complexes with ten schiff bases obtained by the condensation of 3-methoxy-4-hydroxybenzaldehyde (vanillin) and 3,4-dimethoxybenzaldehyde (veratraldehyde) with benzhydrazide, salicyloylhydrazide, anthranilic acid, 2-aminophenol and 4-aminoantipyrine.

Uranyl nitrate (BDH, AR, 99.9% pure) was used as such. The ten schiff bases, viz. N-(3-methoxy-4-hydroxybenzylidene)benzhydrazone (MHBBH), N-(3-methoxy-4-hydroxybenzyli dene)salicyloyldrazone (MHBSH), N^2-(3-methoxy-4-hydroxybenzylidene)aminophenol (MHBAP), N-(3,4-dimethoxybenzylidene)benzhydrazone (DMBBH), N-(3,4-dimethoxybenzylidene) salicyloylhydrazone (DMBSH), N^2-(3,4-dimethoxybenzylidene) aminophenol (DMBAP), N^4-(3-methoxy-4-hydroxybenzylidene)aminoantipyrine (MHBAAP), N^4-(3,4-dimethoxybenzylidene)aminoantipyrine (DMBAAP) and N-(3-methoxy-4-hydroxybenzylidene) anthranilic acid (MHBAA) and N-(3,4-dimethoxybenzylidene) anthranilic acid (DMBAA) were prepared by the literature method and their purities checked by TLC, IR spectra and melting points. The complexes were prepared by the methods described below:

(a) The uranyl complexes of MHBBH, MHBSH, MHBAP, DMBBH, DMBSH and DMBAP were prepared as follows: Solutions of uranyl nitrate (2 mmol) and the ligand (4 mmol) in hot dry acetonitrile were mixed and refluxed on a steam-bath for 3-4 hr and the reaction mixture was concentrated in air. Complexes of MHBBH, DMBBH and DMBSH which separated out on cooling the concentrates were filtered and washed with acetonitrile. Complexes of MHBSH, MHBAP and DMBAP were isolated by the addition of benzene to the concentrates, filtered and washed several times with hot benzene to remove excess ligand. These three complexes were dissolved in minimum quantity of hot acetonitrile and recrystallised by the addition of ether.

(b) For the complexes of MHBAAP and DMBAAP, solutions of uranyl nitrate (2 mmol) and the ligand (4 mmol) in methanol were mixed and refluxed on a steam-bath for 2hr. For the preparation of the complexes of MHBAA and DMBAA the above procedure was adopted in ethanol. The reaction mixture was concentrated. Complexes of MHBAAP and DMBAAP were crystallised on concentration and the complexes of MHBAA and DMBAA were separated by the addition of ether. These four complexes were filtered and washed with ether and methanol or ethanol.

All the ten complexes were dried *in vacuo* over phosphorus(V) oxide.

All the ten complexes are brownish yellow or orange yellow coloured, non-hygroscopic, microcrystalline solids, which are soluble in acetone, acetonitrile, ethanol, methanol and nitrobenzene and insoluble in benzene, carbon tetrachloride, chloroform, diethyl ether and petroleum ether. Analytical and molecular weight data (Table 1) of the complexes show that they have the composition, $UO_2L_2(NO_3)_2$ (where L = MHBBH, MHBSH, MHBAA, MHBAP, MHBAAP, DMBBH, DMBSH, DMBAA, DMBAP and DMBAAP). Molar conductance values of the complexes in acetonitrile and nitrobenzene (Table 1) indicate that all the complexes behave as non-electrolytes suggesting coordination of the nitrate groups. However, in methanol conductance values equal that of 1:1 electrolytes (Table 1), probably due to partial substitution of the solvent molecules for the coordinated nitrate groups.

Electronic spectra of the ligands and the complexes in acetonitrile do not give much structural details. The spectra of the ligands exhibit two strong bands in the regions 210-230 and 300-375 nm, assignable to π-π^*

Table 1—Analytical, Molecular Weight and Conductance Data of Uranyl Nitrate Complexes with Some Schiff Bases

Complex	Found(%) (calc)[a]				Mol. wt[b]	Λ_M(ohm^{-1}cm^{2}mol^{-1}) in $10^{-3}M$		
	Metal	C	H	N		Acetonitrile	Methanol	Nitrobenzene
$[UO_2(MHBBH)_2(NO_3)_2]$	25.30 (25.48)	38.44 (38.54)	3.00 (3.00)	9.02 (8.99)	956 (934)	12.93	95.74	3.15
$[UO_2(MHBSH)_2(NO_3)_2]$	24.46 (24.64)	37.20 (37.27)	2.95 (2.90)	8.57 (8.70)	970 (966)	12.80	97.28	3.40
$[UO_2(MHBAA)_2(NO_3)_2]$	25.70 (25.43)	38.03 (38.46)	2.97 (2.78)	5.71 (5.98)	920 (936)	13.01	72.45	3.38
$[UO_2(MHBAP)_2(NO_3)_2]$	27.35 (27.03)	37.99 (38.18)	3.01 (2.95)	6.21 (6.36)	805 (800)	27.65	80.64	5.98
$[UO_2(MHBAAP)_2(NO_3)_2]$	22.25 (22.28)	43.28 (42.70)	4.10 (3.56)	10.01 (10.49)	1015 (1068)	11.52	91.05	2.97
$[UO_2(DMBBH)_2(NO_3)_2]$	25.11 (24.74)	39.75 (39.92)	3.53 (3.33)	8.47 (8.73)	927 (962)	12.42	90.88	3.46
$[UO_2(DMBSH)_2(NO_3)_2]$	23.91 (23.94)	38.35 (38.63)	3.27 (3.22)	8.01 (8.45)	830 (845)	14.21	96.00	3.49
$[UO_2(DMBAA)_2(NO_3)_2]$	24.53 (24.69)	42.27 (42.62)	3.97 (3.98)	5.73 (5.81)	970 (964)	25.09	92.17	6.14
$[UO_2(DMBAP)_2(NO_3)_2]$	24.89 (26.20)	39.19 (39.65)	3.50 (3.30)	5.88 (6.17)	930 (908)	42.11	96.00	7.15
$[UO_2(DMBAAP)_2(NO_3)_2]$	21.72 (21.89)	43.70 (43.79)	3.98 (3.83)	9.97 (10.02)	1058 (1096)	10.24	90.88	2.18

[a] Calculated values in parentheses; metal contents were determined gravimetrically as U_3O_8.
[b] Molecular weights were determined by cryoscopic method in nitrobenzene; calculated molecular weights are given in parentheses.

type and n-π^* type intraligand charge transfer (CT) transitions, respectively. The spectra of the complexes are quite similar and the absence of any band corresponding to the transition of UO_2^{2+} entity is due to strong absorbance of the CT bands such that other absorptions are almost reduced to non-entities.

The IR spectra of all the ten ligands exhibit a strong or medium band in the region 1580-1620 cm^{-1} assignable to azomethine stretching mode. This band is shifted by ~ 30-40 cm^{-1} to the lower frequency side in the spectra of the complexes suggesting that the nitrogen of the azomethine group is coordinated to the metal ion. In the IR spectra of the MHBAAP and DMBAAP sharp bands are observed around 1640 cm^{-1} which may be assigned to ring $\nu_{C=O}$. In the case of complexes this band is shifted to lower frequency side by ~ 40 cm^{-1} suggesting that the ring carbonyl group is coordinated to the metal ion. The spectra of MHBBH, MHBSH, MHBAA, DMBBH, DMBSH and DMBAA exhibit a strong band in the range of 1630-1685 cm^{-1} assignable to side chain $\nu_{C=O}$ and in the complexes this band is shifted to lower frequency region ($\Delta\nu$ ~ 10-60 cm^{-}) indicating that the side chain carbonyl group also participates in coordination. The appearance of ν_{NH} mode at 3200 cm^{-1} in the spectra of the complexes of MHBBH MHBSH, DMBBH and DMBSH supports that the keto forms of these ligands are involved in coordination.

The IR spectra of MHBSH, MHBAP, DMBSH and DMBAP exhibit bands at 3410-3475 and 1330 cm^{-1} assignable to ν_{OH}(phenolic) and ν_{C-O}, respectively. In the complexes these bands lose sharpness and intensity and are shifted to 3325-3400 and 1360-1380 cm^{-1}, respectively. The shift of ν_{C-O} to higher wavenumber is expected and is due to change of H-bonded structure of the free ligands to covalent metal-bonded structure of the complexes[3,4].

In the spectra of all the complexes four additional bands which are not present in the spectra of the free ligands, are observed. Of these the band around 1020 cm^{-1} is assigned to ν_2 vibration of the NO_3 group. The bands appearing around 1460-1500 and 1260-1300 cm^{-1} in all the complexes are the two split bands of the coordinated nitrate groups, viz. ν_4 and ν_1, respectively. The difference of the order of ~ 220 cm^{-1} in ν_4 and ν_1 confirms that the nitrate groups are coordinated bidentately to the metal ion[5]. The fourth additional band appearing at 910-930 cm^{-1} is attributed to $\nu_{as}O=U=O$ (ν_3) mode. The absence of $\nu_s O=U=O$ (ν_1) mode indicates that the linearity of UO_2^{2+} ion is maintained in the complexes also[6]. Hence, the two oxygen atoms in UO_2^{2+} ion is in *trans* positions.

On the basis of the above observations, the ligands MHBBH, MHBAP, MHBAA, MHBAAP, DMBBH, DMBAA, DMBAP and DMBAAP act as neutral bidentate ligands, while MHBSH and

DMBSH act as terdentate ones. In the present series of complexes a coordination number of ten is suggested for the complexes with MHBSH and DMBSH and a coordination number of eight for the remaining complexes.

We wish to express our sincere thanks to Prof. C G R Nair for his useful suggestions and to the CSIR, New Delhi for the award of a junior research fellowship to one of us (G S D).

References

1 Sobhana Devi G & Indrasenan P, *Inorg chim Acta*, **133** (1987) 157.

2 Babu Kuncheria & Indrasenan P, *Polyhedron* (in press).

3 Doretti L, Sitran S, Madalosso F, Bandoli G & Paolucci G, *J inorg nucl Chem*, **42** (1980) 1060.

4 Syamal A, *Transition met Chem*, **5** (1980) 220.

5 Curtis N F & Curtis Y M, *Inorg Chem*, **4** (1965) 804.

6 Jacob Chacko, *Synth react inorg met-org Chem*, **12** (1982) 361.

Indian Journal of Chemistry
Vol. 27A, September 1988, pp. 812-814

Iron(III) Complexes of 2,4-Dihydroxybenzophenone Semicarbazone (DBPS) & Thiosemicarbazone (DBPT) & Determination of Iron(III) using DBPS & DBPT

K HUSSAIN REDDY, K GIRIDHARA REDDY & D VENKATA REDDY*

Department of Chemistry, Sri Krishnadevaraya University, Anantapur 515 003

Received 8 *September* 1987;
revised and accepted 25 *January* 1988

2,4-Dihydroxybenzophenone semicarbazone (DBPS) and 2,4-dihydroxybenzophenone thiosemicarbazone (DBPT) form coloured complexes with iron(III) in sodium acetate-acetic acid buffer medium. Analytical parameters of iron(III) complexes of DBPS and DBPT have been studied to establish optimum conditions for the determination of iron(III). Solid complexes of the type $[FeL_2]OAc$ (where L = DBPS or DBPT) have been isolated and characterized on the basis of elemental analyses, magnetic susceptibility, infrared and electronic spectral data and conductivity measurements.

Semicarbazone and thiosemicarbazone of 2,4-dihydroxyacetophenone have been earlier used by us for the spectrophotometric determination of copper(II)[1], iron (III)[1] and nickel(II)[2]. In continuation of the earlier work, we report in the present note spectral and anaytical properties of iron(III) complexes of 2,4-dihydroxybenzophenone semicarbazone (DBPS) and 2,4-dihydroxybenzophenone thiosemicarbazone (DBPT).

The instruments used in the present work were the same as described earlier[1,3]. The semicarbazide and thiosemicarbazide derivatives (DBPS and DBPT) of 2,4-dihydroxybenzophenone were prepared by the usual method in 60-70% yield (DBPS—m.p. 214-217°C, DBPT—m.p. 118-120°C). Satisfactory elemental analyses were obtained for the recrystallized samples of the ligands. Solutions (1×10^{-2} *M*) of DBPS and DBPT were prepared in DMF and 30% aq. DMF respectively. The buffers used in the present study were described earlier[2,3]. Ammonium ferric sulphate (AR) was used for the preparation of 0.1 *M* iron (III) solution which was standardized[4]. Experimental solutions were obtained by suitable dilution of the stock solution.

Iron(III) solution instantaneously forms brown and brownish red coloured complexes with DBPS and DBPT respectively in sodium acetate-acetic acid buffer (*p*H 3-5) medium. The order of addition of reagents has no effect on the absorbance. The absorbances of the complexes remain constant for 2 hr.

Procedure for iron(III) determination

Samples were prepared in 25 ml calibrated flasks by taking 10 ml of buffer (DBPS: *p*H 4.0; DBPT: *p*H 4.5) solution, iron(III) solution (11-110 μg for DBPS; 17-117 μg for DBPT), 2.5 ml of DMF and 2 ml of 1×10^{-2} *M* reagent (DBPS or DBPT) solution. Volumes were made upto the mark with distilled water and absorbances measured at 340 nm for DBPS and 360 nm for DBPT against corresponding reagent blanks as references. Calibration plots were prepared accordingly.

Iron(III) reacts instantaneously with DBPS and DBPT and forms 1:2 (M:L) complexes. The stability constants as obtained by the Job's method are 2.8×10^8 and 2.0×10^8 for iron(III) complexes of DBPS and DBPT respectively. The stability constant order, $K_{Fe(DBPS)_2} > K_{Fe(DBPT)_2}$, is compatible with previous observations[1,5] which suggest that iron(III) has a strong tendency to bond with oxygen. The ligand field stabilization energy depends on the charge density distribution and polarizability of the ligand[6]. The $\rangle C=O$ group present in DBPS has higher polarizability in comparison with that of $\rangle C=S$ group of DBPT. Consequently, $Fe(DBPS)_2$ complex has higher stability.

The complexation reactions were studied in detail with a view to finding optimum conditions for the

Table 1—Physicochemical & Analytical Propeties of Complexes

Characteristic	Complexes	
	Fe(III)-DBPS	Fe(III)-DBPT
Colour	Brown	Brownish red
λ_{max}(nm)	340	360
Mol of reagent required per mol of metal ion	10	20
Optimum *p*H range	3-5	3-5.5
Beer's law validity range (ppm)	0.45-4.47	0.67-4.70
Optimum concentration range (ppm)	0.94-3.76	0.83-4.20
Molar absorptivity ($l\ mol^{-1}\ cm^{-1}$)	0.80×10^4	0.75×10^4
Sandell's sensitivity ($\mu g\ cm^{-2}$)	0.00698	0.00745
Standard deviation for ten replicate determinations	0.0050*	0.0070†
Composition (M:L) of complex (Job's and mole ratio methods)	1:2	1:2
Stability constant (Job's method)	2.8×10^8	2.0×10^8

*In the determination of 2.35 ppm of iron.
†In the determination of 2.70 ppm of iron.

Table 2—Analytical, Physicochemical and Spectral Data of Solid Complexes

Complex	Found (Calc), %				$\mu_{eff.}$ (B.M.)	λ_{max} (nm)
	C	H	N	Fe		
$Fe(DBPS)_2CH_3COO$	55.65 (54.94)	3.98 (4.12)	12.63 (12.82)	8.45 (8.52)	5.82	340* 490†
$Fe(DBPT)_2CH_3COO$	52.95 (52.41)	3.87 (3.93)	12.10 (12.23)	7.95 (8.15)	5.68	365* 540†

*$^6A_{1g} \rightarrow {}^4T_{1g}$; †$^6A_{1g} \rightarrow {}^4E_g$

estimation of iron using DBPS and DBPT. The optimum conditions and important physicochemical and analytical characteristics of iron complexes are summarized in Table 1.

For the preparation of the complexes in the solid state, hot aqueous solution of ligand [DBPS or DBPT solution was mixed with buffer (*p*H 4.0) solution] until the metal to ligand ratio reached 1:2. The solid which separated after refluxion for 2 hr was collected after cooling the solution. The solid was washed with hot water and methanol and dried at 80°C for 2 hr in an electric oven.

Elemental analyses, magnetic susceptibility and electronic spectral data of the complexes are presented in Table 2. Positions of νC=N [DBPS 1613, DBPT 1610; Fe(III) complexes 1600 cm^{-1}], νC=O [DBPS 1682, 1593, 1444, 1286, 1247; Fe(III) complex 1649, 1518, 1443, 1277, 1247 cm^{-1}] and νC=S [DBPT 1284, 842; Fe(III) complex 1246, 843(w) cm^{-1}] modes suggest the participation of azomethine nitrogen atom[7], amido oxygen[8] (⟩C=O in Fe-DBPS complex) and thioamido sulphur[9,10] (in Fe-DBPT complex) in coordination. The complexes act as 1:1 electrolytes in DMF (Fe-DBPS: 72; Fe-DBPT: 65 ohm^{-1} cm^2 mol^{-1}) indicating that acetate is outside the coordination sphere.

In the IR spectra of ligands bands, are observed at 3479 (DBPS) and 3592 cm^{-1} (DBPT), which are usually associated with stretching vibrations of phenolic groups. The intensity of these bands decreased considerably indicating the loss of *ortho*-phenolic proton on chelation and formation of bond between metal and oxygen[11]. Based on the data in Table 2, structures (I & II) are assigned to the iron complexes of DBPS and DBPT.

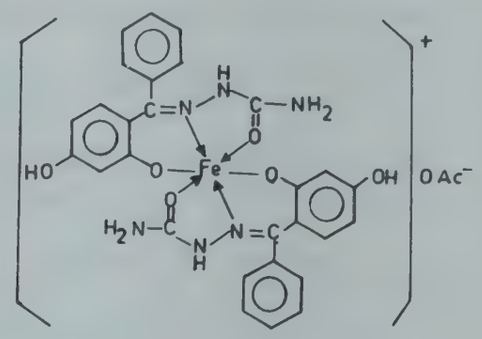

I

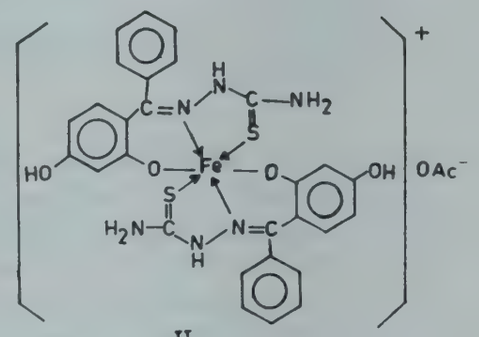

II

Effect of foreign ions

Interference due to associated ions was examined for both the reagents in the determination of 2.35 ppm of iron. The tolerance limit in ppm was taken as the amount of foreign ion required to cause ±2% error in the absorbance. In the determination of 2.5 ppm of iron using DBPS and DBPT reagents respectively fluoride (305, 300); chloride (210, 210); bromide (640, 450); iodide (810, 610); sulphate (2300, 1536); nitrate (745, 490); tetraborate (1140, 860); thiocyanate (280, 300); thiourea (24, 6); thiosulphate (13, 18), bromate (5, 5); citrate (10, 290); tartrate (18, 290); Zn(II) (130, 104); Mn(II) (22, 22); Al(III) (20, 16); W(VI) (4, 5); Pd(II) (17, 16); Ir(III) (5, 10); Cd(II) (17, 10); Sn(II) (2, 3); Zr(IV) (22, 36); Ni(II) (7, 3); Co(II) (10, 2) did not interfere. Cr(III), Ru(III), Ag(I), U(VI), Cu(II), V(V), Os(VIII), Pt(IV) and Au(III) did not interfere when they were present in equal amounts (to iron) in both the systems.

The authors thank the authorities of Sri Krishnadevaraya University, Anantapur for providing necessary facilities. The authors are thankful to the authorities of CDRI, Lucknow and RSIC, IIT, Madras for providing elemental and spectral data respectively.

References

1 Hussain Reddy K, Giridhara Reddy K, Prakash K M M S & Venkata Reddy D, *Indian J Chem*, **23A** (1984) 535.

2 Hussain Reddy K & Venkata Reddy D, *Indian J Chem*, **22A** (1983) 824.

3 Hussain Reddy K & Venkata Reddy D, *Indian J Chem*, **24A** (1985) 154.

4 Vogel A I, *A text book of quantitative inorganic analysis* (ELBS, Longmans Green, London), 1960, 310.

5 Kolthoff I M & Elving P J, *Treatise on analytical chemistry*, Part II, Vol. 2 (Interscience, New York), 260.

6 Olsen E D, *Modern optical methods of analysis* (McGraw Hill, New York), 1975, 105.

7 Sahni S K, Gupta S P, Sangal S K & Rana V B, *J inorg nucl Chem*, **39** (1977) 1098.

8 Chandra S, Bharat B K, Pandeya R B & Singh R P, *J inorg nucl Chem*, **39** (1977) 2079.

9 Venkayappa D & Brown R D, *J inorg nucl Chem*, **36** (1974) 1023.

10 Vigee B G & Selbin J, *J inorg nucl Chem*, **31** (1969) 3187.

11 Jain M C, Sharma R K & Jain P C, *Curr Sci*, **48** (1979) 1056.

Indian Journal of Chemistry
Vol. 27A, September 1988, pp. 815-818

Synthesis, Characterisation & Fungicidal Activity of the Complexes of N-Alkyl phenothiazines with Titanium(IV)

B KESHAVAN* & J SEETHARAMAPPA
Department of Post-graduate Studies & Research in Chemistry, University of Mysore, Mysore 570 006

Received 24 *September* 1987; *revised* 9 *November* 1987; *rerevised and accepted* 4 *February* 1988

Complexes of the type $[Ti(C_2O_4)_2L].2H_2O$ where L = N-alkylphenothiazine (NAP) have been synthesized. The stoichiometry of the complexes has been proposed on the basis of elemental analyses, conductance, magnetic and thermal data. The coordination behaviour of the ligands has been determined with the help of spectroscopic (IR, electronic and ^1H NMR) studies. Probable structures of the complexes have been proposed. The fungicidal activity of the isolated complexes has been investigated.

N-Alkylphenothiazines (NAP) have been reported to be biologically versatile compounds, possessing anticholinergic, antihistamine and antiamoebic activities[1,2]. It is known that the metal complexes have greater activity than the ligands themselves. Recently, a considerable increase in the fungicidal activity of phenothiazines on complexation of phenothiazines with copper(II) and dioxouranium(VI) has been reported[3,4]. In view of the importance of metal-phenothiazine complexes as fungicides, it was considered worthwhile to study the titanium(IV)-NAP complexes.

We report here the synthesis, characterization and fungicidal activity of titanium(IV) complexes with chlorpromazine (CP), promethazine (PM), propericiazine (PPC), methotrimeprazine (MTM), mepazine (M), perazine (P), propionyl promazine (PP) and butaperazine (BP).

Potassium titanyl oxalate dihydrate and N-alkylphenothiazines (structure I) were used as received.

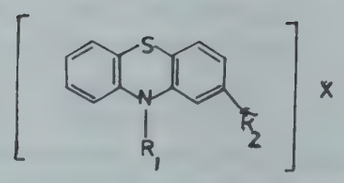

Structure I

Chlorpromazine hydrochloride: $R_1 = CH_2CHMeNMe_2$, $R_2 = Cl$ and X = HCL

Promethazine hydrochloride: $R_1 = CH_2CHMeNMe_2$, $R_2 = H$ and X = HCl

Propericiazine: $R_1 = (CH_2)_3NC_5H_9OH$, $R_2 = CN$ and X = —

Methotrimeprazine: $R_1 = CH_2CHMeCH_2NMe_2$, $R_2 = OMe$ and X = —

Mepazine hydrochloride: $R_1 = CH_2CH(CH_2)_4NMe$, R_2 = —and X = HCl

Perazine dimalonate: $R_1 = (CH_2)_3(CH_2)_4NMe$, R_2 = —and X = dimalonate

Propionylpromazine phosphate: $R_1 = (CH_2)_3NMe_2$, $R_2 = COCH_2Me$ X = phosphate

Butaperazine dimaleinate: $R_1 = (CH_2)_3N(CH_2)_4$ NMe, $R_2 = CO(CH_2)_3Me$ and X = dimaleinate

Synthesis of complexes

Potassium titanyl oxalate dihydrate (1.5 g, 1 mmol) dissolved in distilled water (50 cm^3) was added with vigorous stirring to a solution of N-alkylphenothiazine (1.8 g, 1 mmol) in distilled water (65 cm^3). There was an immediate separation of the solid complex. The suspension was set aside for 1 h, filtered, washed several times with water and finally with ethanol and dried *in vacuo* over fused $CaCl_2$.

Analyses for carbon, hydrogen and nitrogen were performed at the Bio-Organic Chemistry Division, Bhabha Atomic Research Centre, Bombay. Titanium was determined as TiO_2 gravimetrically. The magnetic susceptibilities were determined by the Gouy method at room temperature using $Hg[Co(SCN)_4]$ as the calibrant. The IR spectra of samples in KBr pellets were recorded on a Perkin Elmer spectrophotometer model 781. Far IR spectra were recorded using polythene discs on a polytech far IR spectrophotometer model 30. The visible and UV spectra of the complexes in dimethylformamide (DMF) were measured on a Beckman spectrophotometer model DB. The molar conductances of the complexes were measured with 10^{-3} *M* DMF solutions using Philips PR 9500 conductivity bridge. Thermal analysis was carried out on a Stanton Redcraft TG 750/770 electrobalance with a heating rate 6° min^{-1} in air. The NMR spectral data were recorded on a Hitachi-Perkin Elmer spectrometer, model FT 60 in $CDCl_3$. X-ray diffraction data were obtained with a Jeol X-ray diffractometer, model JDX 8P.

Antifungal studies

The N-alkylphenothiazines and their corresponding complexes (prepared in 10% DMF solution) were tested against *Aspergillus flavous* and *Alternaria tenius* at different concentrations by the poisoned food technique. The experiment was conducted by using potato dextrose agar (PDA), and the solutions

of the ligands and complexes were poured into petri plates containing PDA after solidification.

The test fungi *Alternaria tenius* and *Aspergillus flavous* were taken as 2 mm dishes from 7 days-old culture. The experiment was carried out with four replicates per treatment and incubation was carried out at 22 ± 2° for 8 days. The radial growth of the colony was recorded on the completion of incubation and mean diameter in each concentration was recorded. The average per cent inhibition was calculated by using the equation given by Vincent[5],

$$I = \frac{C - T}{C} \times 100$$

where I = percentage inhibition, C = colony diameter of the control and T = colony diameter of tested plates.

The analytical data of the complexes (Table 1) correspond to the formula $[Ti(C_2O_4)_2L].2H_2O$, where L = NAP. All the complexes are quite stable in air for long periods. They do not possess sharp melting points. The complexes are insoluble in water and soluble in chloroform, dimethylformamide (DMF) and dimethyl sulphoxide. The molar conductances in DMF are in the range 9-15 $ohm^{-1}\ mol^{-1}\ cm^2$ at 10^{-3} *M* concentration indicating the non-electrolytic nature of the complexes. The magnetic susceptibility values at room temperature indicate that the complexes are diamagnetic, as expected for titanium(IV) complexes. These results are consistent with the stoichiometry proposed on the basis of analytical data.

The electronic spectra of all the complexes show a band in the region 404-411 nm, which may be assigned to charge-transfer[6] in accordance with the $(n-1)d^0ns^0$ electronic configuration of titanium. The band at 250-262 nm found in the NAP and the corresponding complexes may be attributed to $\pi \rightarrow \pi^*$ transition. The band found in the region 300-320 nm in the NAP may be assigned to the $n \rightarrow \pi^*$ transition. This band is found slightly shifted towards higher energy region in the spectra of the corresponding titanium(IV)-NAP complexes, evidently due to coordination.

The selected IR frequencies of the titanium(IV)-NAP complexes are given in Table 2.

The absence of $\nu(Ti=0)$ in 1050-950 cm^{-1} region in the isolated complexes rules out the existence of (Ti = 0) moiety in the complexes[7]. In NAP, $-R_3NH^+$ interaction with Cl^- gives rise to a broad band in the 2500-2300 cm^{-1} region[2]. A broad band observed at 2600-2350 cm^{-1} in the IR spectra of the ligands corresponds to the $-CH_2NR_2H^+$ (R = methyl or pentyl) moiety together with X^- (X = chloride, phosphate, malonate or maleinate). In the IR spectra of the corresponding complexes of titanium(IV), this band totally disappears indicating that the tertiary nitrogen atom of the side chain is a site of coordination. The FAR IR bands at 540-520 cm^{-1} may be attributed to $\nu(Ti-N)$ bands[8].

In aromatic derivatives the $\nu(CSC)$ generally appears as a band of weak or moderate intensity in 705-670 cm^{-1} region[9]. However, some difficulty is experienced in recognising the $\nu(CSC)$ mode in NAP due to the presence of the intense CH out-of-plane deformation band in this region[10]. In all the complexes studied $\nu(CSC)$ suffers a significant positive shift $[-\Delta\nu(CSC) = 20\text{-}30\ cm^{-1}]$ due to coordina-

Table 1—Analytical Data of Titanium(IV) – NAP Complexes $[Ti(C_2O_4)_2L].2H_2O$

Ligand	Compound	Colour	Found (Calc.), %			
			C	H	N	Ti
CP	$[Ti(C_2O_4)_2C_{17}H_{19}N_2SCl].2H_2O$	Pale yellow	43.9 (43.5)	4.2 (4.0)	4.7 (4.8)	8.9 (8.3)
PM	$[Ti(C_2O_4)_2C_{17}H_{20}N_2S].2H_2O$	Pale yellow	46.8 (46.3)	4.0 (4.4)	5.3 (5.1)	9.1 (8.8)
PPC	$[Ti(C_2O_4)_2C_{21}H_{23}N_3OS].2H_2O$	Yellow	48.3 (48.0)	4.3 (4.3)	6.8 (6.7)	8.2 (7.7)
MTM	$[Ti(C_2O_4)_2C_{18}H_{22}N_2OS].2H_2O$	Pale blue	46.5 (46.0)	4.8 (4.5)	4.9 (4.9)	8.8 (8.3)
M	$[Ti(C_2O_4)_2C_{19}H_{22}S].2H_2O$	Pale grey	48.8 (48.4)	4.7 (4.6)	5.2 (4.9)	8.1 (8.4)
P	$[Ti(C_2O_4)_2C_{20}H_{25}N_3S].2H_2O$	Orange yellow	48.7 (48.1)	4.6 (4.6)	7.0 (7.0)	7.7 (8.0)
PP	$[Ti(C_2O_4)_2Cl_{21}H_{24}N_2OS].2H_2O$	Yellow	48.8 (49.0)	4.8 (4.6)	4.3 (4.6)	8.1 (7.8)
BP	$[Ti(C_2O_4)_2C_{24}H_{31}N_3OS].2H_2O$	Yellow	50.4 (50.2)	5.0 (5.2)	6.4 (6.3)	7.4 (7.2)

Table 2—Characteristic IR Bands (cm^{-1}) and Screening Data of Titanium(IV)-NAP Complexes, $[Ti(C_2O_4)_2L].2H_2O$

Compound	ν(Ti−N)	ν(Ti−S)	ν(OCO)	Average % Inhibition			
				Aspergillus flavous		*Alternaria tenius*	
				0.01	0.25	0.01	0.25
$[Ti(C_2O_4)_2C_{17}H_{19}N_2SCl].2H_2O$	525	320	1710 1400	44.2	65.6	38.2	71.5
$[Ti(C_2O_4)_2C_{17}H_{20}N_2S].2H_2O$	520	330	1690 1395	38.9	76.8	35.4	72.3
$[Ti(C_2O_4)_2C_{21}H_{23}N_3OS].2H_2O$	524	345	1675 1385	38.2	78.0	43.1	74.5
$[Ti(C_2O_4)_2C_{18}H_{22}N_2OS].2H_2O$	530	324	1685 1390	34.5	68.8	36.7	64.7
$[Ti(C_2O_4)_2C_{19}H_{22}N_2S].2H_2O$	534	338	1710 1375	28.8	58.7	33.4	70.2
$[Ti(C_2O_4)_2C_{20}H_{25}N_3S].2H_2O$	520	335	1700 1395	33.5	63.4	28.4	65.8
$[Ti(C_2O_4)_2C_{21}H_{24}N_2OS].2H_2O$	540	325	1695 1400	32.1	68.7	35.2	74.2
$[Ti(C_2O_4)_2C_{24}H_{23}N_3OS].2H_2O$	535	340	1705 1380	35.4	72.6	36.8	68.7
NAP	—	—	—	5-8	10-18	8-15	20-25

tion of the heterocyclic sulphur atom. This is supported by the far IR bands[8] at 345-320 cm^{-1}. The coordination of the bidentant oxalate is confirmed by the bands of 1710-1675 cm^{-1} (asymmetric COO vibration) and at 1400-1375 cm^{-1} (symmetric COO vibration)[11].

The ^1H NMR spectra of all these complexes recorded in deuterated chloroform exhibit chemical shifts at lower fields for $N-CH_3$ protons which appear at $\delta = 2.7 - 2.95$ ppm compared with the position in the free ligands ($\delta = 2.55 - 2.70$ ppm). This is probably due to the coordinating effect of the tertiary nitrogen atom which results in the deshielding of the protons attached to it. Thus, ^1H NMR studies confirm the participation of the tertiary nitrogen atom of the alkyl side chain of NAP in coordination. The integrated proton ratios correspond to the proposed formula.

Thermogravimetric studies indicate the decomposition of complexes in three steps, namely, the loss of water molecules, decomposition of organic moiety and the loss of oxalate followed by the formation of TiO_2 in the temperature ranges 80-150°, 180-385° and 400-550°, respectively. The intermediates were identified by mass loss and the end product was confirmed by X-ray diffraction data. The differences between found and calculated mass losses lie in the range 0.2-0.9%.

The decomposition scheme of $[Ti(C_2O_4)_2L].2H_2O$ in air and DTA peak temperatures for each step are indicated below:

$$[Ti(C_2O_4)_2L].2H_2O \xrightarrow{90\text{-}110^\circ\,(endo)} [Ti(C_2O_4)_2L] + 2H_2O \quad \ldots (1)$$

$$[Ti(C_2O_4)_2L] \xrightarrow{290\text{-}330^\circ\,(exo)} [Ti(C_2O_4)_2] + L \quad \ldots (2)$$

$$[Ti(C_2O_4)_2] \xrightarrow{480\text{-}540^\circ\,(exo)} TiO_2 + 2CO_2 + 2CO \quad \ldots (3)$$

Antifungal activity

The complexes and the corresponding ligands were tested for their efficacy in controlling the two fungi, *Aspergillus flavous* and *Alternaria tenius* at different concentrations by the poisoned food technique. The screening data of the average percentage inhibition of the fungi at 0.01% and 0.25% concentrations are given in Table 2.

The toxicity of the complexes can be explained on the basis of chelation theory[12]. It has been suggested that chelation reduces the polarity of the metal ion considerably because its positive charge is partially shared with donor atoms and π-electron delocalisation over the whole chelate ring is feasible. This in-

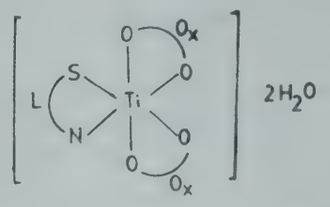

Structure II

creases the lipophilic character of the metal chelate which favours its permeation through lipoid layers of the fungus membrances.

In the light of foregoing discussion, structure (II) has been proposed for titanium(IV)-NAP complexes.

The authors thank M. Krishnappa, Department of Applied Botany, University of Mysore, Mysore for fungicidal investigations. One of them (J.S) thanks the University of Mysore for financial assistance.

References

1 Snyder S H, *Am J Psychiatry*, **133** (1976) 197.

2 Katritzky A R & Boulton A J, *Advances in heterocyclic chemistry*, Vol. 9 (Academic Press, New York) 1968, 336.

3 Keshavan B & Janardhan R, *Indian J Chem*, **25A** (1986) 1954.

4 Keshavan B & Seetharamappa J, *Inorg chim Acta*, **138** (1987) 135.

5 Vincent J M, *Nature*, **189** (1947) 850.

6 Kaushik N K, Bhushan B & Chhatwal C R, *J inorg nucl Chem*, **42** (1980) 457.

7 Weighardt K, Quilitzsch U, Weiss J & Nuber B, *Inorg Chem*, **19** (1980) 2514.

8 Singh R V, *Indian J Chem*, **24A** (1985) 1064.

9 Bellamy L J, *The infrared spectra of complex molecules* (Methuen, London) 1964, 355.

10 Rao C N R, *Chemical applications of infrared spectroscopy*, (Academic Press, London) 1963, 297.

11 Brisse F & Haddad M, *Inorg chim Acta*, **24** (1977) 173.

12 Srivastava R S, *Inorg chim Acta*, **56** (1981) L65.

Indian Journal of Chemistry
Vol. 27A, September 1988, pp. 819-821

Interaction of Divalent Metal Ions with Uracil : Part IV† — Mixed Ligand Complexes of Mn(II), Fe(II), Co(II), Ni(II) & Cu(II) with Uracil & Different Amines

ASIT R SARKAR*, PARTHASARATHI GHOSH & RANAJIT K BANDYOPADHYAY
Department of Chemistry, University of Kalyani, Kalyani 741 235

Received 25 *August* 1987; *revised and accepted* 25 *January* 1988

Mixed ligand complexes of the types $MA_2L_2(H_2O)_2$, $MBL_2(H_2O)_2$ and $MCL_2.2H_2O$ where M = Mn, Fe, Co, Ni and Cu; A = pyridine and 2-picoline; B = ethylenediamine; C = 1,10-phenanthroline, 2,2′-bipyridyl and L = deprotonated uracil have been synthesised and characterisied. The room temperature magnetic moment and electronic spectral studies indicate high-spin octahedral stereochemistry for the complexes. Infrared spectral studies indicate that uracil acts as a monodentate ligand coordinating through N(3) in complexes of the type $MA_2L_2(H_2O)_2$ and $MBL_2(H_2O)_2$ and as a bidentate ligand coordinating through C(2)=O and N(3) in $MCL_2.2H_2O$.

Studies on the interaction of divalent metal ions with the bases which are nucleic acid constituents have been subject of numerous publications in recent years[1-6]. Uracil, which is present in RNA, is a ligand of biochemical importance due to the biological relevance of metal binding to RNA constituents[7]. Until recently, relatively little information was available on the divalent metal complexes of uracil[5,6], particularly on the mixed ligand uracil complexes[8,9]. Synthesis and characterisation of the complexes of divalent 3*d* metal ions with uracil have been earlier reported by us[10-13]. In view of the physiological significance[14,15] of mixed ligand complexes of transition metal ions with uracil, we have prepared some novel mixed ligand complexes of Mn(II), Fe(II), Co(II), Ni(II) and Cu(II) containing uracil and amines such as ethylenediamine, pyridine, 2-picoline, 2,2′-bipyridyl and 1,10-phenanthroline. The complexes have been characterised on the basis of elemental analysis, conductance, thermogravimetric, magnetic moment, electronic and IR spectral studies.

Uracil was a BDH (England) reagent. All the other chemicals used were of analytical reagent grade. Pyridine and 2-picoline were distilled under reduced pressure before use. Conductivity measurements were made with a Philips conductivity bridge (NO. PR 9500). Magnetic susceptibility measurements were made by Gouy method using $Hg[Co(NCS)_4]$ as a calibrant. The experimental magnetic susceptibilities were corrected for diamagnetism[16]. Recording of thermogravimetric analysis, electronic spectra and infrared spectra were as described before[11].

Preparation of the complexes

A calculated amount of uracil was dissolved in boiling methanol and to this was added a methanolic solution of the calculated amount of metal chloride (in case of iron $FeSO_4$ was used). The resulting solution was well stirred. To this resulting solution a methanolic solution of the amine was added so that the overall ratio of metal : uracil : amine was 1:2:2 in cases where pyridine and 2-picoline were used and 1:2:1 in cases where ethylenediamine, 2,2′-bipyridyl and 1,10-phenanthroline were used. The resulting solutions were refluxed for 12 hr. On cooling, crystals appeared in the case of pyridine and 2-picoline complexes. In other cases, the volume of the solution had to be reduced by heating over a water bath to get the crystals. The complexes were separated by filtration through No.4 Gooch crucible, washed with methanol and finally dried *in vacuo* over calcium chloride. Metals in the complexes were estimated by standard methods after decomposing the complexes by heating in a platinum crucible at 800°C and digesting with HNO_3 and finally with H_2SO_4. Carbon, hydrogen and nitrogen were analysed at Dr. Alfred Bernhardt's Mikroanalytische Laboratium, West Germany.

All the complexes are coloured, stable solids in air. Their analytical data (Table 1) suggest the formulation of the complexes as $MA_2L_2(H_2O)_2$, $MBL_2(H_2O)_2$ and $MCL_2.2H_2O$ where M = Mn, Fe, Co, Ni and Cu; A = pyridine, 2-picoline; B = ethylenediamine; C = 2,2′-bipyridyl, 1,10-phenanthroline and L = deprotonated uracil. The molar conductances of these complexes in chloroform ($10^{-3}M$) lie in the range 1-5 mho cm^2 mol^{-1} indicating their nonelectrolytic nature in chloroform.

The TGA curves show that complexes of the types $MA_2L_2(H_2O)_2$ and $MBL_2(H_2O)_2$ begin to decompose round 130°C while complexes of the type $MCL_2.2H_2O$ decompose around 80°C exhibiting a horizontal portion over a very small range

†For Part III please see ref. 13.

Table 1—Analytical Data and Colours of the Complexes[a]

Complex	Colour	Found (Calc.)%			
		M	N	C	H
$Mn(en)L_2(H_2O)_2$	Pale pink	15.03 (14.72)	22.67 (22.52)	32.86 (32.17)	4.23 (4.82)
$Mn(py)_2L_2(H_2O)_2$	Pale pink	11.89 (11.65)	18.00 (17.83)	46.72 (45.86)	3.98 (4.25)
$Mn(pic)_2L_2(H_2O)_2$	Pale pink	11.03 (11.00)	16.67 (16.83)	49.08 (48.10)	4.62 (4.81)
$Fe(py)_2L_2(H_2O)_2$	Yellowish brown	11.55 (11.82)	17.70 (17.79)	45.98 (45.76)	3.87 (4.23)
$Fe(py)_2L_2(H_2O)_2$	Yellowish brown	11.06 (11.16)	17.02 (16.80)	48.79 (48.00)	4.13 (4.80)
$Fe(bipy)L_2.2H_2O$	Reddish brown	11.80 (11.89)	17.89 (17.88)	46.35 (46.97)	3.02 (3.83)
$Fe(phen)L_2.2H_2O$	Reddish brown	11.47 (11.31)	17.25 (17.01)	48.07 (48.60)	3.97 (3.64)
$Co(py)_2L_2(H_2O)_2$	Light violet	12.53 (12.40)	17.76 (17.68)	46.01 (45.47)	3.93 (4.21)
$Co(pic)_2L_2(H_2O)_2$	Light violet	11.78 (11.70)	16.87 (16.70)	48.09 (47.71)	4.25 (4.77)
$Ni(py)_2L_2(H_2O)_2$	Light green	12.43 (12.36)	18.81 (17.69)	45.92 (45.50)	3.89 (4.21)
$Ni(pic)_2L_2(H_2O)_2$	Light green	11.72 (11.68)	17.92 (16.71)	48.23 (47.74)	4.31 (4.77)
$Ni(bipy)L_2.2H_2O$	Greenish blue	12.56 (12.42)	17.65 (17.77)	45.84 (45.70)	3.07 (3.81)
$Ni(phen)L_2.2H_2O$	Greenish blue	11.87 (11.82)	16.93 (16.91)	50.11 (48.32)	3.43 (3.62)
$Cu(en)L_2(H_2O)_2$	Deep blue	16.72 (16.64)	22.17 (22.02)	31.97 (31.45)	4.20 (4.71)
$Cu(py)_2L_2(H_2O)_2$	Blue	13.51 (13.24)	17.56 (17.52)	45.92 (45.05)	3.83 (4.17)
$Cu(pic)_2L_2(H_2O)_2$	Blue	12.67 (12.51)	17.83 (16.55)	47.86 (47.29)	4.22 (4.73)

[a]Abbreviations : L = $C_4H_3N_2O_2^-$; en = ethylenediamine; py = pyridine; pic = 2-picoline; bipy = 2,2'-bipyridyl; phen = 1,10-phenanthroline

Table 2—Electronic Spectral Bands and Magnetic Moments (T = 308°A) of the complexes

Complex	Band Maxima (cm^{-1})	μ_{eff} (B.M.)
$Mn(en)L_2(H_2O)_2$		5.96
$Mn(py)_2L_2(H_2O)_2$		6.01
$Mn(pic)_2L_2(H_2O)_2$		6.03
$Fe(py)_2L_2(H_2O)_2$	7740w,10650w	5.13
$Fe(pic)_2L_2(H_2O)_2$	7760w,10660w	5.28
$Fe(bipy)L_2.2H_2O$	8500w,10750w,15550s,16900s	5.42
$Fe(phen)L_2.2H_2O$	8470w,10510w,16150s,17200s	5.45
$Co(py)_2L_2(H_2O)_2$	8900w,19800m	4.68
$Co(pic)_2L_2(H_2O)_2$	9000w,21100m	4.62
$Ni(py)_2L_2(H_2O)_2$	8650m,14000m,23700s	3.26
$Ni(pic)_2L_2(H_2O)_2$	8900m,14400m,23950s	3.22
$Ni(bipy)L_2.2H_2O$	11000w,11850m,18950m,26000vs	3.36
$Ni(phen)L_2.2H_2O$	11400w,12000m,19200m,26050vs	3.38
$Cu(en)L_2(H_2O)_2$	15150s,br	1.85
$Cu(py)_2L_2(H_2O)_2$	14650s,br	1.96
$Cu(pic)_2L_2(H_2O)_2$	14700s,br	1.96

(10°) around 150-200°C. This indicates the loss of water molecules. But we failed to obtain any definite compound by heating the complexes at constant temperature around 120-150°C.

The corrected magnetic moment data (Table 2) indicate high-spin octahedral geometry for all the complexes.

The electronic spectral data of the complexes are summarised in Table 2. The low energy weak absorption bands in all the iron(II) complexes (Table 2) may be assigned to $^5E_g \leftarrow {}^5T_{2g}$ transition. The doublet arises due to the lifting of the degeneracy of the E_g level by Jahn-Teller distortion[17]. Both the high energy strong bands in the iron-bipyridyl and -*o*-phenanthroline mixed ligand complexes are due to the chargetransfer transitions from the metal t_{2g} orbital to the vacant π^* orbital of bipyridyl or phenanthroline.

For the cobalt(II) complexes, the low energy weak absorption bands (8900-9000 cm^{-1}) may be assigned to the transition $^4T_{2g} \leftarrow {}^4T_{1g}(\nu_1)$ and the high energy medium bands (19000-21000 cm^{-1}) to the transition $^4T_{1g}(P) \leftarrow {}^4T_{1g}(F)$ (ν_3). The values of D_q, B and ν_2 were calculated[15] as 1031, 825 and 18558 cm^{-1} for the cobalt-pyridine and 1013, 844 and 18234 cm^{-1} for the cobalt-picoline mixed ligand complexes, respectively. The ratio of $\nu_2:\nu_1$ is 2.1 for the former and 2.0 for the latter complex indicating distorted octahedral stereochemistry for the cobalt(II) complexes[18]. The bands at 8650, 14000, 23700 cm^{-1} for the nickel-pyridine and at 8900, 14400, 23950 cm^{-1} for the nickel-picoline mixed ligand complexes may be assigned to three spin allowed transitions, $^3T_{2g} \leftarrow {}^3A_{2g}(\nu_1)$, $^3T_{1g}(F) \leftarrow {}^3A_{2g}(\nu_2)$ and $^3T_{1g}(P) \leftarrow {}^3A_{2g}(\nu_3)$ respectively. The values of D_q are 865 and 890 cm^{-1} for the complexes indicating octahedral symmetry for the complexes. For the nickel-bipyridyl and -phenanthroline complexes the bands at 11850, 18950 and 12000, 19200 cm^{-1} respectively may be assigned to ν_1 and ν_2 transitions. The very strong band around 26000 cm^{-1} in both the complexes is due to $t_{2g} \rightarrow \pi^*$ charge-transfer transition[19]. For all the nickel(II) complexes the ratio of $\nu_2:\nu_1$ is found to be around 1.6 which also indicates the octahedral stereochemistry for the nickel(II) complexes[20]. All the copper(II) complexes exhibit a strong broad band, which indicates the hexacoordination of the metal ions[17].

The potential binding sites of the uracil ligand (structure I) are: oxygens of the 2-keto and 4-keto groups and nitrogens at 1 and 3 positions. Free uracil ligand exhibits[21] strong bands at 1716 cm^{-1} due to $\nu C(2) = O$, 1675 cm^{-1} due to $\nu C(4) =$

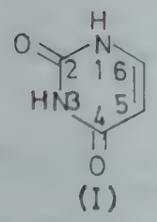

(I)

O, a medium band at 1508 cm^{-1} due to δNH(1) and another strong band at 1417 cm^{-1} due to δNH(3). The infrared spectra of all the mixed ligand complexes involving pyridine and 2-picoline give similar spectra. Since pyridine and 2-picoline absorb strongly around 1500 cm^{-1} where δNH(1) of uracil absorbs, it is not possible from the spectra to infer about the coordination through NH(1) of the uracil. In all these pyridine and 2-picoline mixed ligand complexes the position and intensity of the bands due to the νC(2) = O remain almost unchanged. The band due to νC(4) = O is shifted to lower frequency by 5-10 cm^{-1} whereas that due to the δNH(3) disappears completely. Hence, it may be suggested that in these complexes NH(3) deprotonates and coordination takes place through N(3). The other bands in the spectra of these complexes resemble those of typical complexes containing pyridine and 2-picoline ligands[22].

In the mixed ligand bipyridyl and phenanthroline complexes, position and intensity of the bands due to νC(4) = O remain unchanged but the band due to δNH(3) disappears completely and the strong band at 1716 cm^{-1} due to νC(2) = O is shifted as a weak band to ≃ 1695 cm^{-1}. The disappearance of the δNH(3) band and the appreciable change in position and intensity of the νC(2) = O band in these complexes compared to that of the free uracil indicate bidentate coordination of uracil through C(2) = O and N(3). Other bands in the spectra of these complexes resemble those of the typical chelates containing bipyridyl or phenanthroline ligands[23].

Hence, from the above studies, we conclude that all the complexes are hexacoordinated. In the course of preparation of mixed ligand ethylenediamine, pyridine and 2-picoline complexes, the reaction medium attain a $pH \simeq 9.6$. At first uracil gets deprotonated and coordination takes place through N(3) of uracil. The reaction medium attain a $pH \simeq 7.5$ during the preparation of the mixed ligand bipyridyl or phenanthroline complexes and under these condition uracil acts as a bidentate ligand coordinating through both its donor sites, C(2) = O and N(3).

The authors thank the University of Kalyani for awarding a fellowship to one of them (R.K.B.).

References

1 Eichorn G L, *Adv inorg Biochem*, **3** (1981) 1.
2 Marzilli L G, *Adv inorg Biochem*, **3** (1981) 47.
3 Lippert B, *Inorg Chem*, **20** (1981) 4326.
4 Lippert B & Neugebauer D, *Inorg Chem*,,**21** (1982) 451.
5 Goodgame M & Johns K W, *J chem Soc, Dalton*, (1977) 1680.
6 Geodgame M & Johns K W, *Inorg chim Acta*, **30** (1978) L335.
7 Swartouw B T, *J gen Microb*, **34** (1964) 115.
8 Lumme P & Mutikainen T, *Acta Crystallogr*, **B36** (1980) 2251.
9 Gupta M & Srivastava M N, *Polyhedron*, **4** (1985) 475.
10 Sarkar A R, *Proceedings of the XX international conference on coordination chemistry*, Calcutta (1979), 346.
11 Sarkar A R & Ghosh P, *Inorg chim Acta*, **78** (1983) L39.
12 Sarkar A R, Bandyopadhyay R K & Ghosh P, *J Indian chem Soc*, (In press).
13 Ghosh P, Mukhopadhyay T K & Sarkar A R, *Trans metal chem*, **9** (1984) 46.
14 Siegel H, *Metal ions in biological systems, mixed ligand complexes*, Vol 2 (Marcel Dekker, New York).
15 Sundberg R J & Martin R B, *Chem Rev*, **74** (1974) 471.
16 Earnshaw A, *Introduction to magnetochemistry* (Academic Press, London) 1968, 4.
17 Lever A B P, *Inorganic electronic spectroscopy* (Elsevier, Amsterdam) 1968, 252.
18 Patel K C & Goldberg D E, *J inorg nucl Chem*, **34** (1972) 637.
19 Lever A B P, Lewis J & Nyholm R S, *J chem Soc*, (1964) 1187.
20 Sacconi L, *Trans Metal Chem*, **4** (1968) 199.
21 Susi H & Ard J S, *Spectrochim Acta*, **A27** (1971) 1549.
22 Gill N S, Nuttal R H, Scaife D E & Sharp D W A, *J inorg nucl Chem*, **18** (1961) 79.
23 McWhinnie W R & Miller J D, *Adv inorg Chem radio Chem*, **12** (1969) 159.

Indian Journal of Chemistry
Vol. 27A, September 1988, pp. 822-824

Formation Constants of the Complexes of Some Bivalent Metal Ions with a New Tridentate Schiff Base, 7-Hydroxy-8-[(2-mercaptophenyl)iminomethyl]-4-methyl-2*H*-1-benzopyran-2-one

(Mrs) S V KALAVATHI & K L OMPRAKASH*
Department of Chemistry, P.G. College (Osmania University), Secunderabad 500 003
and
K JAGANNADHA CHARYULU, A V CHANDRA PAL & M L N REDDY*
Department of Chemistry, Osmania University, Hyderabad 500 007

Received 15 *June* 1987; *revised and accepted* 14 *October* 1987

A new tridentate schiff base, 7-hydroxy-8-[(2-mercaptophenyl)-iminomethyl]-4-methyl-2*H*-1-benzopyran-2-one (HMMB), derived from 8-formyl-7-hydroxy-4-methyl-2*H*-1-benzopyran-2-one and 2-mercaptoaniline has been synthesised and characterised by analytical and spectral data. Proton-ligand formation constants of the schiff base and metal-ligand formation constants of its chelates with Cu(II), Co(II), Ni(II), Fe(II), Mn(II), Zn(II), Cd(II), Hg(II) and Pb(II) have been determined *p*H-metrically in 70% (v/v) aq. dioxane medium at 20, 25, 32 and 45° and $I = 0.5\ M(NaClO_4)$. The $\bar{n}$ and *p*L values reveal the formation of only 1:1 chelates with this tridentate ligand. The order of chelate stabilities is found to be almost in conformity with Irving-Williams order. Thermodynamic parameters, ΔG, ΔH, and ΔS, associated with the complex formation reactions, have been evaluated. The schiff base HMMB is suggested as suitable acid-base indicator for the titration of HCO_3^-, HPO_4^{2-} and CH_3COO^- against a strong mineral acid.

Metal complexes of coumarins and schiff bases are reported to be potential biochemical and analytical reagents. This prompted us to study the synergistic effect of these two moieties on the complexing tendencies of the ligands containing them with metal ions. In the present investigation the schiff base 7-hydroxy-8-[(2-mercaptophenyl)iminomethyl] -4-methyl-2*H*-1-benzopyran-2-one (HMMB) has been synthesised by condensing 8-formyl-7-hydroxy-4-methyl-2*H*-1-benzopyran-2-one (FHMB) with 2-mercaptoaniline. The interaction of HMMB with bivalent transition metal ions has been studied *p*H-metrically in 70% (v/v) aq. dioxane at 20, 25, 32 and 45° and $I = 0.05\ M(NaClO_4)$.

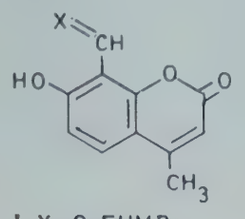

I X = O, FHMB;
X = 2-SH-Ph-N-, HMMB

All the chemicals used were of AR/GR grade. Equimolar quantities of FHMB[1] and 2-mercaptoaniline were refluxed (1 hr) in methanol. The resultant schiff base, HMMB, was repeatedly crystallised from methanol to get TLC-pure sample; m.p. 167°; IR(KBr): 3100-3250br(νOH), 1720(νC = O lactonic), 1620(νC = N) and 2550 cm^{-1}(νSH); PMR: δ 60 MHz ($CDCl_3$; TMS internal ref): 2.06 (3H, *t*, 4-CH_3), 6.0(1H, *s*, 3-H), 6.8-7.8(6H, *m*, Ar − H), (1H, *s*, S − H, D_2O exchangeable), 9.25(1H, *s*, CH = N) and 14.8(1H, *s*, OH, D_2O exchangeable); Mass: M^+ 311 (23%) [Found: C, 65.8; H, 4.1; N, 4.4: S, 10.1, $C_{17}H_{13}O_3NS$ requires: C, 65.6; H, 4.2; N, 4.5; S, 10.3%]. Based on the above analytical and spectral data, structure (I) has been assigned to the schiff base HMMB.

Proton-ligand and metal-ligand formation constants have been determined using Irving-Rossotti *p*H-titration technique[2] in 70% (v/v) aq. dioxane ($I = 0.05\ M$ $NaClO_4$) at 20, 25, 32 and 45°. The experimental details are similar to those described earlier[3]. The *p*H-meter readings (B) in 70% (v/v) aq. dioxane were corrected by the method of Van Uitert and Hass[4]. The titration curve of HMMB showed the liberation of two protons per ligand molecule, corresponding to the − OH and − SH groups. From the proton-ligand formation curve log K_1^H and log K_2^H values have been obtained by various computational methods[2]. As the hydroxyl group is more acidic (due to high electronegativity of oxygen) than mercapto group, log K_1^H and log K_2^H are designated as log K_{SH} and log K_{OH}, respectively.

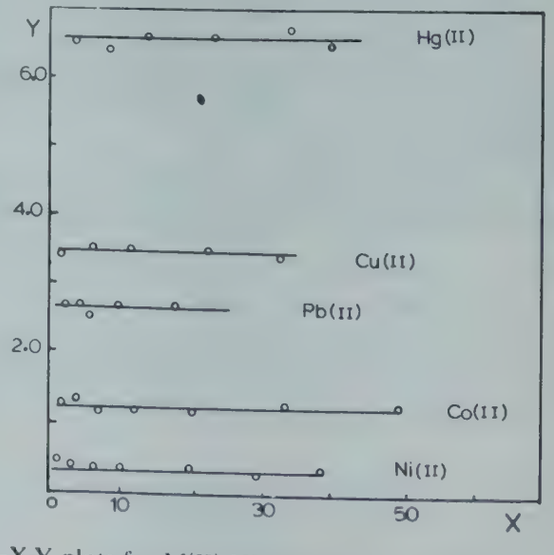

Fig. 1—X-Y plots for M(II)-HMMB systems [Cu, Hg, ($X \times 10^{20}$, $Y \times 10^{-19}$); Co ($X \times 10^{19}$; $Y \times 10^{-19}$); Pb ($X \times 10^{15}$, $Y \times 10^{-15}$) and Ni ($X \times 10^{17}$, $Y \times 10^{-16}$)]

Table 1—Formation Constants and Thermodynamic Parameters Associated with M(II)-HMMB Chelate Systems

[Medium: 70% (v/v) aq. dioxane; $I = 0.05$ M]

	log K_1				$-\Delta G$ (kJ mol^{-1})	$-\Delta H$ (kJ mol^{-1})	$-\Delta S$ (J mol^{-1} K^{-1})
	20	25	32	45°C			
Log K_{SH}	11.73	11.33	11.04	10.33	..	..	..
Log K_{OH}	10.45	10.19	9.85	9.24	..	..	..
Hg(II)	22.40	21.27	19.76	17.25	115.4	382.4	875.8
Cu(II)	22.15	20.98	19.48	16.68	113.8	386.6	895.1
Co(II)	21.70	20.56	19.06	16.32	111.3	382.0	888.1
Ni(II)	18.85	17.81	16.46	14.01	96.1	343.5	811.4
Pb(II)	17.22	16.43	15.42	13.59	90.1	257.3	548.6
Fe(II)	15.37	14.97	14.45	13.48	84.4	133.5	161.3
Zn(II)	14.90	14.52	14.05	13.22	82.2	118.0	117.7
Cd(II)	14.25	14.02	13.66	13.02	79.8	88.7	29.5
Mn(II)	10.83	10.50	10.05	9.22	58.7	114.6	183.5

The metal-ligand titration curves were well below the metal-ion hydrolysis curves. The low concentrations of metals ions (4×10^{-4} M) used are likely to prevent the formation of polynuclear complexes. The maximum $\bar{n}$ values calculated for each metal-ligand system have been found to be around 1.0 indicating the formation of only 1:1 complexes. An attempt has been made to check whether only 1:1 chelate[5-7] is formed by constructing X-Y plots of the Eq. 1 (Fig. 1),

$$\frac{\bar{n}}{(1-\bar{n})[L]} = \beta_1 + \beta_2 \frac{(2-\bar{n})[L]}{(1-\bar{n})} \quad \ldots (1)$$

In the present investigation all the M(II)-HMMB systems gave plots parallel to the abscissa confirming the formation of only 1:1 complex. The ligand is expected to act as a tridentate chelating agent coordinating through the phenolic oxygen, mercapto sulphur and azomethine nitrogen. Therefore, the stereochemistry of the ligand molecule may hinder the formation of a 1:2 complex. The metal-ligand formation constants (log K_1) have been evaluated by various computation techniques[2]. The values obtained by different methods are in agreement with each other. The average log K_1 values are presented in Table 1. The standard deviations are in the range ± 0.03.

The order of stability constants of M(II)-HMMB is: Hg(II) > Cu(II) > Co(II) > Ni(II) > Pb(II) > Fe(II) > Zn (II) > Cd(II) > Mn(II) which is almost in accordance with Irving-Williams natural order of stabilities except for Co(II) > Ni(II) and Fe(II) > Zn(II). The higher values for Co(II) and Fe(II) chelates may be due to the resonance stabilisation in these systems. Further, it has been found that Hg(II) and Pb(II) form more stable chelates compared with those of Zn(II) and Cd(II). Hg(II) and Pb(II) being relatively soft acids (due to their larger size) compared to Zn(II) and Cd(II), such an observation is not unexpected.

The thermodynamic parameters associated with the chelation reactions of M(II)-HMMB systems have been evaluated from the *p*H-metric data at different temperatures and are presented in Table 1. The negative free energy change (ΔG) for M(II)-HMMB reaction in each case indicates that the chelation is spontaneous. Further, ΔG becomes more positive with an increase in temperature suggesting a decrease in the extent of complex formation at higher temperatures. The negative values of enthalpy change (ΔH) indicate exothermic nature of chelation and their magnitudes suggest strong metal-ligand bond. The negative entropy change (ΔS) can be attributed to the extensive solvation[8] of metal chelates in an aquo-organic medium. This may be due to the exposure of the polar oxygen, nitrogen, sulphur and the metal ions of the chelate to solvent molecules[9].

HMMB as an acid-base indicator

The ligand (H_2L) is colourless in the acid medium. In the *p*H-metric titration of the ligand HMMB with the alkali, an intense red colour was observed at the equivalence point. The formation of red colour may be due to the deprotonated form (HL^-) of the ligand. The presence of chromophoric centers like phenolic, mercapto, azomethine and lactonic groups coupled with highly extended conjugation in the ring system may be responsible for the intense red colour of the reagent. Keeping this in view, it was thought worthwhile to examine the suitability of this ligand as an acid-base indicator. It was found that with the aqueous sodium salt solutions of HCO_3^-, HPO_4^{2-}, and CH_3COO^-, the ligand formed intense red colouration instantaneously, whereas no colouration was noted with solutions of HSO_4^-, SO_4^{2-}, ClO_4^-, Cl^-, $H_2PO_4^-$, and NO_3^-. The colour formation reaction of the ligand with HCO_3^-, HPO_4^{2-} and CH_3COO^- was followed spectrophotometrically using a Systronics digital spectrophotometer type 106 with 1 cm quartz cells. Maximum absorption of the colour occurred at 500 nm. Reverse S-shaped curve (absorption vs volume of

HCl) was obtained when 20 ml of 0.05 *M* solution of HCO_3^-, HPO_4^{2-} or CH_3COO^- was titrated against 0.075 *M* standard HCl solution confirming the sharp colour change at the stoichiometric end point. The *p*H range of the colour change interval (as revealed by A vs *p*H plateaus) has been noted to be 4.9-7.1.

To have an insight as to why the reagent gives red colour with the aqueous solutions of HCO_3^-, HPO_4^{2-} and CH_3COO^- only, the proton-ligand stability of the ligand was determined in aqueous medium by extrapolating the plot of log K_{OH} versus mole fraction of dioxane or acetone to zero mole fraction. The value of log K_{OH} of the ligand in aqueous medium was found to be 6.5. This is consistent with the *p*H range of the colour change interval of the reagent.

Standard solutions of $NaHCO_3$, Na_2HPO_4 or CH_3COONa (0.1 *M* to 0.001 *M*) were successfully titrated with standard mineral acids in the presence of this ligand, end point being from dark red to colourless solution. Two drops of 0.1% ligand solution prepared in acetone were added. The titration error was found to be within 0.5-1.5%.

References

1 Parikh S H & Thakur V N, *J Univ Bombay*, **(Sect A), 36** (1954) 37.
2 Irving H & Rossotti H S, *J chem Soc*, (1954) 2904; (1953) 3397.
3 Omprakash K L, Chandra Pal A V & Reddy M L N, *Indian J Chem*, **21A** (1982) 322; **22A** (1983) 546.
4 Van Uitert L G & Hass C G, *J Am chem Soc*, **75** (1953) 451.
5 Ramamoorthy S & Santappa M, *Bull chem Soc Japan*, **4** (1968) 1330.
6 Jagannadha Charyulu K, Omprakash K L, Chandra Pal A V & Reddy M L N, *J Indian chem Soc*, **60** (1983) 236; **62** (1985) 121.
7 Jagannadha Charyulu K, Omprakash K L, Chandra Pal A V & Reddy M L N, *Indian J Chem*, **23A** (1984) 668.
8 Nahar C T & Mukhedkar A J, *J Indian chem Soc*, **57** (1980) 961.
9 Johnston W D & Frieser H, *Analyt chim Acta*, **11** (1954) 201.

Indian Journal of Chemistry
Vol. 27A, September 1988, pp. 825-826

Differential Pulse Polarographic Determination of Proquazone

AYTEKIN TEMIZER*, SEDEF KIR & A NUR ONAR
Department of Analytical Chemistry, Faculty of Pharmacy, Hacettepe University, 06100, Ankara, Turkey

Received 3 *September* 1987; *revised and accepted* 28 *January* 1988

The differential pulse polarographic (DPP) behaviour of proquazone is investigated in different media. The compositions of electrolytes, height of the mercury column, temperature and the other parameters are so selected that the determination of this substance can be accomplished down to sub ppm level. Evidence is presented to show that the reduction of proquazone to proquazole is a reversible reaction with one electron transfer.

Proquazone [1-isopropyl-4-phenyl-7-methyl-2-(1H)-quinazolinone] is a new non-steroidal, anti-inflammatory agent. The compound possesses potent anti-inflammatory, analgesic and antipyretic effects[1].

Earlier, proquazone has been determined in serum and in synovial fluid by means of fluorimetric procedures with detection limit of 0.01 μg/ml[2,3]. The concentrations of the principal metabolite were determined by means of HPLC with the detection limit lying in the range 0.03-0.05 μg/ml[3]. However, the earlier methods of determination are cumbersome. We present here a differential pulse polarographic method of the determination of proquazone which can be used for the pure substance as well as for commercially available pharmaceutical samples.

The electrochemical apparatus used in the present study has been described previously[4]. The tapered dropping mercury electrode capillary that was used had a flow rate of 0.48 mg.s^{-1} at *p*H 5.00 (Britton-Robinson buffer) in open circuit with 80 cm height of mercury column. IR and UV spectrophotometers used were Perkin-Elmer model 457 and Beckman model DB-GT respectively. Controlled-potential electrolysis with a mercury pool cathode was carried out with the Heath model EUA-19-21 instrument. Corning model 12 research *p*H meter was used for *p*H measurements.

Stock solutions of $10^{-3}M$ proquazone were prepared in ethanol. The polarograms were recorded under the following conditions: drop-time, 1 s; modulation amplitude, 50 mV; current range, 2 μA; scan rate, 2 mV-s^{-1}; low pass filter, off; height of mercury column, 80 cm; temperature of the cell, 20 ± 0.1°C.

Controlled-potential electrolysis was performed using 18 ml of proquazone solution (90 μg/ml) in Britton-Robinson buffer at *p*H 5.00. Exhaustive reduction of proquazone at a mercury pool electrode was carried out. The potential of electrolysis was selected (with respect to SCE) so as to be similar to that on the upper plateau of the polarographic wave. At this potential, carbonyl group present on the molecule is reduced to hydroxyl.

In the determination of pharmaceutical samples, 5, 10 and 20 capsules were weighed. After finding the mean weight value of each set of capsules, the material from one capsule was dissolved in ethanol and solution diluted to 100 ml with the same solvent. 0.05 ml of this solution was added to the polarographic cell containing supporting electrolytes. Standard addition technique was used in order to find the concentration of drug.

The polarographic behaviour of proquazone was examined over the *p*H range 2-12. Proquazone gives rise to a single cathodic peak throughout the *p*H region studied. However, the peak potential becomes markedly more negative as the *p*H increases. The current value at peak potential (− 0.8 V) has been found to be highest in a supporting electrolyte composed of BR buffer of *p*H 5.00.

It is worth emphasizing that a buffer system at the usual concentrations used, generally provides adequate capacity only over ± 1 pK_a range. The pK_a of a polarographically active substance can be found by determining the inflection point of a plot of half-wave potential with respect to *p*H[5]. The inflection point for proquazone under the experimental conditions was found to be 4.40. Solutions having *p*H values near to this value seem to be appropriate as supporting electrolytes. In fact, BR buffer of *p*H 5.00 was found to be the best supporting electrolyte.

The characteristics of linear regression of calibration graph for proquazone at *p*H 5.00 BR buffer were: slope, 4.20×10^{-6} nA/*M*, concentration intercept, 0.53×10^{-6} *M* and correlation coefficient was 0.999 for 9 data points. The concentration range of 0.02-20 ppm is appropriate for the determination of proquazone by DPP. At concentrations lower than 0.02 ppm, the peak is not resolved from the noise. At concentrations greater than 20 ppm, deviation from linearity occurs.

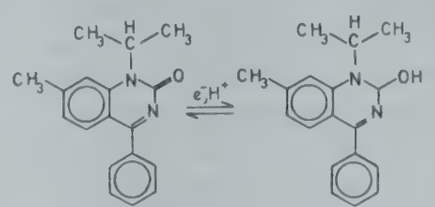

Fig. 1—Reduction mechanism of proquazone to proquazole

The mechanism of reduction of proquazone in aqueous solution involves the addition of one electron and a proton to form the corresponding proquazole (Fig. 1). This is shown by the controlled-potential electrolysis. The electrode product was isolated and identification was made by spectroscopic methods. An absorption peak at 360 nm belonging to the $\pi \rightarrow \pi^*$ transition of proquazone was not observed in the spectrum of proquazole. IR spectra of proquazone and proquazole are similar with the exception of a strong carbonyl stretching absorption at 1659 cm^{-1} in the spectrum of proquazone and a wide hydroxyl stretching vibration at 3400 cm^{-1} in the spectrum of proquazole.

In order to find the current characteristics, which were used in the analysis of proquazone, effect of the height of the mercury column and temperature coefficient have been determined. Linear regression analysis of the limiting current versus the square root of the height of the mercury column showed a linear behaviour. Temperature coefficient of the proquazone was found to be 1.5 %. deg^{-1}. These results indicate that the current is diffusion controlled.

The reversibility test was performed by scan reversal pulse polarography, logarithmic analysis and on the basis of the value of $E_{3/4}$-$E_{1/4}$. The reciprocal slope of the plot of logarithmic functions of current $(i_d\text{-}i)/i$ versus potential give the value 0.062 volt. This is very similar to the theoretical Nernst voltage of 0.059 volt, of 2.303 RT/nF for a reversible reduction involving one electron. The value of $E_{3/4}$-$E_{1/4}$ was found to be 59.375 mV. There was no difference found in reverse scanning. All these results showed that the electrode reaction is a reversible one.

Proquazone is marketed in a capsule form under the name "Biarison" containing 200 mg proquazone per capsule. Differential pulse polarographic analysis of Biarison capsules showed 196.37 ± 3.66 mg proquazone per capsule. Considerable time saving, increased reproducibility and precision were obtained with the use of DPP in determination of proquazone in Biarison capsules.

References

1 Andersen R B & Halskov O, *Scand J Rheumatology Suppl*, **21** (1978) 18.
2 Ross A & Hinderling P H, *J Pharm Sci.*, **70** (1981) 252.
3 Ott H & Meier J, *Scand J Rheumatology Suppl*, **21** (1978) 12.
4 Onar A N & Temizer A, *Analyst*, **112** (1987) 227.
5 Kucharczyk N, Adamovsky M, Horak V & Zuman P, *J electroanal Chem*, **10** (1969) 503.

Indian Journal of Chemistry
Vol. 27A, September 1988, pp. 827-828

BOOK REVIEWS

The Theory of Thermodynamics by J R Waldram (Cambridge University Press) 1985, pp. XV+ 336

The approach adopted in this book is entirely different from the approach in most of the existing books on the subject. The usual approach is to take laws of thermodynamics as generalisations coming from everyday experience and then make deductions from these laws. This approach obviously makes thermodynamics an empirical subject. Such an approach has both an advantage as well as a handicap. The advantage is that generality of thermodynamics is emphasised. The handicap is in terms of loss of information on mechanism, rendering appreciation of the linkup between classical thermodynamics, kinetic theory and statistical thermodynamics a little uneasy.

Since rationale behind these empirical laws is sure to lie in the happenings at the microscopic level, the author starts with the mechanical picture and derives laws of thermodynamics therefrom. This approach, as shown by the author, is quite rewarding from the didactic point of view. The intimate connection between kinetics, thermodynamics and statistical thermodynamics is brought about smoothly and in a natural way. I agree with the author's claim that this book can cater to the needs of the students from first year to final year and beyond. It provides a complete university course. The use of master equation as starting point in statistical thermodynamics has been of definite advantage in exposing the links between kinetics and thermodynamics.

This book, which really deals with the theory of thermodynamics, lucidly exhibits the connection between the approach involving mechanism and the empirical approach. One immediately appreciates that the laws of thermodynamics are no longer empirical in nature. Dr Waldram has done an excellent job. I would recommend this book to all students including those doing research in thermodynamics.

R C Srivastava
Chemistry Department
BITS, Pilani 333 031

High pressure Chemistry and Biochemistry edited by R Van Eldik & J Jones (D. Reidel Publishing Company Dordrecht, Holland) 1987, pp. VI + 468, Price $ 96.00

This book arises from the selected papers presented at a NATO-sponsored advanced study workshop on "Advances in High Pressure Studies of Chemical and Biological Systems" held in Corfu, Greece, during Sept.-Oct. 1986. Through this volume, the authors aim to project the current status of high pressure chemistry. Although improved equipment is available that enables static as well as dynamic measurements at pressures several orders of magnitude higher than before, its impact has been more extensive in physics and experimental petrology than in chemistry, and the book, in a way, is intended to alter this apparent anomaly. A general introduction on high pressure research is followed by nine chapters on theoretical and experimental investigations on physical aspects of fluids as well as solids at high pressure and temperatures. Due stress on instrumental techniques, such as NMR and vibrational spectroscopy, X-ray and neutron scattering, is given in the first section. Applications of high pressure studies in organic and inorganic systems are presented in the second part followed by the past growing area of high pressure researches in biochemistry in the last three chapters. The general review on high pressure chemistry by H C Drickamer is for fast, but enjoyable, reading. What the high pressure has to offer in understanding the atomic and molecular interactions by means of appropriate physical techniques is made abundantly clear in this chapter.

Gases and liquids have curiously anomalous properties at high pressures generated in shockwave experiments as well as under static pressures. Studies on shock-compressed liquids enable one to understand the intermolecular forces, electronic and chemical properties and melting behaviour at extreme conditions. Supercritical fluids containing strongly interacting polar molecules have peculiar thermophysical characteristics. Demonstration of methane combustion flame in supercritical water and the transition of ionic to metallic state in Cs-CsH system by E U Franck are examples worth mentioning. Critical behaviour of liquid metals at high pressures, especially those of alkali metals, illustrates the nature of fluid electronic conductors. Another interesting example is the critical miscibility and phase equilibria in polymerization of monomers in solution or emulsion under pressure wherein the entropy of mixing of the system decreases. The physical techniques utilized to probe the

molecular structure and interactions under pressure are well presented by way of nuclear magnetic resonance, laser-Raman and Rayleigh Scattering pertaining to the dynamics of fluids as also X-ray and neutron scattering with respect to phase transitions in solids. Specific mention may be made of pressure-tuning spectroscopy involving the effect of pressure on electronic excitation.

The section on the chemical aspects of high pressure studies mostly deals with the kinetics and mechanisms of reactions in organic as well as inorganic systems. The core of concept follows the transition rate theory, according to which the volume of activation can be determined from the pressure dependence of the rate constants and combining it with the partial molar volumes of reactant and product molecules, one can construct the volume profile of a given reaction. The structure profile of a chemical reaction, including that of the activated complex can thus be arrived at. Applicability to organic reactions and so also, to transition metal complexes is presented. Further, dynamics of excited state species are attempted by way of pressure effects on photochemical reactions of transition metal complexes in solution. Admittedly, this has introduced ambiguities into the existing understanding of the investigated systems. Utility of high pressure as a variable in synthetic reactions is restricted to selected organic systems. One may contain the disappointment in not finding the inorganic systems, particularly those relating to high pressure synthesis of inorganic solids in the light of the generalisations derivable from the abundance literature on experimental minerology.

The third section is further constrained than the previous one, possibly due to the rapidly growing nature and the abundant possibilities in the near future for high pressure researches in biochemistry. Pressure-induced modifications in the structure and dynamics of lamellar, micellar and reversed-micellar model biomembranes in water have been treated on the basis of infrared and Raman spectroscopic data. High pressure stability of oligomeric proteins and the conformational drift in the dissociated subunits under pressure are illustrative examples. Effect of pressure on spin coupling equilibria and ligand binding processes in methyoglobin is indicative of the possible vistas in high pressure biochemistry.

Though the book falls short of reflecting fully the various aspects of current researches in high pressure chemistry, it evidently compels one to think beyond the boundaries of specific concepts and systems with which one is entangled routinely.

T R N Kutty
Materials Research Laboratory
Indian Institute of Science
Bangalore 560 012

THE WEALTH OF INDIA

An Encyclopaedia of Indian Raw Materials and Industrial Products, published in two series :

(i) Raw Materials, and **(ii) Industrial Products.**

RAW MATERIALS

The articles deal with Animal Products, Dyes & Tans, Essential Oils, Fats & Oils, Fibres & Pulps, Foods & Fodders, Drugs, Minerals, Spices & Flavourings, and Timbers and other Forest products. Names in Indian languages, and trade names are provided.

For important crops, their origin, distribution, evolution of cultivated types and methods of cultivation, harvesting and storage are mentioned in detail. Data regarding area and yield and import and export are provided. Regarding minerals, their occurrence and distribution in the country and modes of exploitation and utilization are given. The articles are well illustrated. Adequate literature references are provided.

Eleven volumes of the series covering letters A–Z have been published.

Vol. I : A (Revised) Rs. 300.00; Vol. I (A-B) Rs. 120.00; Vol. II (C) Rs. 143.00; Vol. III (D-E) with index to Vols. I-III Rs. 158.00; Vol. IV (F-G) Rs. 150.00; Vol. IV Suppl. Fish & Fisheries Rs. 84.00; Vol. V (H-K) Rs. 171.00; Vol. VI (L-M) Rs. 135.00; Vol. VI : Suppl. on Livestock including poultry Rs. 153.00; Vol. VII (N-Pe) Rs. 150.00; Vol. VIII (Ph-Re) Rs. 129.00; Vol. IX (Rh-Sc) Rs. 200.00; Vol. X (Sp-W) Rs. 338.00; Vol. XI (X-Z) with Cumulative Index to Vols. I-XI Rs. 223.00.

INDUSTRIAL PRODUCTS

Includes articles giving a comprehensive account of various large, medium and small scale industries. Some of the major industries included are : Acids, Carriages, Diesel Engines, Fertilizers, Insecticides & Pesticides, Iron & Steel, Paints & Varnishes, Petroleum Refining, Pharmaceuticals, Plastics, Ship & Boatbuilding, Rubber, Silk, etc.

The articles include an account of the raw materials and their availability, manufacturing processes, and uses of products, and industrial potentialities. Specifications of raw materials as well as finished products and statistical data regarding production, demand, exports, imports, prices, etc. are provided. The articles are suitably illustrated. References to the sources of information are provided.

Nine volumes of the series covering letters A–Z have been published.

Part I (A-B) Rs. 87.00; Part II (C) Rs. 111.00; Part III (D-E) with Index to Parts I-III Rs. 150.00; Part IV (F-H) Rs. 189.00; Part V (I-L) Rs. 135.00; Part VI (M-Pi) Rs. 42.00; Part VII (Pl-Sh) Rs. 90.00; Part VIII (Sl-Tl) Rs. 99.00; Part IX (To-Z) with Index to Parts I-IX Rs. 120.00.

HINDI EDITION : BHARAT KI SAMPADA—PRAKRITIK PADARTH

Vols. I to VII and two supplements of Wealth of India—Raw Materials series in Hindi already published.

Published Volumes :

Vol. I (अ-औ) Rs. 57.00; Vol. II (क) Rs. 54.00; Vol. III (ख-न) Rs. 54.00; Vol. IV (प) Rs. 125.00; Vol. V (फ-मेरे) Rs. 90.00; Vol. VI (मेल-रू) Rs. 120.00; Vol. VII (रे-वाटा) Rs. 203.00; Vol. VIII (वाय-सीसे) Rs. 300.00.

Supplements :

Fish & Fisheries (Matsya & Matsyaki) Rs. 74.00;
Livestock (Pashudhan aur Kukkut Palan) Rs. 51.00

Vols. IX to XI under publication.

Please contact :

SENIOR SALES AND DISTRIBUTION OFFICER

PUBLICATIONS & INFORMATION DIRECTORATE, CSIR

Hillside Road, New Delhi 110 012

RN 7090/63

CSIR PUBLICATIONS

WEALTH OF INDIA

An encyclopaedia of the economic products and Industrial resources of India issued in two series.

RAW MATERIALS SERIES – Contains articles on plant, animal and mineral resources.

	Rs.	$	£
Vol. I(A) (Revised)	300.00	94.00	74.00
Vol. I (A-B)	120.00	60.00	26.00
Vol. II (C)	143.00	66.00	34.00
Vol. III (D-E)	158.00	64.00	40.00
Vol. IV (F-G)	98.00	54.00	24.00
Supplement (Fish & Fisheries)	84.00	32.00	21.00
Vol. V (H-K)	171.00	68.00	42.00
Vol. VI (L-M)	135.00	68.00	30.00
Supplement (Livestock including Poultry)	153.00	68.00	39.00
Vol. VII (N-Pe)	150.00	60.00	38.00
Vol. VIII (Ph-Re)	129.00	64.00	28.00
Vol. IX (Rh-Se)	156.00	70.00	38.00
Vol. X (Sp-W)	338.00	150.00	85.00
Vol. XI (X-Z)	223.00	77.00	44.00

INDUSTRIAL PRODUCTS SERIES – Deals with major, Small-Scale and Cottage Industries

Part I (A-B)	87.00	40.00	22.00
Part II (C)	111.00	48.00	28.00
Part III (D-E)	150.00	67.00	39.00
Part IV (F-H)	189.00	84.00	48.00
Part V (I-L)	135.00	46.00	34.00
Part VI (M-Pi)	42.00	16.00	5.60
Part VII (Pl-Sh)	90.00	36.00	12.00
Part VIII (Si-Ti)	99.00	54.00	20.00
Part IX (To-Z)	120.00	68.00	24.00

BHARAT KI SAMPADA (Hindi Edition of Wealth of India, Raw Materials):

Vol. I (अ-औ)	57.00	32.00	13.00
Vol. II (क)	54.00	30.00	12.00
Vol. III (ख-न)	54.00	30.00	12.00
Vol. IV (प)	125.00	68.00	32.00
Vol. V (फ-मेरे)	90.00	44.00	20.00
Vol. VI (मेल-रू)	120.00	54.00	26.00
Vol. VII (रे-वाटा)	203.00	80.00	50.00
Vol. VIII (वाय-सीसे)	300.00	80.00	50.00
Livestock (Kukkut Palan)	51.00	30.00	12.00
Fish & Fisheries (Matsya aur Matsyaki)	74.00	42.00	10.00
A Dictionary of Generic & Specific Names of Plants & Animals Useful to Man	45.00	22.00	10.00

Please Contact :

SENIOR SALES & DISTRIBUTION OFFICER
PUBLICATIONS & INFORMATION
DIRECTORATE, CSIR
HILLSIDE ROAD, NEW DELHI - 110012

OTHER PUBLICATIONS

	Rs.	$	£
The Useful Plants of India	192.00	64.00	48.00
A Dictionary of the Flowering Plants in India by H. Santapau & A.N. Henry	63.00	28.00	16.00
Glossary of Indian Medicinal plants by R.N. Chopra, S.L. Nayar & I.C. Chopra	93.00	32.00	20.00
Supplement to Glossary of Indian Medicinal Plants by R.N. Chopra, I.C. Chopra & B.S. Verma	51.00	18.00	12.00
The Flora of Delhi by J.K. Maheshwari	42.00	16.00	5.50
Illustrations to the Flora of Delhi by J.K. Maheshwari	105.00	44.00	26.00
Herbaceous Flora of Dehra Dun by C.R. Babu	216.00	120.00	44.00
Gnetum by P. Maheshwari & Vimla Vasil	30.00	12.00	4.00
Marsilea by K.M. Gupta	62.00	27.00	16.00
Aquatic Angiosperms	30.00	12.00	4.00
Indian Fossil Pteridophytes by K.R. Surange	99.00	44.00	25.00
Cedrus by P. Maheshwari & Chhaya Biswas	63.00	28.00	16.00
Proteaceae by C. Venkata Rao	108.00	48.00	27.00
Pinus by P. Maheshwari & R.N. Konar	45.00	22.00	16.00
Loranthaceae by B.M. Johri & S.P. Bhatnagar	83.00	37.00	21.00
Abies & Picea by K.A. Chowdhury	21.00	12.00	4.20
Indian Thysanoptera by T.N. Ananthakrishnan	39.00	16.00	5.20
The Millipede Thyropygus by G. Krishnan	18.00	7.00	2.40
Indian Sardines by R.V. Nair	33.00	14.00	4.40
Drug Addiction with special Reference to India by R.N. Chopra & I.C. Chopra	19.00	7.00	2.40
Diosgenin & other Steroid Drug Precursors by L.V. Asolkar & Y.R. Chandha	54.00	26.00	12.00
Cholera Bacteriophages by Dr. Sachimohan Mukerjee	45.00	20.00	12.00
Cottonseed Chemistry & Technology by K.S. Murti & K.T. Achaya	116.00	64.00	26.00
Corrosion Map of India	27.00		3.60
Rural Development and Technology: A Status Report-cum-Bibliography by PR Bose and V.N. Vashist	150.00	76.00	34.00
Termite Problems in India	14.00	6.00	1.80
Research & Development Management	38.00	20.00	
Proceedings of the Seminar on Primary Communications in Science & Technology in India by R.N. Sharma & S. Seetharama	78.00	35.00	68.00

Packing and Postage Extra

Printed & Published by Shri S.S. Saksena, Editor, Publications & Information Directorate (PID), Hillside Road, New Delhi 110012, at PID Photocomposition-cum-Printing Unit

Regd No. D(C)-1018